

Aeronautics Engineering Handbook

Doug Hunsaker

Special thanks to Ben Moulton, Sabrina Snow, and Joseph Hammer for typesetting support

This document compiled on: May 16, 2024

Contents

| | |
|---|-----------|
| 1 Basic Mathematical Properties | 5 |
| 1.A Cartesian Coordinates | 5 |
| 1.B Cylindrical Coordinates | 5 |
| 1.C Spherical Coordinates | 5 |
| 1.D Useful Trigonometric Relations | 6 |
| 2 Fundamentals of Fluids | 7 |
| 2.A Fundamental Equations | 7 |
| 2.B Fluid Properties | 7 |
| 2.C Dimensionless Numbers | 8 |
| 2.D The Standard Atmosphere | 8 |
| 2.D.1 Gravity | 8 |
| 2.D.2 Geopotential Altitude | 8 |
| 2.D.3 Pressure and Temperature | 8 |
| 2.D.4 Density and Speed of Sound | 9 |
| 2.D.5 Dynamic Viscosity | 9 |
| 2.D.6 English Units | 9 |
| 3 Potential Flow Solutions | 10 |
| 3.A Uniform Flow | 10 |
| 3.B Incompressible Line Source | 10 |
| 3.C Incompressible Point Source | 10 |
| 3.D Incompressible Line Vortex | 10 |
| 3.E Incompressible Line Doublet | 10 |
| 3.F Incompressible Circular Cylinder with Circulation | 10 |
| 3.G Incompressible Source Panel | 10 |
| 3.H Incompressible Vortex Panel | 11 |
| 3.I Kutta-Joukowski Law | 11 |
| 4 Airfoil Theory | 12 |
| 4.A Airfoil Geometry | 12 |
| 4.B Thin Airfoil Theory | 12 |
| 4.C Parabolic Flaps | 13 |
| 4.D Vortex Panel Method | 13 |
| 5 Two-Dimensional Conformal Mapping | 15 |
| 5.A Fundamental Concepts | 15 |
| 5.B Elementary Potential Flows | 15 |
| 5.B.1 Uniform Flow | 15 |
| 5.B.2 Source Flow | 15 |
| 5.B.3 Vortex Flow | 15 |
| 5.B.4 Doublet Flow | 15 |
| 5.B.5 Flow over a Circular Cylinder with Circulation | 16 |

| | | |
|----------|--|-----------|
| 5.B.6 | Body of Arbitrary Cross Section | 16 |
| 5.C | Blasius Relations | 16 |
| 5.C.1 | Complex Section Force | 16 |
| 5.C.2 | Section Pitching Moment | 16 |
| 5.D | Kutta-Joukowski Law | 16 |
| 5.E | Conformal Transformations | 16 |
| 5.F | Joukowski Cylinders and Airfoils | 16 |
| 5.F.1 | Joukowski Transformation | 16 |
| 5.F.2 | Joukowski Cylinder | 17 |
| 5.F.3 | Joukowski Airfoils | 17 |
| 6 | Lifting-Line Theory | 18 |
| 6.A | Classical Development | 18 |
| 6.B | Decomposed Fourier Solution | 18 |
| 6.B.1 | Planform | 20 |
| 6.B.2 | Washout | 20 |
| 6.B.3 | Aileron Distribution | 21 |
| 6.C | Lift Distributions | 23 |
| 6.C.1 | Special Class of Lift Distributions | 24 |
| 6.D | Wing Spar Sizing | 27 |
| 7 | Aircraft Performance | 28 |
| 7.A | Lift and Drag | 28 |
| 7.B | Steady-Level Flight | 28 |
| 7.B.1 | Thrust Required and Minimum-Drag Airspeed | 28 |
| 7.B.2 | Power Required | 29 |
| 7.C | Rate of Climb | 30 |
| 7.D | Gliding Flight | 30 |
| 7.D.1 | Sink Rate | 30 |
| 7.D.2 | Glide Ratio | 30 |
| 7.E | Stall | 31 |
| 7.F | Steady Coordinated Turn | 31 |
| 7.G | Takeoff and Landing | 32 |
| 8 | Longitudinal Static Trim and Stability | 33 |
| 8.A | Small-Angle Longitudinal Trim Requirements | 33 |
| 8.B | Longitudinal Stability Requirements | 33 |
| 8.C | Simplified Wing and Tail Model | 33 |
| 8.D | Estimating Downwash | 34 |
| 8.D.1 | General Solution For Wings Without Sweep | 34 |
| 8.D.2 | Plane of Symmetry | 35 |
| 8.D.3 | Sweep Effects | 35 |
| 8.D.4 | Rough Approximation for a Horizontal Stabilizer | 35 |
| 8.E | Generalized Model with Vertical Offsets and Drag | 35 |
| 8.F | Aerodynamic Center | 36 |
| 8.G | Fuselage and External Stores | 37 |
| 8.H | Contribution of Propellers | 37 |
| 8.I | Contribution of Jet Engines | 38 |
| 9 | Lateral Static Trim and Stability | 39 |
| 9.A | Small-Angle Lateral Trim Requirements | 39 |
| 9.B | Lateral Stability Requirements | 39 |
| 9.B.1 | Yaw Stability Requirement | 39 |
| 9.B.2 | Roll Stability Requirement | 39 |
| 9.C | Contributions to Yaw Trim and Stability | 39 |

| | | |
|-----------|---|-----------|
| 9.C.1 | Vertical Tail | 39 |
| 9.C.2 | Fuselage, Nacelles, and Stores | 40 |
| 9.C.3 | Propellers | 40 |
| 9.D | Estimating Sidewash | 40 |
| 9.E | Contributions to Roll Trim and Stability | 41 |
| 9.E.1 | Horizontal and Vertical Tail | 41 |
| 9.E.2 | Rudder | 41 |
| 9.F | Steady-Heading Sideslip | 42 |
| 9.G | Minimum-Control Airspeed | 42 |
| 10 | Equations of Motion | 43 |
| 10.A | Velocity Definitions | 43 |
| 10.B | Newton's Second Law | 43 |
| 10.C | Euler Angle Orientation | 44 |
| 10.D | 6-DOF Rigid-Body Equations of Motion Summary | 45 |
| 10.E | Linearized Equations of Motion | 46 |
| 10.E.1 | Linearized Longitudinal Equations | 47 |
| 10.E.2 | Linearized Lateral Equations | 48 |
| 10.F | Force and Moment Derivatives | 48 |
| 10.F.1 | Derivatives with respect to Velocity | 49 |
| 10.F.2 | Derivatives with respect to Rotation Rates | 50 |
| 10.F.3 | Derivatives with respect to Translational Acceleration | 50 |
| 10.F.4 | Derivatives with respect to Control Deflections | 51 |
| 10.G | Traditional Nondimensional Linearized Equations of Motion | 52 |
| 10.G.1 | Nondimensional Linearized Longitudinal Equations | 53 |
| 10.G.2 | Nondimensional Linearized Lateral Equations | 53 |
| 10.H | Transformation of Stability Axes | 53 |
| 11 | Linearized Dynamics | 55 |
| 11.A | Linearized Longitudinal Dynamics | 56 |
| 11.A.1 | Short-Period | 56 |
| 11.A.2 | Phugoid | 57 |
| 11.B | Linearized Lateral Dynamics | 58 |
| 11.B.1 | Roll Mode | 58 |
| 11.B.2 | Spiral Mode | 58 |
| 11.B.3 | Dutch Roll Approximation | 59 |
| 12 | Maneuverability | 60 |
| 12.A | Longitudinal Trim with a Pitch Rate | 60 |
| 12.B | Elevator Angle per g | 61 |
| 12.C | Dynamic Margin | 61 |
| 13 | Flight Simulation | 62 |
| 13.A | Flat-Earth Euler-Angle Formulation | 62 |
| 13.B | Euler Axis | 62 |
| 13.C | Euler-Rodriguez Quaternion | 63 |
| 13.D | Quaternion Algebra | 63 |
| 13.E | Relations to Other Attitude Descriptors | 64 |
| 13.E.1 | Euler Angles to Quaternion | 64 |
| 13.E.2 | Quaternion to Euler Angles | 64 |
| 13.F | Quaternion Renormalization | 65 |
| 13.F.1 | Exact Solution | 65 |
| 13.F.2 | Approximate Solution | 65 |
| 13.G | Flat-Earth Quaternion Formulation | 65 |
| 13.H | Geographic Coordinates | 65 |

| | |
|---|-----------|
| 13.H.1 Mean-Sea-Level Ellipsoid Approximation | 65 |
| 13.H.2 Spherical Earth Approximation | 66 |
| 14 Aerodynamic Coordinate Transformations | 68 |
| 14.A Traditional Aerodynamic Angles | 68 |
| 14.B Stability Coordinate System | 68 |
| 14.C Wind Coordinate System | 69 |
| 14.C.1 Velocity Components | 69 |
| 14.D Flank Angle | 69 |
| 14.E Aerodynamic Force Components | 70 |
| 14.F Aerodynamic Moment Components | 70 |
| 14.G Pseudo Aerodynamic Forces and Moments | 71 |
| 14.H Center of Gravity Movement | 72 |
| 15 Aerodynamic Models | 73 |
| 15.A Aerodynamic Model Below Stall | 73 |
| 15.B Aerodynamic Coefficient Estimation | 76 |
| 15.C Ground Effect | 76 |
| 15.C.1 Phillips and Hunsaker Model | 76 |
| 15.C.2 Application to a Typical Aerodynamic Model | 77 |
| 15.D Stall | 77 |
| 15.E Propulsion | 78 |
| 15.F Gust Modeling | 79 |
| 15.F.1 Damped Sinusoidal Gust Model | 80 |
| 15.F.2 von Kármán Atmospheric Turbulence Model | 80 |
| 15.F.3 Atmospheric Database | 81 |
| 16 Six-Degree-of-Freedom Static Trim | 82 |
| 16.A Governing Rigid-Body Equations of Motion | 82 |
| 16.B Climb Rate | 83 |
| 16.C Ground Track | 83 |
| 16.C.1 Given Bank Angle | 84 |
| 16.C.2 Given Heading Angle | 84 |
| 16.D Load Factor | 85 |
| 16.D.1 General Relation to Bank Angle | 85 |
| 16.D.2 Traditional Approximation | 85 |
| 16.E Steady-Coordinated Turn | 86 |
| 16.F Steady-Heading Sideslip | 86 |
| 16.G Vertical Barrel Roll | 86 |
| 16.H Solution Process | 87 |
| 16.H.1 Fixed-Point Iteration | 87 |
| 16.H.2 Newton's Method | 89 |

1. Basic Mathematical Properties

A. Cartesian Coordinates

$$\nabla\psi = \frac{\partial\psi}{\partial x}\mathbf{i}_x + \frac{\partial\psi}{\partial y}\mathbf{i}_y + \frac{\partial\psi}{\partial z}\mathbf{i}_z \quad (1.1)$$

$$\nabla \cdot \mathbf{V} = \frac{\partial V_x}{\partial x} + \frac{\partial V_y}{\partial y} + \frac{\partial V_z}{\partial z} \quad (1.2)$$

$$\nabla \times \mathbf{V} = \begin{vmatrix} \mathbf{i}_x & \mathbf{i}_y & \mathbf{i}_z \\ \frac{\partial}{\partial x} & \frac{\partial}{\partial y} & \frac{\partial}{\partial z} \\ V_x & V_y & V_z \end{vmatrix} \quad (1.3)$$

$$= \left(\frac{\partial V_z}{\partial y} - \frac{\partial V_y}{\partial z} \right) \mathbf{i}_x + \left(\frac{\partial V_x}{\partial z} - \frac{\partial V_z}{\partial x} \right) \mathbf{i}_y + \left(\frac{\partial V_y}{\partial x} - \frac{\partial V_x}{\partial y} \right) \mathbf{i}_z \quad (1.4)$$

$$\nabla^2\psi = \frac{\partial^2\psi}{\partial x^2} + \frac{\partial^2\psi}{\partial y^2} + \frac{\partial^2\psi}{\partial z^2} \quad (1.5)$$

$$\nabla^2\mathbf{V} = \left(\nabla^2 V_x \right) \mathbf{i}_x + \left(\nabla^2 V_y \right) \mathbf{i}_y + \left(\nabla^2 V_z \right) \mathbf{i}_z \quad (1.6)$$

B. Cylindrical Coordinates

$$\nabla\psi = \frac{\partial\psi}{\partial r}\mathbf{i}_r + \frac{1}{r}\frac{\partial\psi}{\partial\theta}\mathbf{i}_\theta + \frac{\partial\psi}{\partial z}\mathbf{i}_z \quad (1.7)$$

$$\nabla \cdot \mathbf{V} = \frac{1}{r}\frac{\partial(rV_r)}{\partial r} + \frac{1}{r}\frac{\partial V_\theta}{\partial\theta} + \frac{\partial V_z}{\partial z} = \frac{\partial V_r}{\partial r} + \frac{1}{r}\frac{\partial V_\theta}{\partial\theta} + \frac{\partial V_z}{\partial z} + \frac{V_r}{r} \quad (1.8)$$

$$\nabla \times \mathbf{V} = \begin{vmatrix} (1/r)\mathbf{i}_r & \mathbf{i}_\theta & (1/r)\mathbf{i}_z \\ \frac{\partial}{\partial r} & \frac{\partial}{\partial\theta} & \frac{\partial}{\partial z} \\ V_r & rV_\theta & V_z \end{vmatrix} \quad (1.9)$$

$$= \left(\frac{1}{r}\frac{\partial V_z}{\partial\theta} - \frac{\partial V_\theta}{\partial z} \right) \mathbf{i}_r + \left(\frac{\partial V_r}{\partial z} - \frac{\partial V_z}{\partial r} \right) \mathbf{i}_\theta + \left(\frac{\partial V_\theta}{\partial r} - \frac{1}{r}\frac{\partial V_r}{\partial\theta} + \frac{V_\theta}{r} \right) \mathbf{i}_z \quad (1.10)$$

$$\nabla^2\psi = \frac{1}{r}\frac{\partial}{\partial r} \left(r\frac{\partial\psi}{\partial r} \right) + \frac{1}{r^2}\frac{\partial^2\psi}{\partial\theta^2} + \frac{\partial^2\psi}{\partial z^2} = \frac{\partial^2\psi}{\partial r^2} + \frac{1}{r}\frac{\partial\psi}{\partial r} + \frac{1}{r^2}\frac{\partial^2\psi}{\partial\theta^2} + \frac{\partial^2\psi}{\partial z^2} \quad (1.11)$$

$$\nabla^2\mathbf{V} = \left(\nabla^2 V_r - \frac{V_r}{r^2} - \frac{2}{r^2}\frac{\partial V_\theta}{\partial\theta} \right) \mathbf{i}_r + \left(\nabla^2 V_\theta + \frac{2}{r^2}\frac{\partial V_r}{\partial\theta} - \frac{V_\theta}{r^2} \right) \mathbf{i}_\theta + \left(\nabla^2 V_z \right) \mathbf{i}_z \quad (1.12)$$

$$\mathbf{i}_r = \cos\theta\mathbf{i}_x + \sin\theta\mathbf{i}_y, \quad \mathbf{i}_\theta = -\sin\theta\mathbf{i}_x + \cos\theta\mathbf{i}_y, \quad \mathbf{i}_z = \mathbf{i}_z \quad (1.13)$$

C. Spherical Coordinates

$$\nabla\psi = \frac{\partial\psi}{\partial r}\mathbf{i}_r + \frac{1}{r}\frac{\partial\psi}{\partial\theta}\mathbf{i}_\theta + \frac{1}{r\sin\theta}\frac{\partial\psi}{\partial\varphi}\mathbf{i}_\varphi \quad (1.14)$$

$$\nabla \cdot \mathbf{V} = \frac{1}{r^2}\frac{\partial(r^2V_r)}{\partial r} + \frac{1}{r\sin\theta}\frac{\partial(V_\theta\sin\theta)}{\partial\theta} + \frac{1}{r\sin\theta}\frac{\partial V_\varphi}{\partial\varphi} = \frac{\partial V_r}{\partial r} + \frac{1}{r}\frac{\partial V_\theta}{\partial\theta} + \frac{1}{r\sin\theta}\frac{\partial V_\varphi}{\partial\varphi} + \frac{2V_r}{r} + \frac{V_\theta\cos\theta}{r\sin\theta} \quad (1.15)$$

$$\nabla \times \mathbf{V} = \begin{vmatrix} (1/r^2 \sin \theta) \mathbf{i}_r & (1/r \sin \theta) \mathbf{i}_\theta & (1/r) \mathbf{i}_z \\ \frac{\partial}{\partial r} & \frac{\partial}{\partial \theta} & \frac{\partial}{\partial \varphi} \\ V_r & rV_\theta & rV_\varphi \sin \theta \end{vmatrix} \quad (1.16)$$

$$= \left(\frac{1}{r} \frac{\partial V_\varphi}{\partial \theta} - \frac{1}{r \sin \theta} \frac{\partial V_\theta}{\partial \varphi} + \frac{V_\varphi \cos \theta}{r \sin \theta} \right) \mathbf{i}_r + \left(\frac{1}{r \sin \theta} \frac{\partial V_r}{\partial \varphi} - \frac{\partial V_\varphi}{\partial r} - \frac{V_\varphi}{r} \right) \mathbf{i}_\theta + \left(\frac{\partial V_\theta}{\partial r} - \frac{1}{r} \frac{\partial V_r}{\partial \theta} + \frac{V_\theta}{r} \right) \mathbf{i}_\varphi \quad (1.17)$$

$$\nabla^2 \psi = \frac{1}{r^2} \frac{\partial}{\partial r} \left(r^2 \frac{\partial \psi}{\partial r} \right) + \frac{1}{r^2 \sin \theta} \frac{\partial}{\partial \theta} \left(\sin \theta \frac{\partial \psi}{\partial \theta} \right) + \frac{1}{r^2 \sin^2 \theta} \frac{\partial^2 \psi}{\partial \varphi^2} \quad (1.18)$$

$$= \frac{\partial^2 \psi}{\partial r^2} + \frac{2}{r} \frac{\partial \psi}{\partial r} + \frac{1}{r^2} \frac{\partial^2 \psi}{\partial \theta^2} + \frac{\cos \theta}{r^2 \sin \theta} \frac{\partial \psi}{\partial \theta} + \frac{1}{r^2 \sin^2 \theta} \frac{\partial^2 \psi}{\partial \varphi^2} \quad (1.19)$$

$$\begin{aligned} \nabla^2 \mathbf{V} = & \left(\nabla^2 V_r - \frac{2V_r}{r^2} - \frac{2}{r^2} \frac{\partial V_\theta}{\partial \theta} - \frac{2V_\theta \cos \theta}{r^2 \sin \theta} - \frac{2}{r^2 \sin \theta} \frac{\partial V_\varphi}{\partial \varphi} \right) \mathbf{i}_r \\ & + \left(\nabla^2 V_\theta + \frac{2}{r^2} \frac{\partial V_r}{\partial \theta} - \frac{V_\theta}{r^2 \sin^2 \theta} - \frac{2 \cos \theta}{r^2 \sin^2 \theta} \frac{\partial V_\varphi}{\partial \varphi} \right) \mathbf{i}_\theta \\ & + \left(\nabla^2 V_\varphi + \frac{2}{r^2 \sin^2 \theta} \frac{\partial V_r}{\partial \varphi} - \frac{V_\varphi}{r^2 \sin^2 \theta} + \frac{2 \cos \theta}{r^2 \sin^2 \theta} \frac{\partial V_\theta}{\partial \varphi} \right) \mathbf{i}_\varphi \end{aligned} \quad (1.20)$$

$$\mathbf{i}_r = \sin \theta \cos \varphi \mathbf{i}_x + \sin \theta \sin \varphi \mathbf{i}_y + \cos \theta \mathbf{i}_z \quad (1.21)$$

$$\mathbf{i}_\theta = \cos \theta \cos \varphi \mathbf{i}_x + \cos \theta \sin \varphi \mathbf{i}_y - \sin \theta \mathbf{i}_z \quad (1.22)$$

$$\mathbf{i}_\varphi = -\sin \varphi \mathbf{i}_x + \cos \varphi \mathbf{i}_y \quad (1.23)$$

D. Useful Trigonometric Relations

$$\int \sin^2(\theta) d\theta = \frac{1}{2}\theta - \frac{1}{4} \sin(2\theta)$$

$$\int \sin^3(\theta) d\theta = -\frac{1}{3} \cos(\theta) [\sin^2(\theta) + 2]$$

$$\int \sin^n(\theta) d\theta = \frac{n-1}{n} \int \sin^{n-2}(\theta) d\theta - \frac{1}{n} \sin^{n-1}(\theta) \cos(\theta)$$

$$\int_0^\pi \sin(n\theta) \sin(m\theta) d\theta = 0, \text{ if } n, m = \text{integers and } n \neq m$$

$$\sin(\theta \pm \phi) = \sin(\theta) \cos(\phi) \pm \cos(\theta) \sin(\phi)$$

$$\sin(2\theta) = 2 \sin(\theta) \cos(\theta)$$

$$\int \cos^2(\theta) d\theta = \frac{1}{2}\theta + \frac{1}{4} \sin(2\theta)$$

$$\int \cos^3(\theta) d\theta = \frac{1}{3} \sin(\theta) [\cos^2(\theta) + 2]$$

$$\int \cos^n(\theta) d\theta = \frac{n-1}{n} \int \cos^{n-2}(\theta) d\theta + \frac{1}{n} \cos^{n-1}(\theta) \sin(\theta)$$

$$\int_0^\pi \cos(n\theta) \cos(m\theta) d\theta = 0, \text{ if } n, m = \text{integers and } n \neq m$$

$$\cos(\theta \pm \phi) = \cos(\theta) \cos(\phi) \mp \sin(\theta) \sin(\phi)$$

$$\cos(2\theta) = 2 \cos^2(\theta) - 1$$

2. Fundamentals of Fluids

A. Fundamental Equations

Conservation of Mass:

$$\frac{\partial \rho}{\partial t} + \mathbf{V} \cdot \nabla \rho + \rho \nabla \cdot \mathbf{V} = 0 \quad (2.1)$$

Euler Equations:

$$\rho \left[\frac{\partial \mathbf{V}}{\partial t} + (\mathbf{V} \cdot \nabla) \mathbf{V} \right] = -\nabla p - \rho g \nabla H \quad (2.2)$$

Vorticity:

$$\boldsymbol{\Omega} = \nabla \times \mathbf{V} \quad (2.3)$$

Circulation:

$$\Gamma \equiv - \oint_C \mathbf{V} \cdot d\mathbf{s} \quad (2.4)$$

Net Volume Outflow:

$$\Lambda \equiv \oint_C \mathbf{V} \cdot \mathbf{n} ds \quad (2.5)$$

Velocity Potential:

$$\mathbf{V} = \nabla \phi \quad (2.6)$$

Laplace's Equation:

$$\nabla^2 \phi = 0 \quad (2.7)$$

Bernoulli's Equation:

$$\frac{1}{2} V^2 + \frac{p}{\rho} + gH = C \quad (2.8)$$

Pressure Coefficient:

$$C_p \equiv \frac{p - p_\infty}{\frac{1}{2} \rho V_\infty^2} = 1 - \left(\frac{V}{V_\infty} \right)^2 \quad (2.9)$$

Stagnation Pressure:

$$\text{stagnation pressure} \equiv p_0 = p_\infty + \frac{1}{2} \rho V_\infty^2 \quad (2.10)$$

B. Fluid Properties

Temperature:

$${}^\circ\text{K} \equiv {}^\circ\text{C} + 273.150 \quad (2.11)$$

$${}^\circ\text{F} \equiv 1.8({}^\circ\text{C}) + 32.0 \quad (2.12)$$

$${}^\circ\text{R} \equiv {}^\circ\text{F} + 459.670 \quad (2.13)$$

Density of an Ideal Gas:

$$\rho = \frac{p}{RT} \quad (2.14)$$

Speed of Sound:

$$a = \sqrt{\gamma RT} \quad (2.15)$$

Sutherland's equation for the dynamic viscosity of atmospheric air:

$$\mu = 1.7153 \times 10^{-5} \frac{\text{kg}}{\text{m} \cdot \text{s}} \left(\frac{T}{273\text{K}} \right)^{3/2} \frac{383.4\text{K}}{T + 110.4\text{K}} \quad (2.16)$$

Kinematic Viscosity:

$$\nu \equiv \frac{\mu}{\rho} \quad (2.17)$$

C. Dimensionless Numbers

Mach Number:

$$M \equiv \frac{V}{a} \quad (2.18)$$

Knudsen Number:

$$K_n \equiv \frac{\lambda}{d} \quad (2.19)$$

Reynolds Number:

$$R_e \equiv \frac{\rho V d}{\mu} \quad (2.20)$$

D. The Standard Atmosphere

The relations in this section will first be given in terms of SI units. At the end of this section, a method for converting the solutions to English units is included.

1. Gravity

Gravity as a function of altitude can be computed from

$$g = g_o \left(\frac{R_E}{R_E + H} \right)^2 \quad (2.21)$$

where $g_o = 9.806645 \text{ [m/s}^2\text{]}$ and the mean radius of the earth at sea level is $R_E = 6,356,766 \text{ [m]}$.

2. Geopotential Altitude

The geopotential altitude can be computed from

$$Z \equiv \frac{R_E H}{R_E + H} \quad (2.22)$$

3. Pressure and Temperature

The pressure variation with altitude assuming a static ideal fluid is

$$\frac{dp}{dz} = -\frac{g_o p}{RT} \quad (2.23)$$

where $R = 287.052874 \text{ [J/(kg K)]}$ is the gas constant for dry air. For the standard atmosphere, the temperature is modeled to vary linearly within set ranges of geopotential altitude defined in Table 2.1. The temperature at any geopotential altitude can be found from

$$T(Z) = T(Z_i) + T'_i(Z - Z_i) \quad (2.24)$$

where Z falls in the range

$$Z_i \leq Z < Z_{i+1} \quad (2.25)$$

Table 2.1 Temperature variation with geopotential altitude for the standard atmosphere.

| $Z_i \text{ (m)}$ | $Z_{i+1} \text{ (m)}$ | $T_i \text{ (K)}$ | $T'_i \text{ (K/km)}$ |
|-------------------|-----------------------|-------------------|-----------------------|
| 0 | 11,000 | 288.150 | -6.5 |
| 11,000 | 20,000 | 216.650 | 0.0 |
| 20,000 | 32,000 | 216.650 | 1.0 |
| 32,000 | 47,000 | 228.650 | 2.8 |
| 47,000 | 52,000 | 270.650 | 0.0 |
| 52,000 | 61,000 | 270.650 | -2.0 |
| 61,000 | 79,000 | 252.650 | -4.0 |
| 79,000 | 90,000 | 180.650 | 0.0 |

The pressure at any geopotential altitude can be obtained from the integral of Eq. (2.25)

$$p(Z) = \begin{cases} p_i \exp \left[-\frac{g_o(Z-Z_i)}{RT_i} \right], & T'_i = 0 \\ p_i \left[\frac{T_i + T'_i(Z-Z_i)}{T_i} \right]^{-\frac{g_o}{RT'_i}}, & T'_i \neq 0 \end{cases} \quad (2.26)$$

where the pressure at sea level is $p = 101,325$ [Pa].

4. Density and Speed of Sound

Once the pressure and temperature have been obtained, the density can be estimated from the ideal gas relation

$$\rho = \frac{p}{RT} \quad (2.27)$$

The speed of sound can be computed from

$$a = \sqrt{\gamma RT} \quad (2.28)$$

where $\gamma = 1.4$ for dry air.

5. Dynamic Viscosity

The dynamic viscosity can be estimated using Sutherland's Law according to the relation

$$\mu = \mu_0 \left(\frac{T_0 + C_S}{T + C_S} \right) \left(\frac{T}{T_0} \right)^{3/2} \quad (2.29)$$

where $T_0 = 273.15$ [K], $\mu_0 = 0.00001716$ [kg/(m-s)], and $C_S = 110.4$ is Sutherland's constant for air.

6. English Units

If a function is constructed using the atmospheric properties in SI units listed above, these properties can be translated to English units using the conversion factors shown in Table 2.2.

Table 2.2 SI units to English units conversion factors.

| Parameter | SI Units | Conversion | English Units |
|-------------------|-------------------|-------------------------|----------------------|
| Length | m | /0.3048 = | ft |
| Temperature | K | *1.8 = | R |
| Pressure | N/m ² | *0.020885434304801722 = | lbf/ft ² |
| Density | kg/m ³ | *0.00194032032363104 = | slug/ft ³ |
| Dynamic Viscosity | kg/(m-s) | /47.88025898 = | slug/(ft-s) |

3. Potential Flow Solutions

A. Uniform Flow

$$\phi(r, \theta) = V_\infty r \cos(\theta - \alpha) \quad (3.1)$$

$$\mathbf{V}(r, \theta, z) = \nabla \phi = V_\infty [\cos(\theta - \alpha) \mathbf{i}_r - \sin(\theta - \alpha) \mathbf{i}_\theta + 0 \mathbf{i}_z] \quad (3.2)$$

B. Incompressible Line Source

$$\phi(r, \theta) = \frac{\Lambda}{2\pi} \ln r \quad (3.3)$$

$$\mathbf{V}(r, \theta, z) = \nabla \phi = \frac{\Lambda}{2\pi r} \mathbf{i}_r + 0 \mathbf{i}_\theta + 0 \mathbf{i}_z \quad (3.4)$$

C. Incompressible Point Source

$$\phi(r, \theta) = -\frac{Q}{4\pi r} \quad (3.5)$$

$$\mathbf{V}(r, \theta, \varphi) = \nabla \phi = \frac{Q}{4\pi r^2} \mathbf{i}_r + 0 \mathbf{i}_\theta + 0 \mathbf{i}_\varphi \quad (3.6)$$

D. Incompressible Line Vortex

$$\phi(r, \theta) = -\frac{\Gamma}{2\pi} \theta \quad (3.7)$$

$$\mathbf{V}(r, \theta, z) = \nabla \phi = 0 \mathbf{i}_r - \frac{\Gamma}{2\pi r} \mathbf{i}_\theta + 0 \mathbf{i}_z \quad (3.8)$$

E. Incompressible Line Doublet

$$\phi(r, \theta) = \frac{\kappa}{2\pi} \frac{\cos(\theta - \alpha)}{r} \quad (3.9)$$

$$\mathbf{V}(r, \theta, z) = \nabla \phi = -\frac{\kappa}{2\pi} \frac{\cos(\theta - \alpha)}{r^2} \mathbf{i}_r - \frac{\kappa}{2\pi} \frac{\sin(\theta - \alpha)}{r^2} \mathbf{i}_\theta + 0 \mathbf{i}_z \quad (3.10)$$

F. Incompressible Circular Cylinder with Circulation

$$\phi(r, \theta) = V_\infty \left(r + \frac{R^2}{r} \right) \cos \theta - \frac{\Gamma}{2\pi} \theta \quad (3.11)$$

$$\mathbf{V}(r, \theta, z) = \nabla \phi = V_\infty \left(1 - \frac{R^2}{r^2} \right) \cos \theta \mathbf{i}_r - \left[V_\infty \left(1 + \frac{R^2}{r^2} \right) \sin \theta + \frac{\Gamma}{2\pi r} \right] \mathbf{i}_\theta + 0 \mathbf{i}_z \quad (3.12)$$

G. Incompressible Source Panel

$$\begin{Bmatrix} V_x \\ V_y \end{Bmatrix} = \frac{1}{2\pi l} \begin{bmatrix} [-y\Phi + (l-x)\Psi + l] & (y\Phi + x\Psi - l) \\ [(l-x)\Phi + y\Psi] & (x\Phi - y\Psi) \end{bmatrix} \begin{Bmatrix} \lambda_1 \\ \lambda_2 \end{Bmatrix} \quad (3.13)$$

$$\Phi = \text{atan2}(yl, y^2 + x^2 - xl) \quad (3.14)$$

$$\Psi = \frac{1}{2} \ln \left[\frac{x^2 + y^2}{(x - l)^2 + y^2} \right] \quad (3.15)$$

H. Incompressible Vortex Panel

$$\begin{Bmatrix} V_x \\ V_y \end{Bmatrix} = \frac{1}{2\pi l} \begin{bmatrix} [(l-x)\Phi + y\Psi] & (x\Phi - y\Psi) \\ [y\Phi - (l-x)\Psi - l] & (-y\Phi - x\Psi + l) \end{bmatrix} \begin{Bmatrix} \gamma_1 \\ \gamma_2 \end{Bmatrix} \quad (3.16)$$

$$\Phi = \text{atan2}(yl, y^2 + x^2 - xl) \quad (3.17)$$

$$\Psi = \frac{1}{2} \ln \left[\frac{x^2 + y^2}{(x - l)^2 + y^2} \right] \quad (3.18)$$

I. Kutta-Joukowski Law

$$\tilde{L} = \rho V_\infty \Gamma \quad (3.19)$$

4. Airfoil Theory

A. Airfoil Geometry

The upper and lower surface of an airfoil can be obtained from

$$x_u(x) = x - \frac{t(x)}{2\sqrt{1 + (dy_c/dx)^2}} \frac{dy_c}{dx} \quad (4.1)$$

$$y_u(x) = y_c(x) + \frac{t(x)}{2\sqrt{1 + (dy_c/dx)^2}} \quad (4.2)$$

$$x_l(x) = x + \frac{t(x)}{2\sqrt{1 + (dy_c/dx)^2}} \frac{dy_c}{dx} \quad (4.3)$$

$$y_l(x) = y_c(x) - \frac{t(x)}{2\sqrt{1 + (dy_c/dx)^2}} \quad (4.4)$$

where the camber line and thickness distribution are given. The camber line and thickness distribution for the NACA 4-digit series is

$$y_c(x) = \begin{cases} y_{mc} \left[2 \left(\frac{x}{x_{mc}} \right) - \left(\frac{x}{x_{mc}} \right)^2 \right], & 0 \leq x \leq x_{mc} \\ y_{mc} \left[2 \left(\frac{c-x}{c-x_{mc}} \right) - \left(\frac{c-x}{c-x_{mc}} \right)^2 \right], & x_{mc} \leq x \leq c \end{cases} \quad (4.5)$$

$$t(x) = t_m \left[2.969 \sqrt{\frac{x}{c}} - 1.260 \left(\frac{x}{c} \right) - 3.516 \left(\frac{x}{c} \right)^2 + 2.843 \left(\frac{x}{c} \right)^3 - 1.015 \left(\frac{x}{c} \right)^4 \right] \quad (4.6)$$

B. Thin Airfoil Theory

The fundamental equation for thin airfoil theory at small angles of attack is

$$\frac{1}{2\pi} \int_{x_o=0}^c \frac{\gamma(x_o)}{x - x_o} dx_o = V_\infty \left(\alpha - \frac{dy_c}{dx} \right) \quad (4.7)$$

where the only unknown is the vortex-strength distribution $\gamma(x_o)$. Any solution for $\gamma(x_o)$ that satisfies the fundamental equation will make the camber line of the airfoil a streamline of the flow. We seek a solution that also satisfies the Kutta condition

$$\gamma(c) = 0 \quad (4.8)$$

To find a solution, we apply the change of variables

$$x = \frac{c}{2}(1 - \cos \theta) \quad (4.9)$$

and assume a solution that takes the form of an infinite sine series

$$\gamma(\theta_o) = 2V_\infty \left(A_0 \frac{1 + \cos \theta_o}{\sin \theta_o} + \sum_{j=1}^{\infty} A_j \sin(j\theta_o) \right) \quad (4.10)$$

Using this infinite series in the fundamental equation produces the following series coefficients

$$A_0 = \alpha - \frac{1}{\pi} \int_{\theta=0}^{\pi} \frac{dy_c}{dx} d\theta \quad (4.11)$$

$$A_j = \frac{2}{\pi} \int_{\theta=0}^{\pi} \frac{dy_c}{dx} \cos(j\theta) d\theta \quad (4.12)$$

The resulting lift coefficient is

$$\tilde{C}_L \equiv \frac{\tilde{L}}{\frac{1}{2}\rho V_\infty^2 c} = 2\pi \left(A_0 + \frac{1}{2}A_1 \right) = 2\pi \left(\alpha - \frac{1}{\pi} \int_{\theta=0}^{\pi} \frac{dy_c}{dx} (1 - \cos \theta) d\theta \right) = 2\pi (\alpha - \alpha_{L0}) \quad (4.13)$$

where

$$\alpha_{L0} = \frac{1}{\pi} \int_{\theta=0}^{\pi} \frac{dy_c}{dx} (1 - \cos \theta) d\theta \quad (4.14)$$

The pitching moment about the leading edge is

$$\tilde{C}_{m_{le}} = -\frac{\tilde{C}_L}{4} + \frac{\pi}{4} (A_2 - A_1) = -\frac{\tilde{C}_L}{4} + \frac{1}{2} \int_{\theta=0}^{\pi} \frac{dy_c}{dx} [\cos(2\theta) - \cos \theta] d\theta = -\frac{\tilde{C}_L}{4} + \tilde{C}_{m_{c/4}} \quad (4.15)$$

The pitching moment about the quarter chord is

$$\tilde{C}_{m_{c/4}} = \tilde{C}_{m_{le}} + \frac{\tilde{C}_L}{4} = \frac{\pi}{4} (A_2 - A_1) = \frac{1}{2} \int_{\theta=0}^{\pi} \frac{dy_c}{dx} [\cos(2\theta) - \cos \theta] d\theta \quad (4.16)$$

The location of the center of pressure is

$$\frac{x_{cp}}{c} = \frac{1}{4} + \frac{\pi}{4\tilde{C}_L} (A_1 - A_2) = \frac{1}{4} + \frac{1}{2\tilde{C}_L} \int_{\theta=0}^{\pi} \frac{dy_c}{dx} [\cos \theta - \cos(2\theta)] d\theta \quad (4.17)$$

C. Parabolic Flaps

A special type of flap which deflects in a parabolic shape has increased flap efficiency. The ideal flap effectiveness for this type of flap is given by

$$\varepsilon_{fi} = \frac{(1 + 2 \cos \theta_f)(\pi - \theta_f) + \sin \theta_f (2 + \cos \theta_f)}{\pi(1 + \cos \theta_f)} \quad (4.18)$$

D. Vortex Panel Method

Using the change of variables given in Eq. (4.9), an even number of nodes (corners of the panels) can be specified along the airfoil using

$$\delta\theta = \frac{2\pi}{n-1} \quad (4.19)$$

$$\begin{Bmatrix} x_N(n/2+i) \\ y_N(n/2+i) \\ x_N(n/2+1-i) \\ y_N(n/2+1-i) \end{Bmatrix} = \begin{Bmatrix} x_u \\ y_u \\ x_l \\ y_l \end{Bmatrix}, \quad \frac{x}{c} = 0.5 \{ 1. - \cos [(i - 0.5)\delta\theta] \}, \quad i = 1, n/2 \quad (4.20)$$

The control points are located using

$$\begin{Bmatrix} x_c(i) \\ y_c(i) \end{Bmatrix} = \begin{Bmatrix} \frac{x_N(i) + x_N(i+1)}{2} \\ \frac{y_N(i) + y_N(i+1)}{2} \end{Bmatrix}, \quad i = 1, n-1 \quad (4.21)$$

The Kutta Condition is enforced at the trailing edge by requiring

$$\gamma_1 + \gamma_n = 0 \quad (4.22)$$

The influence of a single panel extending from node (x_j, y_j) to node (x_{j+1}, y_{j+1}) on a point located at (x, y) can be computed from

$$l_j = \sqrt{(x_{j+1} - x_j)^2 + (y_{j+1} - y_j)^2} \quad (4.23)$$

$$\begin{Bmatrix} \xi \\ \eta \end{Bmatrix} = \frac{1}{l_j} \begin{bmatrix} (x_{j+1} - x_j) & (y_{j+1} - y_j) \\ -(y_{j+1} - y_j) & (x_{j+1} - x_j) \end{bmatrix} \begin{Bmatrix} (x - x_j) \\ (y - y_j) \end{Bmatrix} \quad (4.24)$$

$$\Phi = \text{atan2}(\eta l_j, \eta^2 + \xi^2 - \xi l_j) \quad (4.25)$$

$$\Psi = \frac{1}{2} \ln \left[\frac{\xi^2 + \eta^2}{(\xi - l_j)^2 + \eta^2} \right] \quad (4.26)$$

$$[\mathbf{P}]_{j(x,y)} = \frac{1}{2\pi l_j^2} \begin{bmatrix} (x_{j+1} - x_j) & -(y_{j+1} - y_j) \\ (y_{j+1} - y_j) & (x_{j+1} - x_j) \end{bmatrix} \begin{bmatrix} [(l_j - \xi)\Phi + \eta\Psi] & (\xi\Phi - \eta\Psi) \\ [\eta\Phi - (l_j - \xi)\Psi - l_j] & (-\eta\Phi - \xi\Psi + l_j) \end{bmatrix} \quad (4.27)$$

With these definitions, the coefficient matrix $[A]$ is constructed by computing the influence of every j th panel on every i th point. This can be constructed from the algorithm

$$A_{ij} = 0.0, \quad i = 1, n; \quad j = 1, n \quad (4.28)$$

$$\begin{aligned} A_{ij} &= A_{ij} + \frac{x_{i+1} - x_i}{l_i} P_{21ji} - \frac{y_{i+1} - y_i}{l_i} P_{11ji} \\ A_{ij+1} &= A_{ij+1} + \frac{x_{i+1} - x_i}{l_i} P_{22ji} - \frac{y_{i+1} - y_i}{l_i} P_{12ji} \end{aligned} \quad i = 1, n-1; \quad j = 1, n-1 \quad (4.29)$$

$$A_{nn} = 1.0 \quad (4.30)$$

$$A_{nn} = 1.0 \quad (4.31)$$

The vortex strength at each node is then computed by solving the system of equations

$$[\mathbf{A}] \begin{Bmatrix} \gamma_1 \\ \gamma_2 \\ \vdots \\ \gamma_{n-1} \\ \gamma_n \end{Bmatrix} = V_\infty \begin{Bmatrix} [(y_2 - y_1) \cos \alpha - (x_2 - x_1) \sin \alpha]/l_1 \\ [(y_3 - y_2) \cos \alpha - (x_3 - x_2) \sin \alpha]/l_2 \\ \vdots \\ [(y_n - y_{n-1}) \cos \alpha - (x_n - x_{n-1}) \sin \alpha]/l_{n-1} \\ 0.0 \end{Bmatrix} \quad (4.32)$$

The velocity and pressure at any point in space can be computed by

$$\begin{Bmatrix} V_x \\ V_y \end{Bmatrix} = V_\infty \begin{Bmatrix} \cos \alpha \\ \sin \alpha \end{Bmatrix} + \sum_{i=1}^{n-1} [\mathbf{P}]_{i(x,y)} \begin{Bmatrix} \gamma_i \\ \gamma_{i+1} \end{Bmatrix} \quad (4.33)$$

$$V^2 = V_x^2 + V_y^2 \quad (4.34)$$

$$C_p \equiv \frac{p - p_\infty}{\frac{1}{2}\rho V_\infty^2} = 1 - \frac{V^2}{V_\infty^2} \quad (4.35)$$

The section lift and pitching-moment coefficients can be computed from the know vortex strengths from

$$\tilde{C}_L = \sum_{i=1}^{n-1} \frac{l_i}{c} \frac{\gamma_i + \gamma_{i+1}}{V_\infty} \quad (4.36)$$

$$\tilde{C}_{mle} = -\frac{1}{3} \sum_{i=1}^{n-1} \frac{l_i}{c} \left[\frac{2x_i \gamma_i + x_i \gamma_{i+1} + x_{i+1} \gamma_i + 2x_{i+1} \gamma_{i+1}}{c V_\infty} \cos \alpha + \frac{2y_i \gamma_i + y_i \gamma_{i+1} + y_{i+1} \gamma_i + 2y_{i+1} \gamma_{i+1}}{c V_\infty} \sin \alpha \right] \quad (4.37)$$

5. Two-Dimensional Conformal Mapping

A. Fundamental Concepts

The complex velocity potential is

$$\Phi = \phi + i\psi \quad (5.1)$$

The Cauchy-Riemann conditions in Cartesian coordinates are

$$\frac{\partial f_r}{\partial x} = \frac{\partial f_i}{\partial y} \quad (5.2)$$

$$\frac{\partial f_i}{\partial x} = -\frac{\partial f_r}{\partial y} \quad (5.3)$$

The Cauchy-Riemann conditions in polar coordinates are

$$\frac{\partial f_r}{\partial r} = \frac{1}{r} \frac{\partial f_i}{\partial \theta} \quad (5.4)$$

$$\frac{\partial f_i}{\partial r} = -\frac{1}{r} \frac{\partial f_r}{\partial \theta} \quad (5.5)$$

The complex velocity potential satisfies the Cauchy-Riemann conditions. Therefore, Φ is an analytic function of $z = x + iy$. The complex velocity is

$$w(z) \equiv \frac{d\Phi}{dz} = \frac{\partial \phi}{\partial x} + i \frac{\partial \psi}{\partial x} = \frac{\partial \psi}{\partial y} - i \frac{\partial \phi}{\partial y} = V_x - iV_y \quad (5.6)$$

B. Elementary Potential Flows

1. Uniform Flow

$$\Phi(z) = V_\infty(\cos \alpha - i \sin \alpha)z + C \quad (5.7)$$

$$w(z) = \frac{d\Phi}{dz} = V_\infty(\cos \alpha - i \sin \alpha) \quad (5.8)$$

2. Source Flow

$$\Phi(z) = \frac{\Lambda}{2\pi} \ln z + C \quad (5.9)$$

$$w(z) = \frac{d\Phi}{dz} = \frac{\Lambda}{2\pi z} \quad (5.10)$$

3. Vortex Flow

$$\Phi(z) = i \frac{\Gamma}{2\pi} \ln z + C \quad (5.11)$$

$$w(z) = \frac{d\Phi}{dz} = i \frac{\Gamma}{2\pi z} \quad (5.12)$$

4. Doublet Flow

$$\Phi(z) = \frac{\kappa}{2\pi z} + C \quad (5.13)$$

$$w(z) = \frac{d\Phi}{dz} = -\frac{\kappa}{2\pi z^2} \quad (5.14)$$

5. Flow over a Circular Cylinder with Circulation

$$\Phi(z) = V_\infty \left[z e^{-i\alpha} + i \frac{\Gamma}{2\pi V_\infty} \ln(z - z_0) + \frac{R^2 e^{i\alpha}}{z - z_0} \right] + C \quad (5.15)$$

$$w(z) = \frac{d\Phi}{dz} = V_\infty \left[e^{-i\alpha} + i \frac{\Gamma}{2\pi V_\infty} \frac{1}{z - z_0} - \frac{R^2 e^{i\alpha}}{(z - z_0)^2} \right] \quad (5.16)$$

6. Body of Arbitrary Cross Section

$$\Phi(z) = V_\infty z e^{-i\alpha} + A_1 \ln z - \sum_{j=2}^{\infty} \frac{A_j}{j-1} \frac{1}{z^{j-1}} + C \quad (5.17)$$

$$w(z) = \frac{d\Phi}{dz} = V_\infty e^{-i\alpha} + \sum_{j=1}^{\infty} \frac{A_j}{z^j} \quad (5.18)$$

C. Blasius Relations

1. Complex Section Force

$$\tilde{A} - i\tilde{N} = i \frac{1}{2} \rho \oint_C [w(z)]^2 dz \quad (5.19)$$

2. Section Pitching Moment

$$\tilde{m}_0 = \frac{1}{2} \rho \operatorname{real} \left\{ \oint_C [w(z)]^2 z dz \right\} \quad (5.20)$$

D. Kutta-Joukowski Law

Flow over an arbitrary cross section

$$w(z) = V_\infty e^{-i\alpha} + \frac{\Lambda + i\Gamma}{2\pi z} + \sum_{n=2}^{\infty} \frac{A_n}{z^n} \quad (5.21)$$

Resulting Forces

$$\tilde{A} - i\tilde{N} = -\rho V_\infty e^{-i\alpha} (\Lambda + i\Gamma) \quad (5.22)$$

$$\tilde{L} = \rho V_\infty \Gamma \quad \text{and} \quad \tilde{D} = 0 \quad (5.23)$$

Resulting Moment

$$\tilde{m}_0 = \pi \rho \operatorname{real} \left\{ i \left[\frac{(\Lambda + i\Gamma)^2}{4\pi^2} + 2V_\infty e^{-i\alpha} A_2 \right] \right\} \quad (5.24)$$

E. Conformal Transformations

Definition

$$\Phi_2(z) = \Phi_1[\zeta(z)] \quad (5.25)$$

F. Joukowski Cylinders and Airfoils

1. Joukowski Transformation

$$z = \zeta + \frac{(R - \varepsilon)^2}{\zeta} \quad \text{or} \quad \zeta = \frac{z \pm \sqrt{z^2 - 4(R - \varepsilon)^2}}{2} \quad (5.26)$$

2. Joukowski Cylinder

$$\Phi(z) = V_\infty \left[\zeta e^{-i\alpha} + i \frac{\Gamma}{2\pi V_\infty} \ln(\zeta - z_0) + R^2 e^{i\alpha} \frac{1}{\zeta - z_0} \right] + C \quad (5.27)$$

$$w(z) = V_\infty \left[e^{-i\alpha} + i \frac{\Gamma}{2\pi V_\infty} \frac{1}{\zeta - z_0} - R^2 e^{i\alpha} \frac{1}{(\zeta - z_0)^2} \right] \Bigg/ \left[1 - \frac{(R - \varepsilon)^2}{\zeta^2} \right] \quad (5.28)$$

3. Joukowski Airfoils

$$\varepsilon = R - \sqrt{R^2 - \eta_0^2} - \xi_0 \quad (5.29)$$

$$z_t = 2 \left(\sqrt{R^2 - \eta_0^2} + \xi_0 \right) \quad (5.30)$$

$$z_l = -2 \frac{R^2 - \eta_0^2 + \xi_0^2}{\sqrt{R^2 - \eta_0^2} - \xi_0} \quad (5.31)$$

$$z_t - z_l = 4 \frac{R^2 - \eta_0^2}{\sqrt{R^2 - \eta_0^2} - \xi_0} \quad (5.32)$$

$$\Gamma = 4\pi V_\infty \left(\sqrt{R^2 - \eta_0^2} \sin \alpha + \eta_0 \cos \alpha \right) \quad (5.33)$$

$$\tilde{L} = \rho V_\infty \Gamma = 4\pi \rho V_\infty^2 \left(\sqrt{R^2 - \eta_0^2} \sin \alpha + \eta_0 \cos \alpha \right) \quad (5.34)$$

$$\tilde{C}_L = \frac{\tilde{L}}{\frac{1}{2} \rho V_\infty^2 (z_t - z_l)} = 2\pi \frac{\sin \alpha + \eta_0 \cos \alpha / \sqrt{R^2 - \eta_0^2}}{1 + \xi_0 / \left(\sqrt{R^2 - \eta_0^2} - \xi_0 \right)} \quad (5.35)$$

$$\tilde{C}_{L,\alpha} = \frac{2\pi}{1 + \xi_0 / \left(\sqrt{R^2 - \eta_0^2} - \xi_0 \right)} \quad (5.36)$$

$$\alpha_{L0} = -\tan^{-1} \left(\eta_0 / \sqrt{R^2 - \eta_0^2} \right) \quad (5.37)$$

$$\tilde{C}_{m_z} = \frac{\pi}{4} \left(\frac{R^2 - \eta_0^2 - \xi_0^2}{R^2 - \eta_0^2} \right)^2 \sin 2\alpha + \frac{1}{4} \tilde{C}_L \frac{(x - \xi_0) \cos \alpha + (y - \eta_0) \sin \alpha}{R^2 - \eta_0^2} \left(\sqrt{R^2 - \eta_0^2} - \xi_0 \right) \quad (5.38)$$

6. Lifting-Line Theory

A. Classical Development

The fundamental lifting-line equation is

$$\frac{2\Gamma(z)}{V_\infty c(z)} + \frac{\tilde{C}_{L,\alpha}}{4\pi V_\infty} \int_{\zeta=-b/2}^{b/2} \frac{1}{z-\zeta} \left(\frac{d\Gamma}{dz} \right)_{z=\zeta} d\zeta = \tilde{C}_{L,\alpha} [\alpha(z) - \alpha_{L0}(z)] \quad (6.1)$$

We assume a circulation distribution that can be written in terms of a Fourier sine series

$$\Gamma(\theta) = 2bV_\infty \sum_{j=1}^N A_j \sin(j\theta) \quad (6.2)$$

with the change of variables given by

$$\theta = \cos^{-1}(-2z/b) \quad (6.3)$$

The Fourier coefficients are found by satisfying Eq. (1) at N locations along the wing. This results in the system of equations

$$\sum_{j=1}^N A_j \left[\frac{4b}{\tilde{C}_{L,\alpha} c(\theta)} + \frac{j}{\sin(\theta)} \right] \sin(j\theta) = \alpha(\theta) - \alpha_{L0}(\theta) \quad (6.4)$$

where the right-hand side depends only on the combination of geometric and aerodynamic twist as a function of spanwise location. When rolling rate is included, the resulting integrated forces and moments can be computed from the Fourier coefficients

$$C_L = \pi R_A A_1 \quad (6.5)$$

$$C_{D_i} = \left[\pi R_A \sum_{j=1}^N j A_j^2 \right] - \frac{\pi R_A \bar{p}}{2} A_2 \quad (6.6)$$

$$C_\ell = -\frac{\pi R_A}{4} A_2 \quad (6.7)$$

$$C_n = \left[\frac{\pi R_A}{4} \sum_{j=2}^N (2j-1) A_{j-1} A_j \right] - \frac{\pi R_A \bar{p}}{8} (A_1 + A_3) \quad (6.8)$$

where the wing aspect ratio is defined as

$$R_A \equiv \frac{b^2}{S} = \frac{b}{c} \quad (6.9)$$

B. Decomposed Fourier Solution

Phillips published a decomposed Fourier sine series development of the classical lifting-line theory that can be used to evaluate the influence of planform, twist, and roll rate on the resulting forces and moments. In this development, the Fourier coefficients are a summation of the decomposed Fourier coefficients

$$A_j = a_j (\alpha - \alpha_{L0})_{\text{root}} - b_j \Omega + c_j \delta_a + d_j \bar{p} \quad (6.10)$$

where Ω is the washout amount, δ_a is the aileron deflection, and \bar{p} is the dimensionless rolling rate defined as $\bar{p} = pb/2V_\infty$. The decomposed Fourier coefficients can be computed from the planform distribution $c(\theta)$, the washout distribution $\omega(\theta)$, aileron distribution $\chi(\theta)$, and linear change in angle of attack due to rolling rate $\cos(\theta)$

$$\sum_{j=1}^N a_j \left[\frac{4b}{\tilde{C}_{L,\alpha} c(\theta)} + \frac{j}{\sin(\theta)} \right] \sin(j\theta) = 1 \quad (6.11)$$

$$\sum_{j=1}^N b_j \left[\frac{4b}{\tilde{C}_{L,\alpha} c(\theta)} + \frac{j}{\sin(\theta)} \right] \sin(j\theta) = \omega(\theta) \quad (6.12)$$

$$\sum_{j=1}^N c_j \left[\frac{4b}{\tilde{C}_{L,\alpha} c(\theta)} + \frac{j}{\sin(\theta)} \right] \sin(j\theta) = \chi(\theta) \quad (6.13)$$

$$\sum_{j=1}^N d_j \left[\frac{4b}{\tilde{C}_{L,\alpha} c(\theta)} + \frac{j}{\sin(\theta)} \right] \sin(j\theta) = \cos(\theta) \quad (6.14)$$

Once the decomposed Fourier coefficients have been computed, the integrated forces and moments on the wing can be computed by evaluating the Fourier coefficients given in Eq. (10) and using these in Eqs. (5-8).

For the special case of **steady level flight when the aileron deflection and rolling rate are zero**, the induced-drag coefficient can be computed from

$$C_{D_i} = \frac{C_L^2(1 + \kappa_D) - \kappa_{DL} C_L C_{L,\alpha} \Omega + \kappa_{D\Omega} (C_{L,\alpha} \Omega)^2}{\pi R_A} \quad (6.15)$$

where

$$\kappa_D \equiv \sum_{j=2}^N j \frac{a_j^2}{a_1^2} \quad (6.16)$$

$$\kappa_{DL} \equiv 2 \frac{b_1}{a_1} \sum_{j=2}^N j \frac{a_j}{a_1} \left(\frac{b_j}{b_1} - \frac{a_j}{a_1} \right) \quad (6.17)$$

$$\kappa_{D\Omega} \equiv \left(\frac{b_1}{a_1} \right)^2 \sum_{j=2}^N j \left(\frac{b_j}{b_1} - \frac{a_j}{a_1} \right)^2 \quad (6.18)$$

For the special case when the **wing planform and washout distribution are both symmetric, and when the aileron distribution and effects of rolling rate are antisymmetric**, the lift can be computed from

$$C_L = C_{L,\alpha} [(\alpha - \alpha_{L0})_{\text{root}} - \varepsilon_\Omega \Omega] \quad (6.19)$$

where

$$C_{L,\alpha} = \pi R_A a_1 = \frac{\tilde{C}_{L,\alpha}}{\left(1 + \frac{\tilde{C}_{L,\alpha}}{\pi R_A} \right) (1 + \kappa_L)} \quad (6.20)$$

$$\kappa_L \equiv \frac{1 - (1 + \pi R_A / \tilde{C}_{L,\alpha}) a_1}{(1 + \pi R_A / \tilde{C}_{L,\alpha}) a_1} \quad (6.21)$$

$$\varepsilon_\Omega \equiv \frac{b_1}{a_1} \quad (6.22)$$

and the integrated rolling moment can be computed from

$$C_\ell = C_{\ell,\delta_a} \delta_a + C_{\ell,\bar{p}} \bar{p} \quad (6.23)$$

where

$$C_{\ell,\delta_a} = -\frac{\pi R_A}{4} c_2 \quad (6.24)$$

$$C_{\ell,\bar{p}} = -\frac{\pi R_A}{4} d_2 = -\frac{\kappa_{\ell\bar{p}} C_{L,\alpha}}{8}, \quad \kappa_{\ell\bar{p}} \equiv \frac{2d_2}{a_1} \quad (6.25)$$

The roll damping factor is plotted below for various planforms (assuming an airfoil lift slope of $\tilde{C}_{L,\alpha} = 2\pi$)

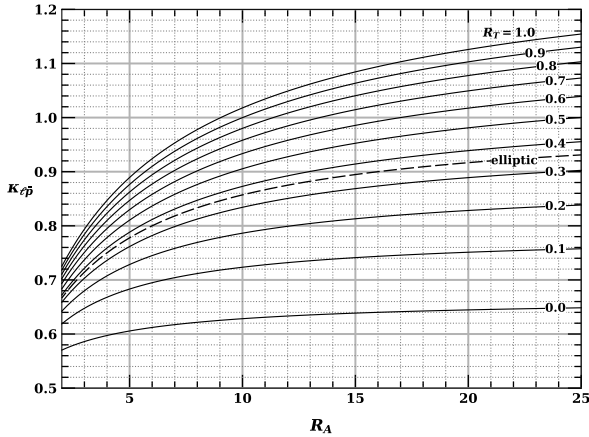


Fig. 6.1 Roll damping factor for wings of various planforms from Prandtl's classical lifting-line theory.

The steady-state rolling rate can be found from Eq. (6.23) by recognizing that the rolling moment at a steady rolling rate is zero. Using this in Eq. (6.23) and solving for the rolling rate gives

$$\bar{p}_{\text{steady}} = -\frac{C_{\ell,\delta_a}}{C_{\ell,\bar{p}}} \delta_a \quad (6.26)$$

1. Planform

The chord distribution of an elliptic wing is given by

$$\frac{c(z)}{b} = \frac{4}{\pi R_A} \sqrt{1 - (2z/b)^2} \quad \text{or} \quad \frac{c(\theta)}{b} = \frac{4}{\pi R_A} \sin(\theta) \quad (6.27)$$

The chord distribution of a wing with a tapered planform is given by

$$\frac{c(z)}{b} = \frac{2}{R_A(1+R_T)} [1 - (1-R_T)|2z/b|] \quad \text{or} \quad \frac{c(\theta)}{b} = \frac{2}{R_A(1+R_T)} [1 - (1-R_T)|\cos(\theta)|] \quad (6.28)$$

2. Washout

The washout distribution is defined as

$$\omega(\theta) \equiv \frac{\alpha(\theta) - \alpha_{L0}(\theta) - (\alpha - \alpha_{L0})_{\text{root}}}{(\alpha - \alpha_{L0})_{\text{max}} - (\alpha - \alpha_{L0})_{\text{root}}} \quad (6.29)$$

Linear washout is given by

$$\omega(z) = |2z/b| \quad \text{or} \quad \omega(\theta) = |\cos(\theta)| \quad (6.30)$$

For any given planform, the optimum distribution of washout to minimize induced drag is

$$\omega_{\text{opt}}(z) = 1 - \frac{\sqrt{1 - (2z/b)^2}}{c(z)/c_{\text{root}}} \quad \text{or} \quad \omega_{\text{opt}}(\theta) = 1 - \frac{\sin(\theta)}{c(\theta)/c_{\text{root}}} \quad (6.31)$$

The optimum amount of washout to minimize induced drag during steady-level flight at a given lift coefficient is

$$\Omega_{\text{opt}} = \frac{\kappa_{DL} C_{Ld}}{2\kappa_{D\Omega} C_{L,\alpha}} \quad (6.32)$$

For the special case of an elliptic lift distribution, this gives

$$\Omega = \frac{4C_L}{\pi R_A \tilde{C}_{L,\alpha} \frac{c_{\text{root}}}{b}} \quad (6.33)$$

with a required root angle of attack of

$$(\alpha - \alpha_{L0})_{\text{root}} = \frac{C_L}{\pi R_A} \left(\frac{4}{\tilde{C}_{L,\alpha} \frac{c_{\text{root}}}{b}} + 1 \right) \quad (6.34)$$

3. Aileron Distribution

The aileron distribution can be defined as

$$\chi(z) \equiv \begin{cases} 0, & z < -z_{at} \\ \varepsilon_f(z), & -z_{at} < z < -z_{ar} \\ 0, & -z_{ar} < z < z_{ar} \\ -\varepsilon_f(z), & z_{ar} < z < z_{at} \\ 0, & z > z_{at} \end{cases} \quad (6.35)$$

where ε_f is the section flap effectiveness. This effectiveness can be computed from

$$\varepsilon_f = \eta_h \eta_d \varepsilon_{fi} \quad (6.36)$$

where η_h is the hinge efficiency, η_d is the deflection efficiency, and ε_{fi} is the ideal flap effectiveness given by

$$\varepsilon_{fi} = 1 - \frac{\theta_f - \sin \theta_f}{\pi} \quad (6.37)$$

where

$$\theta_f = \cos^{-1} \left(2 \frac{c_f}{c} - 1 \right) \quad (6.38)$$

The factors contributing to lift and induced drag defined above are plotted below for various planforms (assuming an airfoil lift slope of $\tilde{C}_{L,\alpha} = 2\pi$)

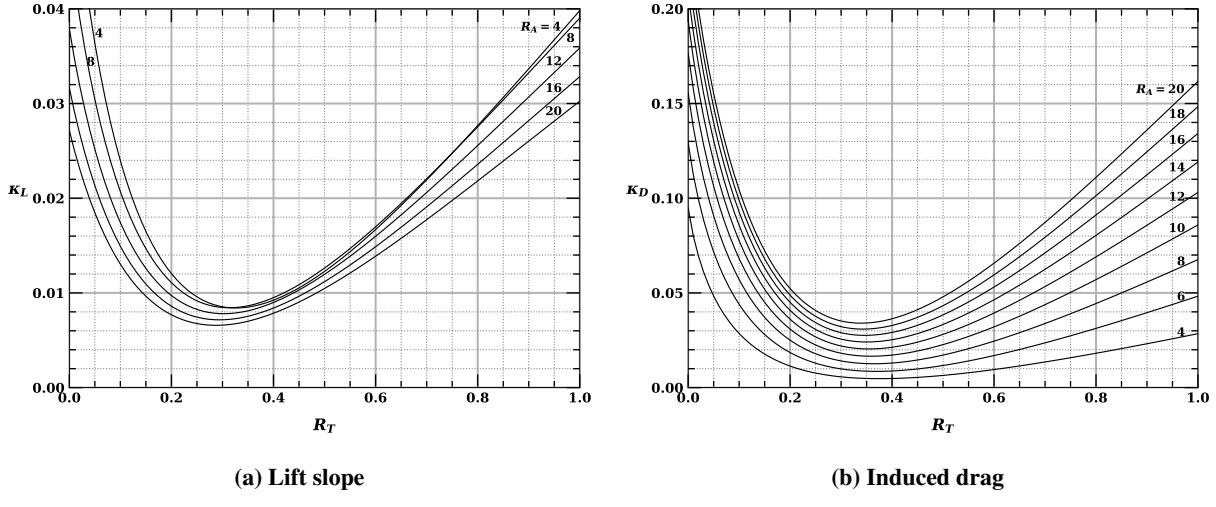


Fig. 6.2 Factors for untwisted tapered wings from Prandtl's classical lifting-line theory.

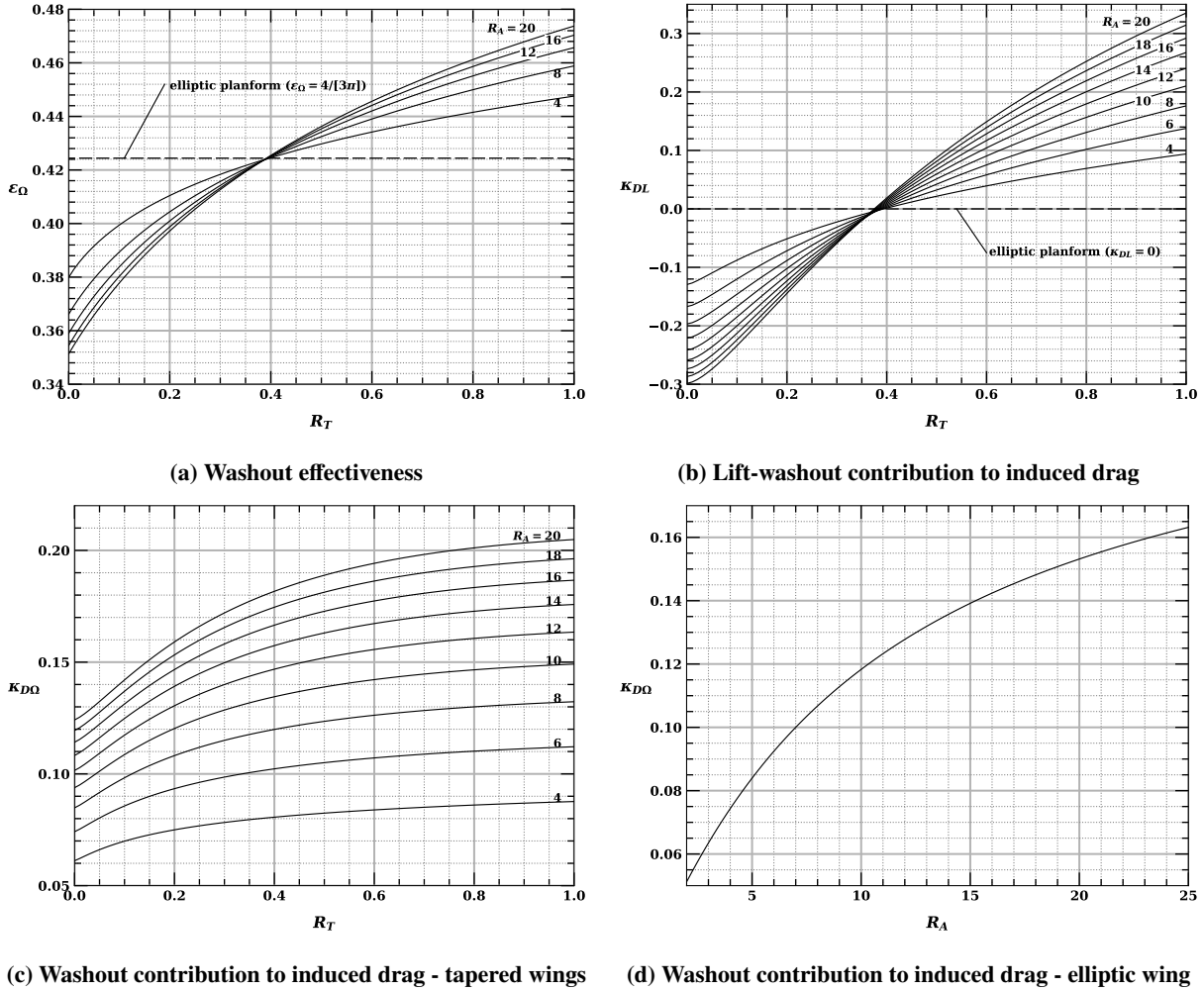


Fig. 6.3 Factors for linearly twisted tapered wings from Prandtl's classical lifting-line theory.

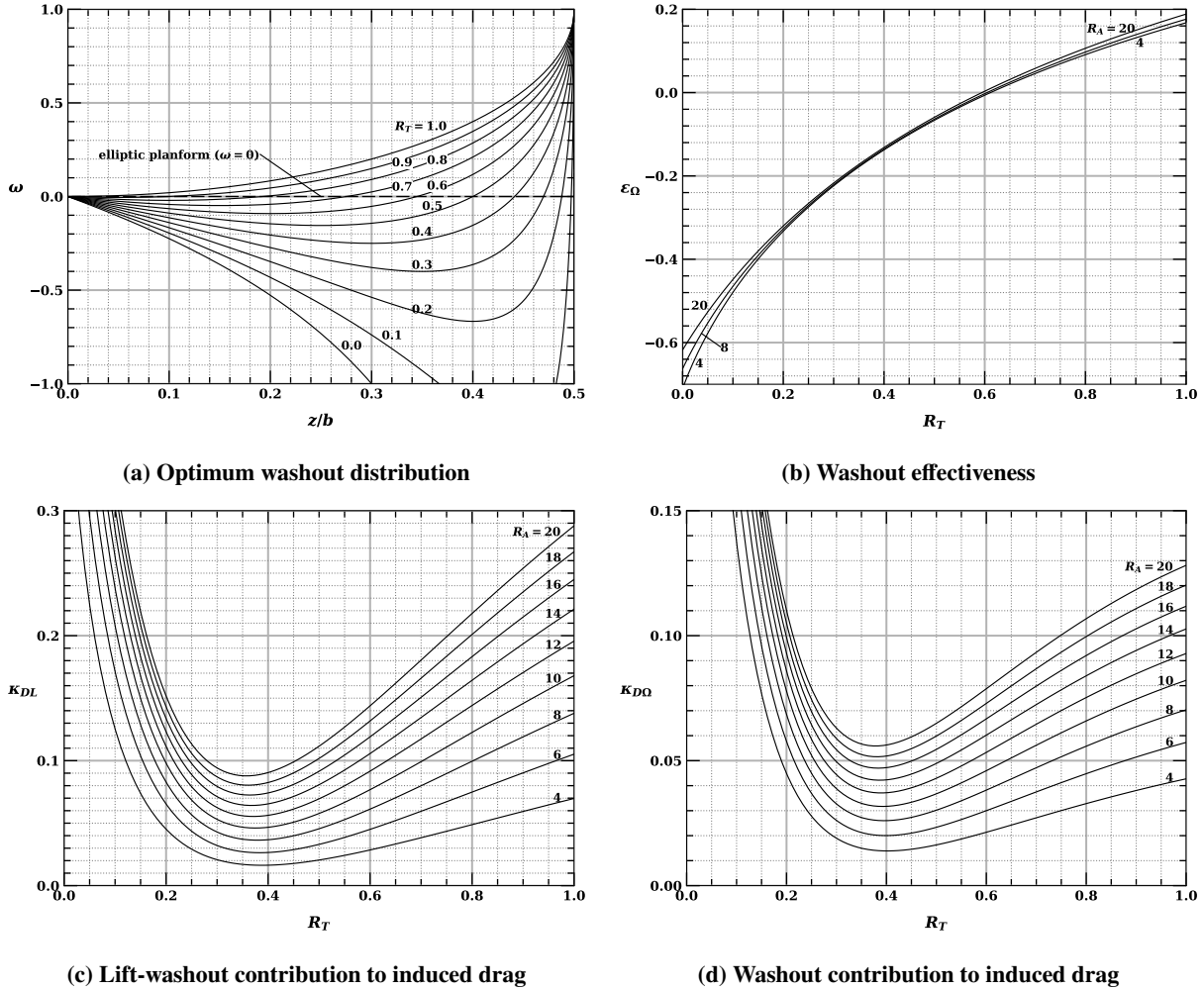


Fig. 6.4 Factors for optimally twisted tapered wings ($B_3 = 0$) from Prandtl's classical lifting-line theory.

C. Lift Distributions

The lift distribution can be computed by using Eq. (6.2) with the Kutta-Joukowski Law

$$\tilde{L}(\theta) = \rho V_\infty \Gamma(\theta) \quad (6.39)$$

A dimensionless lift distribution can be defined by dividing by the dynamic pressure and wingspan

$$\hat{C}_L(\theta) = \frac{\tilde{L}(\theta)}{\frac{1}{2} \rho V_\infty^2 b} \quad (6.40)$$

The contributions to this dimensionless lift distribution from planform, washout, aileron deflection, and rolling rate can be computed from

$$\hat{C}_L(\theta) = \hat{C}_{L_{\text{planform}}} + \hat{C}_{L_{\text{washout}}} + \hat{C}_{L_{\text{aileron}}} + \hat{C}_{L_{\text{roll}}} \quad (6.41)$$

where

$$\hat{C}_{L_{\text{planform}}}(\theta) = 4(\alpha - \alpha_{L0})_{\text{root}} \sum_{j=1}^N a_j \sin(j\theta) \quad (6.42)$$

$$\hat{C}_{L_{\text{washout}}}(\theta) = -4\Omega \sum_{j=1}^N b_j \sin(j\theta) \quad (6.43)$$

$$\hat{C}_{L_{\text{aileron}}}(\theta) = 4\delta_a \sum_{j=1}^N c_j \sin(j\theta) \quad (6.44)$$

$$\hat{C}_{L_{\text{roll}}}(\theta) = 4\bar{\rho} \sum_{j=1}^N d_j \sin(j\theta) \quad (6.45)$$

At any spanwise section, the **local section lift coefficient** is

$$\tilde{C}_L = \frac{\tilde{L}(\theta)}{\frac{1}{2}\rho V_\infty^2 c(\theta)} = \hat{C}_L \frac{b}{c(\theta)} \quad (6.46)$$

The contributions of planform, washout, aileron deflection, and rolling rate to the local section lift coefficient can be found from

$$\tilde{C}_L(\theta) = \tilde{C}_{L_{\text{planform}}} + \tilde{C}_{L_{\text{washout}}} + \tilde{C}_{L_{\text{aileron}}} + \tilde{C}_{L_{\text{roll}}} \quad (6.47)$$

where

$$\tilde{C}_{L_{\text{planform}}}(\theta) = \hat{C}_{L_{\text{planform}}} \frac{b}{c(\theta)} \quad (6.48)$$

$$\tilde{C}_{L_{\text{washout}}}(\theta) = \hat{C}_{L_{\text{washout}}} \frac{b}{c(\theta)} \quad (6.49)$$

$$\tilde{C}_{L_{\text{aileron}}}(\theta) = \hat{C}_{L_{\text{aileron}}} \frac{b}{c(\theta)} \quad (6.50)$$

$$\tilde{C}_{L_{\text{roll}}}(\theta) = \hat{C}_{L_{\text{roll}}} \frac{b}{c(\theta)} \quad (6.51)$$

1. Special Class of Lift Distributions

A special class of lift distributions is of interest in the design of wings to minimize induced drag. This class is defined by the case where $A_j = 0$ for all $n > 1$ and $n \neq 3$, which gives

$$\frac{b\tilde{L}(\theta)}{L} = \frac{4}{\pi} [\sin(\theta) + B_3 \sin(3\theta)] \quad (6.52)$$

or

$$\frac{\hat{C}_L}{C_L} = \frac{4}{\pi R_A} [\sin(\theta) + B_3 \sin(3\theta)] \quad (6.53)$$

where

$$B_3 \equiv \frac{A_3}{A_1} \quad (6.54)$$

This class of lift distributions includes the elliptic lift distribution ($B_3 = 0$), Prandtl's 1933 bell-shaped lift distribution ($B_3 = -1/3$), and others. For example, the lift distributions that minimize induced drag for a rectangular wing with all-positive spanwise symmetric lift and an optimum weight distribution, under the following constraints are as follows:

- prescribed gross weight, prescribed maximum stress, and prescribed chord length: $B_3 = -1/3$
- prescribed gross weight, prescribed maximum stress, and prescribed wing loading: $B_3 = -0.13564322$
- prescribed gross weight, prescribed maximum deflection, and prescribed wing loading: $B_3 = -0.05971587$
- prescribed net weight, prescribed maximum deflection, and prescribed stall speed: $B_3 = -0.17714856$

Any wing can be designed to produce these lift distributions by applying the twist distribution, twist amount, and root angle of attack of

$$\omega(\theta) = \frac{\frac{4}{\tilde{C}_{L,\alpha}} \left[\frac{1-B_3}{c_{\text{root}}/b} - \frac{\sin \theta + B_3 \sin(3\theta)}{c(\theta)/b} \right] - 3B_3 \left[1 + \frac{\sin(3\theta)}{\sin \theta} \right]}{\frac{4(1-B_3)}{\tilde{C}_{L,\alpha} c_{\text{root}}/b} - 12B_3} \quad (6.55)$$

$$\Omega = \frac{C_L}{\pi R_A} \left[\frac{4(1-B_3)}{\tilde{C}_{L,\alpha} c_{\text{root}}/b} - 12B_3 \right] \quad (6.56)$$

$$(\alpha - \alpha_{L0})_{\text{root}} = \frac{C_L}{\pi R_A} \left[\frac{4(1 - B_3)}{\tilde{C}_{L,\alpha} c_{\text{root}} / b} + 1 - 3B_3 \right] \quad (6.57)$$

The factors contributing to lift and induced drag defined above are plotted below for various planforms with optimum twist with $B_3 = -1/3$ (assuming an airfoil lift slope of $\tilde{C}_{L,\alpha} = 2\pi$)

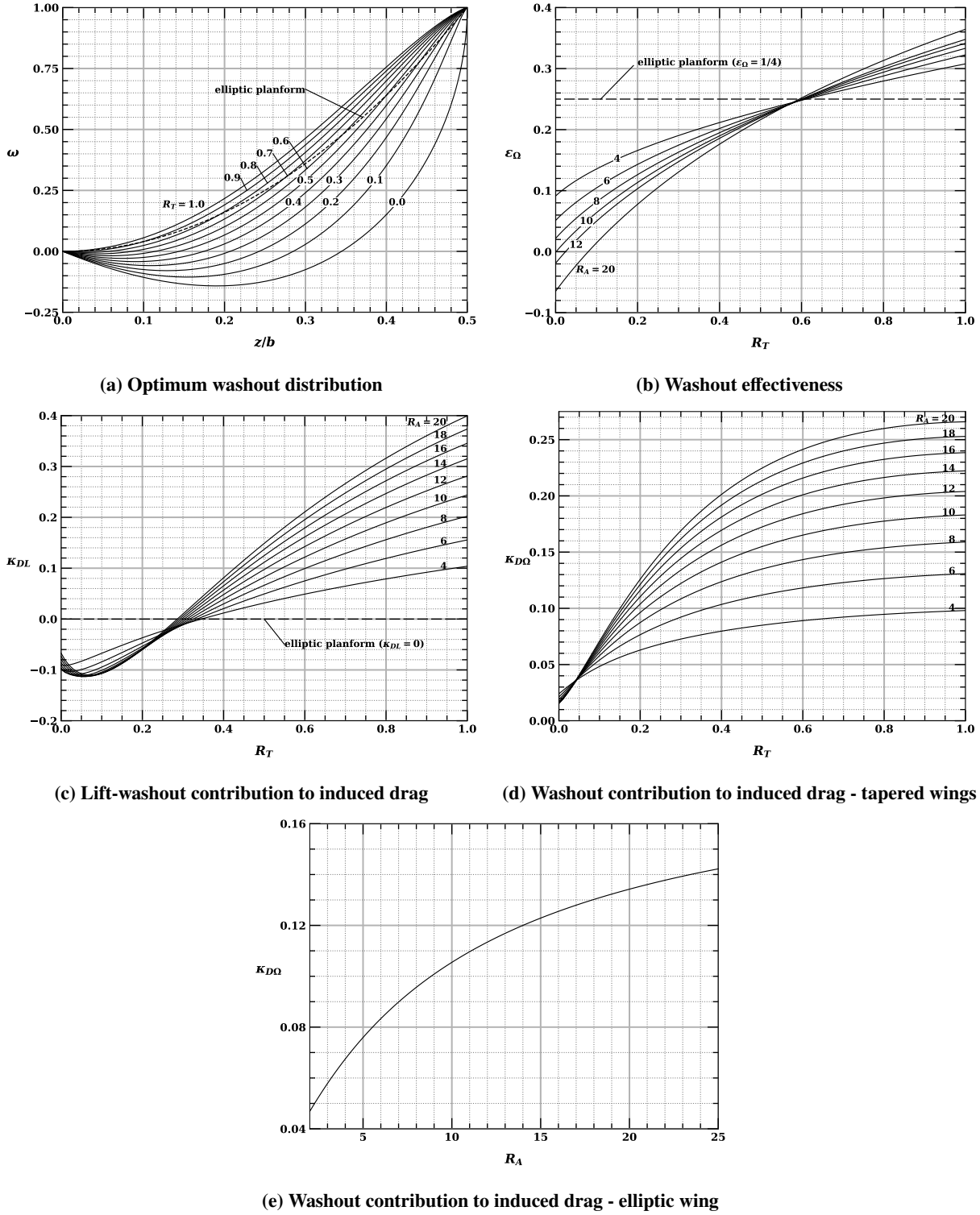


Fig. 6.5 Factors for optimally twisted tapered wings ($B_3 = -1/3$) from Prandtl's classical lifting-line theory.

D. Wing Spar Sizing

In order to carry the loads on a wing, the wing structure must be sized appropriately. The wing spar typically is designed primarily to support the bending moments, which are produced by the weight and its distribution in the wing, as well as the lift distribution. The wing structure is generally sized to support the loads at various loading conditions, described by a load factor n_a . At a given loading condition, the wing bending moments at any location z along the wing can be written as

$$\tilde{M}_b(z) = \int_{z'=z}^{b/2} [\tilde{L}(z') - n_a \tilde{W}_s(z') - n_a \tilde{W}_n(z')] (z' - z) dz' \quad (6.58)$$

where $\tilde{L}(z')$ is the lift distribution, $\tilde{W}_s(z')$ is the distribution of wing-structure (spar) weight, and $\tilde{W}_n(z')$ is the distribution of all other non-structural components in the wing.

7. Aircraft Performance

A. Lift and Drag

Lift and drag are two important aerodynamic forces on an aircraft. The lift is the force perpendicular to the freestream velocity, and the drag is the force in the direction of the freestream velocity. Dimensionless lift and drag coefficients are defined using the freestream velocity, density, and main wing area

$$C_L \equiv \frac{L}{\frac{1}{2}\rho V^2 S_w} \quad (7.1)$$

$$C_D \equiv \frac{D}{\frac{1}{2}\rho V^2 S_w} \quad (7.2)$$

The drag coefficient is nearly parabolic with lift, and is usually expressed as a function of the lift coefficient in the form

$$C_D = C_{D_0} + C_{D_1} C_L + \frac{C_L^2}{\pi e R_A} \quad (7.3)$$

where e is called the Oswald Efficiency. This form of the drag coefficient includes both induced and parasitic drag.

An important measure of aircraft performance is the lift-to-drag ratio L/D . From the definitions above, this can be written as

$$\frac{L}{D} = \frac{\frac{1}{2}\rho V^2 S_w C_L}{\frac{1}{2}\rho V^2 S_w C_D} = \frac{C_L}{C_D} = \frac{C_L}{C_{D_0} + C_{D_1} C_L + \frac{C_L^2}{\pi e R_A}} \quad (7.4)$$

Taking the derivative of Eq. (7.4) with respect to the lift coefficient, we see that the lift-to-drag ratio is maximized when

$$C_{D_0} = \frac{C_L^2}{\pi e R_A} \quad (7.5)$$

This results if often referred to in the field of aeronautics by stating that L/D is maximized when the parasitic drag is equal to the induced drag. Because parasitic drag dominates the term C_{D_0} and induced drag dominates the term on the right-hand side of Eq. (7.5), this statement is roughly true. However, it is not exactly true, since all three components of drag in the drag polar shown in Eq. (7.3) can include both induced-drag and parasitic drag. Using Eq. (7.5) in Eq. (7.4) we find the maximum L/D is

$$(L/D)_{\max} = \frac{\sqrt{\pi e R_A}}{2\sqrt{C_{D_0}} + C_{D_1} \sqrt{\pi e R_A}} \quad (7.6)$$

B. Steady-Level Flight

A free-body diagram of steady-level flight shows that

$$L = W - T \sin \alpha_T \quad (7.7)$$

$$D = T \cos \alpha_T \quad (7.8)$$

1. Thrust Required and Minimum-Drag Airspeed

The thrust required to sustain steady-level flight will be referred to here as the *thrust required* and given the symbol T_R . The previous two equations can be combined to solve for the thrust required as a function of L/D

$$T_R = \frac{W}{(L/D) \cos \alpha_T + \sin \alpha_T} \quad (7.9)$$

Thrust required is minimized when L/D is maximized. Using the results for maximum L/D above, it can be shown that in steady-level flight, maximum L/D is achieved at the minimum-drag velocity

$$V_{MD} = \frac{\sqrt{2}}{\sqrt[4]{\pi e R_A C_{D_0}}} \sqrt{\frac{W/S_w}{\rho}} \sqrt{1 / \left[1 + \left(2 \sqrt{\frac{C_{D_0}}{\pi e R_A}} + C_{D_1} \right) \tan \alpha_T \right]} \quad (7.10)$$

which is the velocity that minimizes T_R .

For the case of $\alpha_T = 0$ in steady-level flight, Eqs. (7.7) and (7.8) simplify to

$$L = W \quad (7.11)$$

$$D = T \quad (7.12)$$

and

$$C_L = C_W \equiv \frac{W}{\frac{1}{2}\rho V^2 S_w} \quad (7.13)$$

The thrust required to sustain steady-level flight is then

$$T_R = \frac{W}{(L/D)} = \frac{C_D}{C_L} W = \left(\frac{\frac{1}{2}\rho V^2 C_{D_0}}{W/S_w} + C_{D_1} + \frac{W/S_w}{\frac{1}{2}\pi e R_A \rho V^2} \right) W \quad (7.14)$$

The velocity that minimizes the thrust required when $\alpha_T = 0$ is then

$$V_{MD} = \frac{\sqrt{2}}{\sqrt[4]{\pi e R_A C_{D_0}}} \sqrt{\frac{W/S_w}{\rho}} \quad (7.15)$$

and the minimum thrust required which results at the minimum drag airspeed is

$$T_{R_{\min}} = \left(2 \sqrt{\frac{C_{D_0}}{\pi e R_A}} + C_{D_1} \right) W \quad (7.16)$$

2. Power Required

The power required is defined as the dot product of the thrust vector and the velocity vector

$$P_R = T_R V \cos \alpha_T = DV \quad (7.17)$$

Using the small-thrust approximation to equate the lift to the weight, the power required can be written in terms of lift coefficient as

$$P_R = \sqrt{2} \left(\frac{C_{D_0}}{C_L^{3/2}} + \frac{C_{D_1}}{C_L^{1/2}} + \frac{C_L^{1/2}}{\pi e R_A} \right) W \sqrt{\frac{W/S_w}{\rho}} \quad (7.18)$$

or in terms of velocity as

$$P_R = \left(\frac{C_{D_0} \rho V^3}{2(W/S_w)} + C_{D_1} V + \frac{2(W/S_w)}{\pi e R_A \rho V} \right) W \quad (7.19)$$

The power required is minimized when

$$3C_{D_0} + C_{D_1} C_L = \frac{C_L^2}{\pi e R_A} \quad (7.20)$$

This occurs at a velocity of

$$V_{MDV} = \frac{2}{\sqrt{\pi e R_A C_{D_1} + \sqrt{(\pi e R_A C_{D_1})^2 + 12\pi e R_A C_{D_0}}}} \sqrt{\frac{W/S_w}{\rho}} \quad (7.21)$$

and results in a power required of

$$P_{R_{\min}} = (DV)_{\min} \tilde{=} \frac{4\sqrt{2} C_{D_0}^{1/4}}{(3\pi e R_A)^{3/4}} W \sqrt{\frac{W/S_w}{\rho}} \quad (7.22)$$

C. Rate of Climb

A free-body diagram of steady-climbing flight shows that

$$L = W \cos \gamma - T \sin \alpha_T \quad (7.23)$$

$$D = T \cos \alpha_T - W \sin \gamma \quad (7.24)$$

The climb rate is defined as the velocity multiplied by the sine of the climb angle. From Eq. (7.24) this gives

$$V_c \equiv V \sin \gamma = \frac{VT \cos \alpha_T - VD}{W} \quad (7.25)$$

For small climb angles, we can approximate the drag as the drag in steady-level flight. This gives

$$V_c \approx \frac{VT \cos \alpha_T - VT_R \cos \alpha_T}{W} = \frac{P - P_R}{W} \quad (7.26)$$

Hence we see that the climb rate at small climb angles is directly proportional to the *excess power*, where the excess power is the power minus the power required to sustain steady-level flight.

D. Gliding Flight

1. Sink Rate

The sink rate is the negative of the climb rate with zero power

$$V_s = \frac{P_R}{W} = \frac{DV}{W} \quad (7.27)$$

This can be written in terms of velocity as

$$V_s = \frac{P_R}{W} = \frac{C_{D_0}\rho V^3}{2(W/S_w)} + C_{D_1}V + \frac{2(W/S_w)}{\pi e R_A \rho V} \quad (7.28)$$

The sink rate is minimized at the same speed that minimizes power required

$$V_{MS} = V_{MDV} = \frac{2}{\sqrt{\pi e R_A C_{D_1} + \sqrt{(\pi e R_A C_{D_1})^2 + 12\pi e R_A C_{D_0}}}} \sqrt{\frac{W/S_w}{\rho}} \quad (7.29)$$

2. Glide Ratio

The glide ratio is defined as

$$R_G = \frac{V_g}{V_s} \quad (7.30)$$

With zero wind, the glide ratio is equal to the lift-to-drag ratio

$$R_G = \frac{L}{D} \quad (7.31)$$

Hence, the maximum zero-wind glide ratio is the max lift-to-drag ratio

$$(R_{G0})_{\max} = (C_L/C_D)_{\max} = \frac{\sqrt{\pi e R_A}}{2\sqrt{C_{D_0}} + C_{D_1}\sqrt{\pi e R_A}} \quad (7.32)$$

and the velocity that maximizes the zero-wind glide ratio is the same velocity that maximizes the lift-to-drag ratio

$$V_{BG0} = V_{MD} \approx \frac{\sqrt{2}}{\sqrt[4]{\pi e R_A C_{D_0}}} \sqrt{\frac{W/S_w}{\rho}} \quad (7.33)$$

In general, the glide ratio depends on wind and can be expressed as a function of velocity as

$$R_G \approx \frac{\sqrt{1 - \frac{V_w^2 \sin^2 \varphi_w}{V^2}} - \frac{V_w \cos \varphi_w}{V}}{\frac{\frac{1}{2} \rho V^2 C_{D0}}{W/S_w} + C_{D1} + \frac{W/S_w}{\frac{1}{2} \pi e R_A \rho V^2}} \quad (7.34)$$

The velocity that maximizes the glide ratio with wind is found by numerically solving the equation

$$2(V^4 - V_{MD}^4)V - (3V^4 - V_{MD}^4)V_w \left(\cos \varphi_w \sqrt{1 - \frac{V_w^2 \sin^2 \varphi_w}{V^2}} + \frac{V_w \sin^2 \varphi_w}{V} \right) = 0 \quad (7.35)$$

E. Stall

The stall speed is often considered the minimum velocity for an aircraft. In steady-level flight with the thrust aligned with the direction of flight, the stall speed can be computed from

$$V_{\min} = \sqrt{\frac{2}{C_{L \max}}} \sqrt{\frac{W/S_w}{\rho}} \quad (7.36)$$

F. Steady Coordinated Turn

The radius of a steady coordinated turn is related to climb angle and bank angle

$$R = \frac{V^2 \cos \gamma}{g \tan \phi} \quad (7.37)$$

The stall-limited bank angle can be found from

$$\cos \phi_{\max} = \frac{W}{\frac{1}{2} \rho V^2 S_w C_{L \max}} \quad (7.38)$$

The load factor is defined as

$$n \equiv \frac{L}{W} \quad (7.39)$$

The load-limited bank angle can be found from

$$\cos \phi_{\max} = \frac{1}{n_{\max}} = \frac{W}{L_{pll}} = \frac{W}{n_{pll} W_{\max}} \quad (7.40)$$

The turn radius is related to load factor for a nearly-level turn according to

$$R = \frac{V^2}{g \sqrt{n^2 - 1}} \quad (7.41)$$

The maneuvering speed is the velocity at which the tightest turns can be performed. This is also called the corner velocity and is the same velocity that gives us the maximum turning rate

$$V_M = \sqrt{\frac{2 n_{pll}}{C_{L \max}}} \sqrt{\frac{W_{\max}/S_w}{\rho}} = \sqrt{n_{pll}} V_{smgw} \quad (7.42)$$

The maximum turning rate is

$$\Omega_{\max} = \sqrt{\frac{C_{L \max}}{2} \left(\frac{n_{pll} W_{\max}}{W} - \frac{W}{n_{pll} W_{\max}} \right)} g \sqrt{\frac{\rho}{W/S_w}} \quad (7.43)$$

G. Takeoff and Landing

The distance between two points on the runway can be found from the integral

$$s_{i+1} - s_i = \frac{W}{g} \int_{V_i}^{V_{i+1}} \frac{(V - V_{hw})dV}{T - D - F_r} \quad (7.44)$$

where thrust, drag, and rolling friction are all functions of velocity

$$T = (T_0)_i + (T')_i V + (T'')_i V^2 \quad (7.45)$$

$$D = \frac{1}{2} \rho V^2 S_w C_D \approx \frac{1}{2} \rho V^2 S_w \left(C_{D_0} + C_{D_1} C_L + \frac{(16h_w/b_w)^2}{1 + (16h_w/b_w)^2} \frac{C_L^2}{\pi e R_A} \right) \quad (7.46)$$

$$F_r = \mu_r (W - L) = \mu_r (W - \frac{1}{2} \rho V^2 S_w C_L) \quad (7.47)$$

Notice that the drag equation has been altered slightly to account for ground effect on the induced drag.

The liftoff speed is 10% above the stall speed

$$V_{LO} = 1.1 \sqrt{\frac{2}{C_{L \max}}} \sqrt{\frac{W/S_w}{\rho}} \quad (7.48)$$

The rotation distance is

$$s_r = (V_{LO} - V_{hw}) t_r \quad (7.49)$$

The total ground roll is

$$s_g = s_a + s_r \quad (7.50)$$

An estimate for the total ground roll is

$$s_g \approx \frac{1.21 W^2}{\rho g S_w C_{L \max} (T - D - F_r) 0.7 V_{LO}} + 1.1 t_r \sqrt{\frac{2}{C_{L \max}}} \sqrt{\frac{W/S_w}{\rho}} \quad (7.51)$$

8. Longitudinal Static Trim and Stability

The longitudinal forces and moment can be written in nondimensional form as

$$C_A \equiv \frac{A}{\frac{1}{2}\rho V_\infty^2 S_w} \quad (8.1)$$

$$C_N \equiv \frac{N}{\frac{1}{2}\rho V_\infty^2 S_w} \quad (8.2)$$

$$C_m \equiv \frac{m}{\frac{1}{2}\rho V_\infty^2 S_w \bar{c}_w} \quad (8.3)$$

A. Small-Angle Longitudinal Trim Requirements

For an aircraft to be trim, the summation of forces and moments about the center of gravity must be zero. The longitudinal components require

$$\sum F_x = \sum F_z = \sum M_y = 0 \quad (8.4)$$

B. Longitudinal Stability Requirements

For an aircraft to be longitudinally stable, the pitch stability derivative must be negative

$$C_{m,\alpha} < 0 \quad (8.5)$$

Assuming that the vertical offset between the center of gravity and the aircraft neutral point is small, and applying the small angle approximation, the traditional estimate for the static margin can be written as

$$\sigma = \frac{l_{np}}{\bar{c}_w} = -\frac{C_{m,\alpha}}{C_{L,\alpha}} \quad (8.6)$$

The static margin is related to the location of the neutral point relative to the center of gravity, and can be estimated from the pitch stability derivative and the lift slope.

C. Simplified Wing and Tail Model

In order to gain some insight into the longitudinal effects of a main wing and tail, we can use a simplified wing-tail model. Assuming the center of gravity and aerodynamic centers of the main wing and tail all lie on a fuselage reference line, and assuming that the thrust is aligned with the fuselage reference line, and applying the small-angle approximation for angle of attack and downwash, the summation of forces in the direction of lift can be written as

$$C_L = C_{L_w} + \frac{S_h}{S_w} \eta_h C_{L_h} = \frac{W \cos \gamma}{\frac{1}{2}\rho V_\infty^2 S_w} \quad (8.7)$$

and the summation of pitching moment about the center of gravity can be written as

$$C_m = C_{m_w} + \frac{S_h \bar{c}_h}{S_w \bar{c}_w} \eta_h C_{m_h} - \frac{l_w}{\bar{c}_w} C_{L_w} - \frac{S_h l_h}{S_w \bar{c}_w} \eta_h C_{L_h} = 0 \quad (8.8)$$

where

$$C_{L_w} = C_{L_w, \alpha} (\alpha + \alpha_{0w} - \alpha_{L0w}) \quad (8.9)$$

$$C_{L_h} = C_{L_h, \alpha} [(1 - \varepsilon_{d,\alpha})\alpha + \alpha_{0h} - \alpha_{L0h} - \varepsilon_{d0} + \varepsilon_e \delta_e] \quad (8.10)$$

$$C_{m_h} = C_{m_h, 0} + C_{m_h, \delta_e} \delta_e \quad (8.11)$$

If all geometric properties are known, Eqs. (8.7) and (8.8) can be combined into a system of equations to solve for the required angle of attack and elevator deflection for a given operating condition

$$\begin{bmatrix} C_{L,\alpha} & C_{L,\delta_e} \\ C_{m,\alpha} & C_{m,\delta_e} \end{bmatrix} \begin{Bmatrix} \alpha \\ \delta_e \end{Bmatrix} = \begin{bmatrix} C_L - C_{L0} \\ -C_{m0} \end{bmatrix} \quad (8.12)$$

where

$$C_{L,\alpha} = C_{L_w,\alpha} + \frac{S_h}{S_w} \eta_h C_{L_h,\alpha} (1 - \varepsilon_{d,\alpha}) \quad (8.13)$$

$$C_{L,\delta_e} = \frac{S_h}{S_w} \eta_h C_{L_h,\alpha} \varepsilon_e \quad (8.14)$$

$$C_L = \frac{W \cos \gamma}{\frac{1}{2} \rho V_\infty^2 S_w} \quad (8.15)$$

$$C_{L0} = C_{L_w,\alpha} (\alpha_{0w} - \alpha_{L0w}) + \frac{S_h}{S_w} \eta_h C_{L_h,\alpha} (\alpha_{0h} - \alpha_{L0h} - \varepsilon_{d0}) \quad (8.16)$$

$$C_{m,\alpha} = -\frac{l_w}{c_w} C_{L_w,\alpha} - \frac{S_h l_h}{S_w c_w} \eta_h C_{L_h,\alpha} (1 - \varepsilon_{d,\alpha}) \quad (8.17)$$

$$C_{m,\delta_e} = \frac{S_h \bar{c}_h}{S_w \bar{c}_w} \eta_h C_{m_h,\delta_e} - \frac{S_h l_h}{S_w \bar{c}_w} \eta_h C_{L_h,\alpha} \varepsilon_e \quad (8.18)$$

$$C_{m0} = C_{m_w} + \frac{S_h \bar{c}_h}{S_w \bar{c}_w} \eta_h C_{m_h0} - \frac{l_w}{\bar{c}_w} C_{L_w,\alpha} (\alpha_{0w} - \alpha_{L0w}) - \frac{S_h l_h}{S_w \bar{c}_w} \eta_h C_{L_h,\alpha} (\alpha_{0h} - \alpha_{L0h} - \varepsilon_{d0}) \quad (8.19)$$

and $C_{m,\alpha}$ is the pitch stability derivative.

D. Estimating Downwash

Downwash is a complex phenomenon that can only be accurately predicted or measured from high-fidelity CFD simulations, inviscid solutions, panel codes, or experimental results. However, during the early phases of design, approximations for downwash can be very useful. This section presents relations that can be used to estimate downwash or upwash in the vicinity of a main wing.

1. General Solution For Wings Without Sweep

From lifting-line theory and the Biot-Savart law, and applying the small-downwash-angle approximation, the downwash angle can be estimated as

$$\begin{aligned} \varepsilon_d(x, y, z) = -\frac{V_y}{V_\infty} &= \frac{C_{L_w} \kappa_v}{\pi^2 R_{A_w} \kappa_b} \left\{ \frac{1 - \hat{z}}{\hat{y}^2 + (1 - \hat{z})^2} \left[1 + \frac{\hat{x}}{\sqrt{\hat{x}^2 + \hat{y}^2 + (1 - \hat{z})^2}} \right] \right. \\ &\quad + \frac{\hat{x}}{\hat{x}^2 + \hat{y}^2} \left[\frac{1 - \hat{z}}{\sqrt{\hat{x}^2 + \hat{y}^2 + (1 - \hat{z})^2}} + \frac{1 + \hat{z}}{\sqrt{\hat{x}^2 + \hat{y}^2 + (1 + \hat{z})^2}} \right] \\ &\quad \left. + \frac{1 + \hat{z}}{\hat{y}^2 + (1 + \hat{z})^2} \left[1 + \frac{\hat{x}}{\sqrt{\hat{x}^2 + \hat{y}^2 + (1 + \hat{z})^2}} \right] \right\} \end{aligned} \quad (8.20)$$

where

$$\hat{x} = \frac{2x}{b_w \kappa_b}, \quad \hat{y} = \frac{2y}{b_w \kappa_b}, \quad \hat{z} = \frac{2z}{b_w \kappa_b} \quad (8.21)$$

are evaluated in the aerodynamic coordinate system with the origin at the aerodynamic center of the main wing, x pointing aft, y pointing up, and z pointing out the left wing. The vortex-strength factor κ_v is the ratio of the vortex strength produced by the wing to that produced by an elliptic lift distribution on a wing of the same aspect ratio and at the same lift coefficient. It can be computed from lifting-line theory as

$$\kappa_v = 1 + \sum_{j=2}^{\infty} \frac{A_j}{A_1} \sin(j\pi/2) \quad (8.22)$$

The vortex-span factor κ_b is the ratio of the distance between the two trailing vortices and the wing span. It can be computed from lifting-line theory as

$$\kappa_b \equiv \frac{b'}{b} = \left[\frac{\pi}{4} + \sum_{j=2}^{\infty} \frac{j A_j}{(j^2 - 1) A_1} \cos(j\pi/2) \right] \Bigg| \kappa_v \quad (8.23)$$

For an elliptic lift distribution, $\kappa_v = 1$ and $\kappa_b = \pi/4$.

2. Plane of Symmetry

The downwash angle in the plane of symmetry of the aircraft ($z = 0$) can be estimated from

$$\varepsilon_d(x, y, 0) = \frac{\kappa_v \kappa_p}{\kappa_b} \frac{C_{L_w}}{R_{A_w}} \quad (8.24)$$

where

$$\kappa_p = \frac{2}{\pi^2(\hat{y}^2 + 1)} \left[1 + \frac{\hat{x}(\hat{x}^2 + 2\hat{y}^2 + 1)}{(\hat{x}^2 + \hat{y}^2)\sqrt{\hat{x}^2 + \hat{y}^2 + 1}} \right] \quad (8.25)$$

3. Sweep Effects

Effects of sweep can be approximated by neglecting the effect of sweep on κ_v and κ_b and including a correction factor that accounts for the change in position of the tips of the main wing

$$\varepsilon_d(x, y, 0) = \frac{\kappa_v \kappa_p \kappa_s}{\kappa_b} \frac{C_{L_w}}{R_{A_w}} \quad (8.26)$$

The sweep correction factor κ_s can be approximated as

$$\kappa_s = \frac{1 + \frac{\hat{x} - \tan \Lambda}{\hat{r}} + \frac{\hat{x}(\hat{r} + \hat{t})(\hat{t}_0^2 - \hat{x}^2)}{\hat{r}\hat{t}(\hat{r}\hat{t} + \hat{r}^2 - \hat{x}\tan \Lambda)}}{1 + \frac{\hat{x}(\hat{r}^2 + \hat{t}_0^2 - \hat{x}^2)}{\hat{r}^2\hat{t}_0}} \quad (8.27)$$

where

$$\hat{r} \equiv \sqrt{\hat{x}^2 + \hat{y}^2} \quad (8.28)$$

$$\hat{t} \equiv \sqrt{(\hat{x} - \tan \Lambda)^2 + \hat{y}^2 + 1} \quad (8.29)$$

$$\hat{t}_0 \equiv \sqrt{\hat{x}^2 + \hat{y}^2 + 1} \quad (8.30)$$

4. Rough Approximation for a Horizontal Stabilizer

A rough approximation for downwash on an aft tail can be obtained by considering the case that the horizontal stabilizer sits very far aft of the main wing and in the same plane as the main wing. In the limit as $x \rightarrow \infty$ the downwash in the plane of symmetry can be estimated from the factors $\kappa_p = 4/\pi^2$ and $\kappa_s = 1.0$. Additionally, for the case of an elliptic lift distribution, $\kappa_v = 1$ and $\kappa_b = \pi/4$. Combining these results gives a very rough approximation for the downwash in the plane of symmetry far downstream from the main wing

$$\varepsilon_d(x \rightarrow \infty, 0, 0) = \frac{16}{\pi^3} \frac{C_{L_w}}{R_{A_w}} \quad (8.31)$$

E. Generalized Model with Vertical Offsets and Drag

Allowing for vertical offsets of the wing, horizontal control surface, and thrust vector from the fuselage reference line that runs through the center of gravity, and accounting for trigonometric nonlinearities, trim requires

$$C_A = C_{D_w} \cos(\alpha - \varepsilon_w) - C_{L_w} \sin(\alpha - \varepsilon_w) + \frac{S_h}{S_w} \eta_h [C_{D_h} \cos(\alpha - \varepsilon_h) - C_{L_h} \sin(\alpha - \varepsilon_h)] = C_T - C_W \sin \theta \quad (8.32)$$

$$C_N = C_{L_w} \cos(\alpha - \varepsilon_w) + C_{D_w} \sin(\alpha - \varepsilon_w) + \frac{S_h}{S_w} \eta_h [C_{L_h} \cos(\alpha - \varepsilon_h) + C_{D_h} \sin(\alpha - \varepsilon_h)] = C_W \cos \theta \quad (8.33)$$

$$C_m = C_{m_w} - \frac{l_w C_{L_w} - h_w C_{D_w}}{\bar{c}_w} \cos(\alpha - \varepsilon_w) - \frac{h_w C_{L_w} + l_w C_{D_w}}{\bar{c}_w} \sin(\alpha - \varepsilon_w) \\ + \frac{S_h}{S_w} \eta_h \left[\frac{\bar{c}_h}{\bar{c}_w} C_{m_h} - \frac{l_h C_{L_h} - h_h C_{D_h}}{\bar{c}_w} \cos(\alpha - \varepsilon_h) - \frac{h_h C_{L_h} + l_h C_{D_h}}{\bar{c}_w} \sin(\alpha - \varepsilon_h) \right] = \frac{h_T}{\bar{c}_w} C_T \quad (8.34)$$

where

$$C_T = \frac{T}{\frac{1}{2} \rho V_\infty^2 S_w} \quad (8.35)$$

The lift on the main wing can include upwash or downwash

$$C_{L_w} = C_{L_w, \alpha} (\alpha + \alpha_{0w} - \alpha_{L0w} - \varepsilon_w) \quad (8.36)$$

and the lift on the horizontal control surface can be computed from

$$C_{L_h} = C_{L_h, \alpha} (\alpha + \alpha_{0h} - \alpha_{L0h} - \varepsilon_h + \varepsilon_e \delta_e) \quad (8.37)$$

The drag on the main wing and horizontal control surface can be computed from

$$C_{D_w} = C_{D_{0w}} + C_{D_{1w}} C_{L_w} + \frac{C_{L_w}^2}{\pi e_w R_{A_w}} \quad (8.38)$$

$$C_{D_h} = C_{D_{0h}} + C_{D_{1h}} C_{L_h} + \frac{C_{L_h}^2}{\pi e_h R_{A_h}} \quad (8.39)$$

The pitching moment on the horizontal control surface can be computed from Eq. (8.8). The system of equations given in Eqs. (8.29)-(8.31) are nonlinear. Given a geometry and flight condition, the angle of attack and elevator deflection required to trim the aircraft must be solved iteratively.

The pitch stability derivative can be found from Eq. (8.31) by taking the first derivative with respect to angle of attack

$$\begin{aligned} \frac{\partial C_m}{\partial \alpha} &= \left[\frac{l_w C_{L_w} - h_w C_{D_w}}{\bar{c}_w} \sin(\alpha - \varepsilon_w) - \frac{h_w C_{L_w} + l_w C_{D_w}}{\bar{c}_w} \cos(\alpha - \varepsilon_w) \right] (1 - \varepsilon_{w,\alpha}) \\ &\quad - \left[\frac{l_w}{\bar{c}_w} \cos(\alpha - \varepsilon_w) + \frac{h_w}{\bar{c}_w} \sin(\alpha - \varepsilon_w) \right] C_{L_w, \alpha} (1 - \varepsilon_{w,\alpha}) \\ &\quad + \left[\frac{h_w}{\bar{c}_w} \cos(\alpha - \varepsilon_w) - \frac{l_w}{\bar{c}_w} \sin(\alpha - \varepsilon_w) \right] \left(C_{D_{1w}} + \frac{2C_{L_w}}{\pi e_w R_{A_w}} \right) C_{L_w, \alpha} (1 - \varepsilon_{w,\alpha}) \\ &\quad + \frac{S_h}{S_w} \eta_h \left[\frac{l_h C_{L_h} - h_h C_{D_h}}{\bar{c}_w} \sin(\alpha - \varepsilon_h) - \frac{h_h C_{L_h} + l_h C_{D_h}}{\bar{c}_w} \cos(\alpha - \varepsilon_h) \right] (1 - \varepsilon_{h,\alpha}) \\ &\quad - \frac{S_h}{S_w} \eta_h \left[\frac{l_h}{\bar{c}_w} \cos(\alpha - \varepsilon_h) + \frac{h_h}{\bar{c}_w} \sin(\alpha - \varepsilon_h) \right] C_{L_h, \alpha} (1 - \varepsilon_{h,\alpha}) \\ &\quad + \frac{S_h}{S_w} \eta_h \left[\frac{h_h}{\bar{c}_w} \cos(\alpha - \varepsilon_h) - \frac{l_h}{\bar{c}_w} \sin(\alpha - \varepsilon_h) \right] \left(C_{D_{1h}} + \frac{2C_{L_h}}{\pi e_h R_{A_h}} \right) C_{L_h, \alpha} (1 - \varepsilon_{h,\alpha}) \end{aligned} \quad (8.40)$$

F. Aerodynamic Center

The aerodynamic center of an airfoil, wing, or entire aircraft can be found from the following development. The aerodynamic center is the point that satisfies the two conditions

$$\frac{\partial C_{m_{ac}}}{\partial \alpha} \equiv 0 \quad (8.41)$$

and

$$\frac{\partial x_{ac}}{\partial \alpha} \equiv 0, \quad \frac{\partial y_{ac}}{\partial \alpha} \equiv 0 \quad (8.42)$$

The pitching moment about the origin can be expressed in terms of the pitching moment about the aerodynamic center as

$$C_{m0} = C_{m_{ac}} - \frac{x_{ac}}{c_{ref}} C_N + \frac{y_{ac}}{c_{ref}} C_A \quad (8.43)$$

Taking the first derivative with respect to alpha and applying Eq. (8.38) gives the neutral axis line

$$\frac{x_{ac}}{c_{ref}} C_{N,\alpha} - \frac{y_{ac}}{c_{ref}} C_{A,\alpha} = -C_{m0,\alpha} \quad (8.44)$$

Taking the derivative of Eq. (8.41) with respect to alpha gives a second line

$$\frac{x_{ac}}{c_{ref}} C_{N,\alpha,\alpha} - \frac{y_{ac}}{c_{ref}} C_{A,\alpha,\alpha} = -C_{m0,\alpha,\alpha} \quad (8.45)$$

The intercept of these two lines is the aerodynamic center. The intersection of these two lines is

$$\frac{x_{ac}}{c_{ref}} = \frac{C_{A,\alpha} C_{m0,\alpha,\alpha} - C_{m0,\alpha} C_{A,\alpha,\alpha}}{C_{N,\alpha} C_{A,\alpha,\alpha} - C_{A,\alpha} C_{N,\alpha,\alpha}} \quad (8.46)$$

$$\frac{y_{ac}}{c_{ref}} = \frac{C_{N,\alpha} C_{m0,\alpha,\alpha} - C_{m0,\alpha} C_{N,\alpha,\alpha}}{C_{N,\alpha} C_{A,\alpha,\alpha} - C_{A,\alpha} C_{N,\alpha,\alpha}} \quad (8.47)$$

In general, the aerodynamic center is a function of angle of attack.

G. Fuselage and External Stores

An approximation for the pitching moment produced by the fuselage, a nacelle, or an external store can be obtained from that given by Hoak (1960). This is

$$C_{m_f} \equiv \frac{m_f}{\frac{1}{2} \rho V_\infty^2 S_f c_f} = -2 \frac{l_f}{c_f} \left[1 - 1.76 \left(\frac{d_f}{c_f} \right)^{3/2} \right] \alpha_f \quad (8.48)$$

where

$$d_f \equiv 2 \sqrt{S_f / \pi} \quad (8.49)$$

This can be written in terms of the pitching-moment effect on the entire aircraft as

$$(C_m)_f = (C_{m0})_f + (C_{m,\alpha})_f \alpha \quad (8.50)$$

where

$$(C_{m0})_f = -2 \frac{S_f l_f}{S_w \bar{c}_w} \left[1 - 1.76 \left(\frac{d_f}{c_f} \right)^{3/2} \right] \alpha_{0f} \quad (8.51)$$

$$(C_{m,\alpha})_f = -2 \frac{S_f l_f}{S_w \bar{c}_w} \left[1 - 1.76 \left(\frac{d_f}{c_f} \right)^{3/2} \right] \quad (8.52)$$

H. Contribution of Propellers

The contribution of a running propeller can be written as

$$(C_m)_p = (C_{m0})_p + (C_{m,\alpha})_p \alpha \quad (8.53)$$

where

$$(C_{m0})_p = -\frac{h_p}{\bar{c}_w} C_D - \frac{2d_p^2 l_p}{S_w \bar{c}_w} \frac{C_{Np,\alpha}}{J^2} (\alpha_{0p} - \varepsilon_{d0p}) \quad (8.54)$$

$$(C_{m,\alpha})_p = -\frac{2d_p^2 l_p}{S_w \bar{c}_w} (1 - \varepsilon_{d,\alpha})_p \frac{C_{Np,\alpha}}{J^2} \quad (8.55)$$

I. Contribution of Jet Engines

The contribution of an operating jet engine can be written as

$$(C_m)_j = (C_{m0})_j + (C_{m,\alpha})_j \alpha \quad (8.56)$$

where

$$(C_{m0})_j = -\frac{T}{\frac{1}{2}\rho V_\infty^2 S_w} \left[\frac{h_j}{\bar{c}_w} + \frac{\eta_{p_i} l_j}{2(1-\eta_{p_i})\bar{c}_w} (\alpha_{0j} - \varepsilon_{d0j}) \right] \quad (8.57)$$

$$(C_{m,\alpha})_j = -\frac{T}{\frac{1}{2}\rho V_\infty^2 S_w} \frac{\eta_{p_i} l_j}{2(1-\eta_{p_i})\bar{c}_w} (1 - \varepsilon_{d,\alpha j}) \quad (8.58)$$

9. Lateral Static Trim and Stability

The lateral force and moments can be written in nondimensional form as

$$C_\ell \equiv \frac{\ell}{\frac{1}{2}\rho V_\infty^2 S_w b_w} \quad (9.1)$$

$$C_n \equiv \frac{n}{\frac{1}{2}\rho V_\infty^2 S_w b_w} \quad (9.2)$$

$$C_Y \equiv \frac{Y}{\frac{1}{2}\rho V_\infty^2 S_w} \quad (9.3)$$

A. Small-Angle Lateral Trim Requirements

For an aircraft to be trim, the summation of forces and moments about the center of gravity must be zero. The lateral components require

$$\sum F_y = \sum M_x = \sum M_z = 0 \quad (9.4)$$

Using small-angle approximations and within linear aerodynamics, lateral trim requires

$$\begin{bmatrix} C_{Y,\beta} & C_{Y,\delta_a} & C_{Y,\delta_r} \\ C_{\ell,\beta} & C_{\ell,\delta_a} & C_{\ell,\delta_r} \\ C_{n,\beta} & C_{n,\delta_a} & C_{n,\delta_r} \end{bmatrix} \begin{bmatrix} \beta \\ \delta_a \\ \delta_r \end{bmatrix} + \begin{bmatrix} (C_Y)_P \\ (C_\ell)_P \\ (C_n)_P \end{bmatrix} = \begin{bmatrix} 0 \\ 0 \\ 0 \end{bmatrix} \quad (9.5)$$

B. Lateral Stability Requirements

1. Yaw Stability Requirement

For an aircraft to be stable in yaw, the change in yawing moment with respect to sideslip angle must be positive, i.e.

$$\frac{\partial C_n}{\partial \beta} \equiv C_{n,\beta} > 0 \quad (9.6)$$

A good range for typical airplanes is $0.06 < C_{n,\beta} < 0.15$ per radian.

2. Roll Stability Requirement

For an aircraft to be stable in roll, the change in rolling moment with respect to sideslip angle must be negative, i.e.

$$\frac{\partial C_\ell}{\partial \beta} \equiv C_{\ell,\beta} < 0 \quad (9.7)$$

A good range for typical airplanes is $-0.10 < C_{\ell,\beta} < 0.0$ per radian.

C. Contributions to Yaw Trim and Stability

1. Vertical Tail

The largest contributor to yaw stability and trim is the vertical tail. The yawing moment due to the vertical tail can be estimated from

$$(C_n)_v = \eta_v \frac{S_v l_v}{S_w b_w} \left[C_{L_v,\alpha} (1 - \varepsilon_{s,\beta})_v \beta - C_{L_v,\alpha} \varepsilon_{s0} - \left(\varepsilon_r C_{L_v,\alpha} - \frac{\bar{c}_v}{l_v} C_{m_v,\delta_r} \right) \delta_r \right] \quad (9.8)$$

and the change in yaw stability derivative due to the vertical tail can be estimated from

$$(C_{n,\beta})_v = \eta_v \frac{S_v l_v}{S_w b_w} C_{L_v,\alpha} (1 - \varepsilon_{s,\beta})_v \quad (9.9)$$

The change in yawing moment due to rudder deflection can be estimated from

$$C_{n,\delta_r} \equiv \frac{\partial C_n}{\partial \delta_r} = -\eta_v \frac{S_v l_v}{S_w b_w} \left(\varepsilon_r C_{L_v,\alpha} - \frac{\bar{c}_v}{l_v} C_{m_v,\delta_r} \right) \quad (9.10)$$

2. Fuselage, Nacelles, and Stores

An estimate for the contribution of the fuselage, nacelles, and stores can be taken from Hoak (1960)

$$(C_n)_f \equiv \frac{n_{cg_f}}{\frac{1}{2}\rho V_\infty^2 S_w b_w} = \frac{S_f c_f}{S_w b_w} C_{n_f} = (C_{n,\beta})_f \beta \quad (9.11)$$

where the contribution to yaw stability is

$$(C_{n,\beta})_f = 2 \frac{S_f l_f}{S_w b_w} \left[1 - 1.76 \left(\frac{d_f}{c_f} \right)^{3/2} \right] \quad (9.12)$$

3. Propellers

An estimate for the contribution of propellers can be expressed as

$$(C_n)_p = (C_{n0})_p + (C_{n,\alpha})_p \alpha + (C_{n,\beta})_p \beta \quad (9.13)$$

where

$$(C_{n0})_p = \frac{2d_p^3}{S_w b_w} \frac{C_{n_p,\alpha}}{J^2} (\alpha_{0p} - \varepsilon_{d0p}) - \frac{y_{bp}}{b_w} f_T C_D \quad (9.14)$$

$$(C_{n,\alpha})_p = \frac{2d_p^3}{S_w b_w} (1 - \varepsilon_{d,\alpha})_p \frac{C_{n_p,\alpha}}{J^2} \quad (9.15)$$

$$(C_{n,\beta})_p = \frac{2d_p^2 l_p}{S_w b_w} (1 - \varepsilon_{s,\beta})_p \frac{C_{N_p,\alpha}}{J^2} \quad (9.16)$$

D. Estimating Sidewash

Sidewash is positive from left to right. For small sideslip angles, it can be expressed as

$$\varepsilon_s = \varepsilon_{s0} + \varepsilon_{s,\beta} \beta \quad (9.17)$$

Using the same simplified model for downwash as was used in the longitudinal section, we can estimate the sidewash at any point in the flowfield from the relations

$$\begin{aligned} \frac{\partial \varepsilon_s}{\partial \beta}(x, y, z) = & -\frac{\kappa_v x_d C_{L_w}}{\kappa_b \pi^2 R_{A_w}} \left\{ \frac{-2\hat{y}(\hat{z}-1)}{[\hat{y}^2 + (\hat{z}-1)^2]^2} \left[1 + \frac{x_d}{\sqrt{(x_d^2 + \hat{y}^2 + (\hat{z}-1)^2)}} \right] \right. \\ & + \frac{2\hat{y}(\hat{z}+1)}{[\hat{y}^2 + (\hat{z}+1)^2]^2} \left[1 + \frac{x_d}{\sqrt{(x_d^2 + \hat{y}^2 + (\hat{z}+1)^2)}} \right] - \frac{\hat{y}}{\hat{y}^2 + (\hat{z}-1)^2} \left[\frac{x_d(\hat{z}-1)}{[(x_d^2 + \hat{y}^2 + (\hat{z}-1)^2)]^{3/2}} \right] \\ & \left. + \frac{\hat{y}}{\hat{y}^2 + (\hat{z}+1)^2} \left[\frac{x_d(\hat{z}+1)}{[(x_d^2 + \hat{y}^2 + (\hat{z}+1)^2)]^{3/2}} \right] \right\} \quad (9.18) \end{aligned}$$

where \hat{x} , \hat{y} , \hat{z} , κ_v , and κ_b are calculated from Eqs. (8.21) - (8.23), and

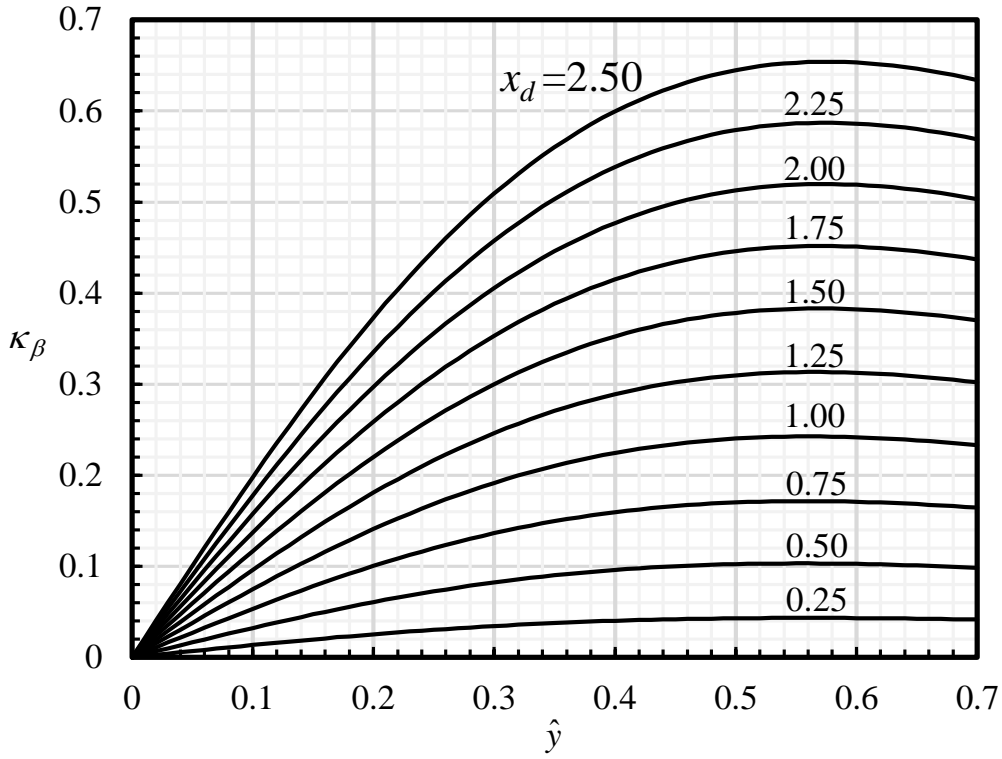
$$x_d = \hat{x} - \tan \Lambda \quad (9.19)$$

Along the symmetry plane of the aircraft ($z = 0$ in the aerodynamic coordinate system), the sidewash gradient can be estimated from

$$\frac{\partial \varepsilon_s}{\partial \beta}(x, y, 0) = -\frac{\kappa_v \kappa_b}{\kappa_b} \frac{C_{L_w}}{R_{A_w}} \quad (9.20)$$

where

$$\kappa_\beta(\hat{x}, \hat{y}, 0) = \frac{4\hat{y}x_d}{\pi^2(\hat{y}^2 + 1)^2} \left[1 + \frac{x_d}{\sqrt{x_d^2 + \hat{y}^2 + 1}} \right] + \frac{2\hat{y}}{\pi^2(\hat{y}^2 + 1)} \left[\frac{x_d^2}{[x_d^2 + \hat{y}^2 + 1]^{3/2}} \right] \quad (9.21)$$



E. Contributions to Roll Trim and Stability

1. Horizontal and Vertical Tail

$$(C_{\ell,\beta})_v = -\eta_v \frac{S_v h_v}{S_w b_w} (1 - \varepsilon_{s,\beta})_v C_{L_v, \alpha} \quad (9.22)$$

$$(C_{\ell,\beta})_h = \pm 0.08 \eta_v \frac{S_v b_h}{S_w b_w} (1 - \varepsilon_{s,\beta})_v C_{L_v, \alpha} \quad (9.23)$$

2. Rudder

$$(C_{\ell,\delta_r})_v = \eta_v \frac{S_v h_v}{S_w b_w} \varepsilon_r C_{L_v, \alpha} \quad (9.24)$$

$$(C_{\ell,\delta_r})_h = \pm 0.08 \eta_v \frac{S_v b_h}{S_w b_w} \varepsilon_r C_{L_v, \alpha} \quad (9.25)$$

F. Steady-Heading Sideslip

For an aircraft with no assymmetries due to propulsion, the general small-angle lateral trim equations simplify to

$$\begin{bmatrix} C_{Y,\delta_a} & C_{Y,\delta_r} & C_W \\ C_{\ell,\delta_a} & C_{\ell,\delta_r} & 0 \\ C_{n,\delta_a} & C_{n,\delta_r} & 0 \end{bmatrix} \begin{Bmatrix} \delta_a \\ \delta_r \\ \phi \end{Bmatrix} = - \begin{Bmatrix} C_{Y,\beta} \\ C_{\ell,\beta} \\ C_{n,\beta} \end{Bmatrix} \beta \quad (9.26)$$

This can be rearranged to yield the bank angle and control deflections required to trim the aircraft, which are proportional to the bank angle

$$\begin{Bmatrix} \delta_a \\ \delta_r \\ \phi \end{Bmatrix} = - \begin{bmatrix} C_{Y,\delta_a} & C_{Y,\delta_r} & C_W \\ C_{\ell,\delta_a} & C_{\ell,\delta_r} & 0 \\ C_{n,\delta_a} & C_{n,\delta_r} & 0 \end{bmatrix}^{-1} \begin{Bmatrix} C_{Y,\beta} \\ C_{\ell,\beta} \\ C_{n,\beta} \end{Bmatrix} \beta = \begin{Bmatrix} \left(\frac{\partial \delta_a}{\partial \beta} \right)_{SHSS} \\ \left(\frac{\partial \delta_r}{\partial \beta} \right)_{SHSS} \\ \left(\frac{\partial \phi}{\partial \beta} \right)_{SHSS} \end{Bmatrix} \beta \quad (9.27)$$

where the steady-heading sideslip gradients are

$$\left(\frac{\partial \delta_a}{\partial \beta} \right)_{SHSS} = \frac{C_{\ell,\delta_r} C_{n,\beta} - C_{\ell,\beta} C_{n,\delta_r}}{C_{\ell,\delta_a} C_{n,\delta_r} - C_{\ell,\delta_r} C_{n,\delta_a}} \quad (9.28)$$

$$\left(\frac{\partial \delta_r}{\partial \beta} \right)_{SHSS} = \frac{C_{\ell,\beta} C_{n,\delta_a} - C_{\ell,\delta_a} C_{n,\beta}}{C_{\ell,\delta_a} C_{n,\delta_r} - C_{\ell,\delta_r} C_{n,\delta_a}} \quad (9.29)$$

$$\left(\frac{\partial \phi}{\partial \beta} \right)_{SHSS} = - \left[C_{Y,\delta_a} \left(\frac{\partial \delta_a}{\partial \beta} \right)_{SHSS} + C_{Y,\delta_r} \left(\frac{\partial \delta_r}{\partial \beta} \right)_{SHSS} + C_{Y,\beta} \right] / C_W \quad (9.30)$$

G. Minimum-Control Airspeed

The general small-angle lateral trim equations can be rearranged to yield

$$\begin{bmatrix} C_{Y,\beta} & C_{Y,\delta_a} & C_{Y,\delta_r} \\ C_{\ell,\beta} & C_{\ell,\delta_a} & C_{\ell,\delta_r} \\ C_{n,\beta} & C_{n,\delta_a} & C_{n,\delta_r} \end{bmatrix} \begin{Bmatrix} \beta \\ \delta_a \\ \delta_r \end{Bmatrix} = - \begin{Bmatrix} (C_Y)_p + C_W \phi \\ (C_\ell)_p \\ (C_n)_p \end{Bmatrix} \quad (9.31)$$

Dividing by the weight coefficient gives

$$\begin{Bmatrix} \beta/C_W \\ \delta_a/C_W \\ \delta_r/C_W \end{Bmatrix} = \begin{bmatrix} C_{Y,\beta} & C_{Y,\delta_a} & C_{Y,\delta_r} \\ C_{\ell,\beta} & C_{\ell,\delta_a} & C_{\ell,\delta_r} \\ C_{n,\beta} & C_{n,\delta_a} & C_{n,\delta_r} \end{bmatrix}^{-1} \begin{Bmatrix} -Y_p/W - \phi \\ -\ell_p/(b_w W) \\ -n_p/(b_w W) \end{Bmatrix} \quad (9.32)$$

Once values for the ratios on the left-hand side of Eq. (9.32) have been found, the minimum-control airspeed for the aileron and rudder are

$$(V_{mc})_{\text{aileron}} = \sqrt{\frac{2W(\delta_a/C_W)}{\rho S_w \delta_{a_{sat}}}} \quad (9.33)$$

$$(V_{mc})_{\text{rudder}} = \sqrt{\frac{2W(\delta_r/C_W)}{\rho S_w \delta_{r_{sat}}}} \quad (9.34)$$

10. Equations of Motion

A. Velocity Definitions

The freestream velocity relative to the aircraft coordinate system can be expressed either as components ($V_{x_b} = u$, $V_{y_b} = v$, $V_{z_b} = w$) or as a magnitude V with two aerodynamic angles (α and β). The definition for the angle of attack is universally accepted

$$\alpha \equiv \tan^{-1} \left(\frac{w}{u} \right) \quad (10.1)$$

There are two definitions for the sideslip angle β . The most common is what Phillips refers to as the *experimental* definition of sideslip angle, which he subscripts with an e

$$\beta = \beta_e \equiv \sin^{-1} \left(\frac{v}{V} \right) \quad (10.2)$$

A secondary definition that is sometimes used and is analogous to angle of attack is what is commonly referred to as the *flank* angle, or what Phillips refers to as the *analytical* definition of sideslip angle

$$\beta_f = \beta_a \equiv \tan^{-1} \left(\frac{v}{u} \right) \quad (10.3)$$

If either form for the sideslip angle is known along with the angle of attack, the other can be found through the relation

$$\tan \beta_a = \frac{\tan \beta_e}{\cos \alpha} \quad (10.4)$$

For small angles of attack, these two definitions are nearly identical. In fact, the small-angle approximation for the sideslip angle is the same for either definition

$$\alpha \approx \frac{w}{u} \quad (10.5)$$

$$\beta \approx \frac{v}{u} \quad (10.6)$$

If the velocity magnitude and aerodynamic angles are known, the velocity components in the body-fixed coordinate system can be found from

$$u = V \frac{\cos \alpha \cos \beta_a}{\sqrt{1 - \sin^2 \alpha \sin^2 \beta_a}} = V \cos \alpha \cos \beta_e \quad (10.7)$$

$$v = V \frac{\cos \alpha \sin \beta_a}{\sqrt{1 - \sin^2 \alpha \sin^2 \beta_a}} = V \sin \beta_e \quad (10.8)$$

$$w = V \frac{\sin \alpha \cos \beta_a}{\sqrt{1 - \sin^2 \alpha \sin^2 \beta_a}} = V \sin \alpha \cos \beta_e \quad (10.9)$$

B. Newton's Second Law

Newton's second law requires

$$\mathbf{F}_S + \mathbf{W} = \frac{d}{dt}(m\mathbf{V}) + \boldsymbol{\omega} \times (m\mathbf{V}) \quad (10.10)$$

and for an aircraft with propellers rotating at a constant angular velocity, the angular momentum equation can be written as

$$\mathbf{M}_S = \frac{d}{dt}([\mathbf{I}]\boldsymbol{\omega}) + \boldsymbol{\omega} \times ([\mathbf{I}]\boldsymbol{\omega} + \mathbf{h}) \quad (10.11)$$

where \mathbf{h} is the angular momentum of spinning rotors relative to the body-fixed coordinate system. The inertia tensor can be written as

$$[\mathbf{I}] = \begin{bmatrix} I_{xx_b} & -I_{xy_b} & -I_{xz_b} \\ -I_{yx_b} & I_{yy_b} & -I_{yz_b} \\ -I_{zx_b} & -I_{zy_b} & I_{zz_b} \end{bmatrix} \quad (10.12)$$

where

$$I_{xx_b} = \iiint_m (y_b^2 + z_b^2) dm \quad (10.13)$$

$$I_{yy_b} = \iiint_m (x_b^2 + z_b^2) dm \quad (10.14)$$

$$I_{zz_b} = \iiint_m (x_b^2 + y_b^2) dm \quad (10.15)$$

$$I_{xy_b} = I_{yx_b} = \iiint_m x_b y_b dm \quad (10.16)$$

$$I_{yz_b} = I_{zy_b} = \iiint_m y_b z_b dm \quad (10.17)$$

$$I_{xz_b} = I_{zx_b} = \iiint_m x_b z_b dm \quad (10.18)$$

Equations (10.10) and (10.11) can be rearranged to yield

$$\frac{W}{g} \begin{Bmatrix} \dot{u} \\ \dot{v} \\ \dot{w} \end{Bmatrix} = \begin{Bmatrix} F_{x_b} + W_{x_b} + (rv - qw)W/g \\ F_{y_b} + W_{y_b} + (pw - ru)W/g \\ F_{z_b} + W_{z_b} + (qu - pv)W/g \end{Bmatrix} \quad (10.19)$$

$$\begin{bmatrix} I_{xx_b} & -I_{xy_b} & -I_{xz_b} \\ -I_{xy_b} & I_{yy_b} & -I_{yz_b} \\ -I_{xz_b} & -I_{yz_b} & I_{zz_b} \end{bmatrix} \begin{Bmatrix} \dot{p} \\ \dot{q} \\ \dot{r} \end{Bmatrix} = \begin{Bmatrix} M_{x_b} \\ M_{y_b} \\ M_{z_b} \end{Bmatrix} + \begin{bmatrix} 0 & -h_{z_b} & h_{y_b} \\ h_{z_b} & 0 & -h_{x_b} \\ -h_{y_b} & h_{x_b} & 0 \end{bmatrix} \begin{Bmatrix} p \\ q \\ r \end{Bmatrix} + \begin{Bmatrix} (I_{yy_b} - I_{zz_b})qr + I_{yz_b}(q^2 - r^2) + I_{xz_b}pq - I_{xy_b}pr \\ (I_{zz_b} - I_{xx_b})pr + I_{xz_b}(r^2 - p^2) + I_{xy_b}qr - I_{yz_b}pq \\ (I_{xx_b} - I_{yy_b})pq + I_{xy_b}(p^2 - q^2) + I_{yz_b}pr - I_{xz_b}qr \end{Bmatrix} \quad (10.20)$$

where F_b and M_b are the aerodynamic forces and moments including thrust. For an aircraft that is symmetric about the $x - z$ plane and neglecting any gyroscopic effects, Eqs. (10.19) and (10.20) reduce to

$$\frac{W}{g} \begin{Bmatrix} \dot{u} \\ \dot{v} \\ \dot{w} \end{Bmatrix} = \begin{Bmatrix} F_{x_b} + W_{x_b} + (rv - qw)W/g \\ F_{y_b} + W_{y_b} + (pw - ru)W/g \\ F_{z_b} + W_{z_b} + (qu - pv)W/g \end{Bmatrix} \quad (10.21)$$

$$\begin{bmatrix} I_{xx_b} & 0 & -I_{xz_b} \\ 0 & I_{yy_b} & 0 \\ -I_{xz_b} & 0 & I_{zz_b} \end{bmatrix} \begin{Bmatrix} \dot{p} \\ \dot{q} \\ \dot{r} \end{Bmatrix} = \begin{Bmatrix} M_{x_b} + (I_{yy_b} - I_{zz_b})qr + I_{xz_b}pq \\ M_{y_b} + (I_{zz_b} - I_{xx_b})pr + I_{xz_b}(r^2 - p^2) \\ M_{z_b} + (I_{xx_b} - I_{yy_b})pq - I_{xz_b}qr \end{Bmatrix} \quad (10.22)$$

C. Euler Angle Orientation

The Euler angles are

$$\phi = \text{Bank Angle}$$

$$\theta = \text{Elevation Angle}$$

$$\psi = \text{Azimuth Angle}$$

They are defined with limits

$$\begin{aligned}-180^\circ < \phi &\leq +180^\circ \\ -90^\circ &\leq \theta \leq +90^\circ \\ 0^\circ &\leq \psi < +360^\circ\end{aligned}$$

To obtain the correct rotation matrix, the angles are applied in the order ψ, θ, ϕ . Any vector in body-fixed coordinates can be obtained in earth-fixed coordinates from the rotation

$$\begin{pmatrix} v_{x_f} \\ v_{y_f} \\ v_{z_f} \end{pmatrix} = \begin{bmatrix} C_\theta C_\psi & S_\phi S_\theta C_\psi - C_\phi S_\psi & C_\phi S_\theta C_\psi + S_\phi S_\psi \\ C_\theta S_\psi & S_\phi S_\theta S_\psi + C_\phi C_\psi & C_\phi S_\theta S_\psi - S_\phi C_\psi \\ -S_\theta & S_\phi C_\theta & C_\phi C_\theta \end{bmatrix} \begin{pmatrix} v_{x_b} \\ v_{y_b} \\ v_{z_b} \end{pmatrix} \quad (10.23)$$

Any vector in earth-fixed coordinates can be obtained in body-fixed coordinates from the rotation

$$\begin{pmatrix} v_{x_b} \\ v_{y_b} \\ v_{z_b} \end{pmatrix} = \begin{bmatrix} C_\theta C_\psi & C_\theta S_\psi & -S_\theta \\ S_\phi S_\theta C_\psi - C_\phi S_\psi & S_\phi S_\theta S_\psi + C_\phi C_\psi & S_\phi C_\theta \\ C_\phi S_\theta C_\psi + S_\phi S_\psi & C_\phi S_\theta S_\psi - S_\phi C_\psi & C_\phi C_\theta \end{bmatrix} \begin{pmatrix} v_{x_f} \\ v_{y_f} \\ v_{z_f} \end{pmatrix} \quad (10.24)$$

For example, the velocity of the aircraft in body-fixed coordinates can be used to obtain the velocity of the aircraft relative to the ground through the rotation

$$\begin{pmatrix} \dot{x}_f \\ \dot{y}_f \\ \dot{z}_f \end{pmatrix} = \begin{bmatrix} C_\theta C_\psi & S_\phi S_\theta C_\psi - C_\phi S_\psi & C_\phi S_\theta C_\psi + S_\phi S_\psi \\ C_\theta S_\psi & S_\phi S_\theta S_\psi + C_\phi C_\psi & C_\phi S_\theta S_\psi - S_\phi C_\psi \\ -S_\theta & S_\phi C_\theta & C_\phi C_\theta \end{bmatrix} \begin{pmatrix} u \\ v \\ w \end{pmatrix} + \begin{pmatrix} V_{w,x_f} \\ V_{w,y_f} \\ V_{w,z_f} \end{pmatrix} \quad (10.25)$$

Likewise, the weight vector can be obtained in body-fixed coordinates

$$\begin{pmatrix} W_{x_b} \\ W_{y_b} \\ W_{z_b} \end{pmatrix} = W \begin{pmatrix} -\sin(\theta) \\ \sin(\phi) \cos(\theta) \\ \cos(\phi) \cos(\theta) \end{pmatrix} \quad (10.26)$$

Using a similar transformation method, the change in orientation can be found as a function of the current orientation and rotation rates of the aircraft

$$\begin{pmatrix} \dot{\phi} \\ \dot{\theta} \\ \dot{\psi} \end{pmatrix} = \begin{bmatrix} 1 & S_\phi S_\theta / C_\theta & C_\phi S_\theta / C_\theta \\ 0 & C_\phi & -S_\phi \\ 0 & S_\phi / C_\theta & C_\phi / C_\theta \end{bmatrix} \begin{pmatrix} p \\ q \\ r \end{pmatrix} \quad (10.27)$$

D. 6-DOF Rigid-Body Equations of Motion Summary

For an aircraft that is symmetric about the $x - z$ plane, and neglecting gyroscopic effects, the equations of motion can be summarized as

$$V = \sqrt{u^2 + v^2 + w^2} \quad (10.28)$$

$$\alpha \equiv \tan^{-1} \left(\frac{w}{u} \right) \quad (10.29)$$

$$\beta = \beta_e \equiv \sin^{-1} \left(\frac{v}{V} \right), \quad \beta_f = \beta_a \equiv \tan^{-1} \left(\frac{v}{u} \right) \quad (10.30)$$

$$\begin{pmatrix} \dot{u} \\ \dot{v} \\ \dot{w} \end{pmatrix} = \frac{g}{W} \begin{pmatrix} F_{x_b} \\ F_{y_b} \\ F_{z_b} \end{pmatrix} + g \begin{pmatrix} -S_\theta \\ S_\phi C_\theta \\ C_\phi C_\theta \end{pmatrix} + \begin{pmatrix} rv - qw \\ pw - ru \\ qu - pv \end{pmatrix} \quad (10.31)$$

$$\begin{pmatrix} \dot{p} \\ \dot{q} \\ \dot{r} \end{pmatrix} = \begin{bmatrix} I_{xx_b} & 0 & -I_{xz_b} \\ 0 & I_{yy_b} & 0 \\ -I_{zx_b} & 0 & I_{zz_b} \end{bmatrix}^{-1} \begin{pmatrix} M_{x_b} + (I_{yy_b} - I_{zz_b})qr + I_{xz_b}pq \\ M_{y_b} + (I_{zz_b} - I_{xx_b})pr + I_{xz_b}(r^2 - p^2) \\ M_{z_b} + (I_{xx_b} - I_{yy_b})pq - I_{xz_b}qr \end{pmatrix} \quad (10.32)$$

$$\begin{Bmatrix} \dot{x}_f \\ \dot{y}_f \\ \dot{z}_f \end{Bmatrix} = \begin{bmatrix} C_\theta C_\psi & S_\phi S_\theta C_\psi - C_\phi S_\psi & C_\phi S_\theta C_\psi + S_\phi S_\psi \\ C_\theta S_\psi & S_\phi S_\theta S_\psi + C_\phi C_\psi & C_\phi S_\theta S_\psi - S_\phi C_\psi \\ -S_\theta & S_\phi C_\theta & C_\phi C_\theta \end{bmatrix} \begin{Bmatrix} u \\ v \\ w \end{Bmatrix} + \begin{Bmatrix} V_{wx_f} \\ V_{wy_f} \\ V_{wz_f} \end{Bmatrix} \quad (10.33)$$

$$\begin{Bmatrix} \dot{\phi} \\ \dot{\theta} \\ \dot{\psi} \end{Bmatrix} = \begin{bmatrix} 1 & S_\phi S_\theta / C_\theta & C_\phi S_\theta / C_\theta \\ 0 & C_\phi & -S_\phi \\ 0 & S_\phi / C_\theta & C_\phi / C_\theta \end{bmatrix} \begin{Bmatrix} p \\ q \\ r \end{Bmatrix} \quad (10.34)$$

Equations (10.31) and (10.32) are Newton's second law. The pseudo aerodynamic forces and moments in these two equations include thrust, and are functions of the velocity and aerodynamic angles, as well as pilot control inputs. Equations (10.33) and (10.34) are kinematic transformation equations based on the aircraft orientation. At any point in time, all the information on the right of Eqs. (10.31) – (10.34) is known. The left-hand side of these equations represents the change of the state of the aircraft with respect to time, and can then be integrated forward to find the new state of the aircraft.

E. Linearized Equations of Motion

$$\begin{aligned} u &= u_o + \Delta u & v &= v_o + \Delta v & w &= w_o + \Delta w \\ p &= p_o + \Delta p & q &= q_o + \Delta q & r &= r_o + \Delta r \\ x_f &= x_o + \Delta x_f & y_f &= y_o + \Delta y_f & z_f &= z_o + \Delta z_f \\ \phi &= \phi_o + \Delta \phi & \theta &= \theta_o + \Delta \theta & \psi &= \psi_o + \Delta \psi \\ F_{x_b} &= F_{x_b o} + \Delta F_{x_b} & F_{y_b} &= F_{y_b o} + \Delta F_{y_b} & F_{z_b} &= F_{z_b o} + \Delta F_{z_b} \\ W_{x_b} &= W_{x_b o} + \Delta W_{x_b} & W_{y_b} &= W_{y_b o} + \Delta W_{y_b} & W_{z_b} &= W_{z_b o} + \Delta W_{z_b} \\ M_{x_b} &= M_{x_b o} + \Delta M_{x_b} & M_{y_b} &= M_{y_b o} + \Delta M_{y_b} & M_{z_b} &= M_{z_b o} + \Delta M_{z_b} \\ \delta_a &= \delta_{ao} + \Delta \delta_a & \delta_e &= \delta_{eo} + \Delta \delta_e & \delta_r &= \delta_{ro} + \Delta \delta_r \end{aligned} \quad (10.35)$$

For the particular solution, we will choose steady-level flight at a velocity of V_o with zero sideslip, and zero angular rates. We will align the x -axis of the aircraft with the direction of flight ($u_o = V_o$). For simplicity, we will also align the x -axis of the aircraft with the x -axis of the earth-fixed frame, since the dynamics of the aircraft do not depend on the direction we are flying. This gives

$$v_o = w_o = p_o = q_o = r_o = \phi_o = \psi_o = F_{y_b o} = W_{y_b o} = M_{x_b o} = M_{y_b o} = M_{z_b o} = 0 \quad (10.36)$$

Using these simplifications along with Eq. (10.35) in Eqs. (10.21) and (10.22) and dropping second-order disturbance terms gives

$$\begin{bmatrix} W/g & 0 & 0 & 0 & 0 & 0 \\ 0 & W/g & 0 & 0 & 0 & 0 \\ 0 & 0 & W/g & 0 & 0 & 0 \\ 0 & 0 & 0 & I_{xx_b} & 0 & -I_{xz_b} \\ 0 & 0 & 0 & 0 & I_{yy_b} & 0 \\ 0 & 0 & 0 & -I_{xz_b} & 0 & I_{zz_b} \end{bmatrix} \begin{Bmatrix} \Delta \dot{u} \\ \Delta \dot{v} \\ \Delta \dot{w} \\ \Delta \dot{p} \\ \Delta \dot{q} \\ \Delta \dot{r} \end{Bmatrix} = \begin{Bmatrix} \Delta F_{x_b} + \Delta W_{x_b} \\ \Delta F_{y_b} + \Delta W_{y_b} - \Delta r V_o W/g \\ \Delta F_{z_b} + \Delta W_{z_b} - \Delta q V_o W/g \\ \Delta M_{x_b} \\ \Delta M_{y_b} \\ \Delta M_{z_b} \end{Bmatrix} \quad (10.37)$$

The pseudo aerodynamic force and moment derivatives are functions of the velocity, angular rates, acceleration,

and control-surface deflections. Expanding these in a Taylor series and retaining only the linear terms gives

$$\begin{aligned} \begin{Bmatrix} \Delta F_{x_b} \\ \Delta F_{y_b} \\ \Delta F_{z_b} \end{Bmatrix} &= \begin{bmatrix} \frac{\partial F_{x_b}}{\partial u} & \frac{\partial F_{x_b}}{\partial v} & \frac{\partial F_{x_b}}{\partial w} \\ \frac{\partial F_{y_b}}{\partial u} & \frac{\partial F_{y_b}}{\partial v} & \frac{\partial F_{y_b}}{\partial w} \\ \frac{\partial F_{z_b}}{\partial u} & \frac{\partial F_{z_b}}{\partial v} & \frac{\partial F_{z_b}}{\partial w} \end{bmatrix} \begin{Bmatrix} \Delta u \\ \Delta v \\ \Delta w \end{Bmatrix} + \begin{bmatrix} \frac{\partial F_{x_b}}{\partial p} & \frac{\partial F_{x_b}}{\partial q} & \frac{\partial F_{x_b}}{\partial r} \\ \frac{\partial F_{y_b}}{\partial p} & \frac{\partial F_{y_b}}{\partial q} & \frac{\partial F_{y_b}}{\partial r} \\ \frac{\partial F_{z_b}}{\partial p} & \frac{\partial F_{z_b}}{\partial q} & \frac{\partial F_{z_b}}{\partial r} \end{bmatrix} \begin{Bmatrix} \Delta p \\ \Delta q \\ \Delta r \end{Bmatrix} \\ &+ \begin{bmatrix} \frac{\partial F_{x_b}}{\partial \dot{u}} & \frac{\partial F_{x_b}}{\partial \dot{v}} & \frac{\partial F_{x_b}}{\partial \dot{w}} \\ \frac{\partial F_{y_b}}{\partial \dot{u}} & \frac{\partial F_{y_b}}{\partial \dot{v}} & \frac{\partial F_{y_b}}{\partial \dot{w}} \\ \frac{\partial F_{z_b}}{\partial \dot{u}} & \frac{\partial F_{z_b}}{\partial \dot{v}} & \frac{\partial F_{z_b}}{\partial \dot{w}} \end{bmatrix} \begin{Bmatrix} \Delta \dot{u} \\ \Delta \dot{v} \\ \Delta \dot{w} \end{Bmatrix} + \begin{bmatrix} \frac{\partial F_{x_b}}{\partial \delta_a} & \frac{\partial F_{x_b}}{\partial \delta_e} & \frac{\partial F_{x_b}}{\partial \delta_r} \\ \frac{\partial F_{y_b}}{\partial \delta_a} & \frac{\partial F_{y_b}}{\partial \delta_e} & \frac{\partial F_{y_b}}{\partial \delta_r} \\ \frac{\partial F_{z_b}}{\partial \delta_a} & \frac{\partial F_{z_b}}{\partial \delta_e} & \frac{\partial F_{z_b}}{\partial \delta_r} \end{bmatrix} \begin{Bmatrix} \Delta \delta_a \\ \Delta \delta_e \\ \Delta \delta_r \end{Bmatrix} \end{aligned} \quad (10.38)$$

$$\begin{aligned} \begin{Bmatrix} \Delta M_{x_b} \\ \Delta M_{y_b} \\ \Delta M_{z_b} \end{Bmatrix} &= \begin{bmatrix} \frac{\partial M_{x_b}}{\partial u} & \frac{\partial M_{x_b}}{\partial v} & \frac{\partial M_{x_b}}{\partial w} \\ \frac{\partial M_{y_b}}{\partial u} & \frac{\partial M_{y_b}}{\partial v} & \frac{\partial M_{y_b}}{\partial w} \\ \frac{\partial M_{z_b}}{\partial u} & \frac{\partial M_{z_b}}{\partial v} & \frac{\partial M_{z_b}}{\partial w} \end{bmatrix} \begin{Bmatrix} \Delta u \\ \Delta v \\ \Delta w \end{Bmatrix} + \begin{bmatrix} \frac{\partial M_{x_b}}{\partial p} & \frac{\partial M_{x_b}}{\partial q} & \frac{\partial M_{x_b}}{\partial r} \\ \frac{\partial M_{y_b}}{\partial p} & \frac{\partial M_{y_b}}{\partial q} & \frac{\partial M_{y_b}}{\partial r} \\ \frac{\partial M_{z_b}}{\partial p} & \frac{\partial M_{z_b}}{\partial q} & \frac{\partial M_{z_b}}{\partial r} \end{bmatrix} \begin{Bmatrix} \Delta p \\ \Delta q \\ \Delta r \end{Bmatrix} \\ &+ \begin{bmatrix} \frac{\partial M_{x_b}}{\partial \dot{u}} & \frac{\partial M_{x_b}}{\partial \dot{v}} & \frac{\partial M_{x_b}}{\partial \dot{w}} \\ \frac{\partial M_{y_b}}{\partial \dot{u}} & \frac{\partial M_{y_b}}{\partial \dot{v}} & \frac{\partial M_{y_b}}{\partial \dot{w}} \\ \frac{\partial M_{z_b}}{\partial \dot{u}} & \frac{\partial M_{z_b}}{\partial \dot{v}} & \frac{\partial M_{z_b}}{\partial \dot{w}} \end{bmatrix} \begin{Bmatrix} \Delta \dot{u} \\ \Delta \dot{v} \\ \Delta \dot{w} \end{Bmatrix} + \begin{bmatrix} \frac{\partial M_{x_b}}{\partial \delta_a} & \frac{\partial M_{x_b}}{\partial \delta_e} & \frac{\partial M_{x_b}}{\partial \delta_r} \\ \frac{\partial M_{y_b}}{\partial \delta_a} & \frac{\partial M_{y_b}}{\partial \delta_e} & \frac{\partial M_{y_b}}{\partial \delta_r} \\ \frac{\partial M_{z_b}}{\partial \delta_a} & \frac{\partial M_{z_b}}{\partial \delta_e} & \frac{\partial M_{z_b}}{\partial \delta_r} \end{bmatrix} \begin{Bmatrix} \Delta \delta_a \\ \Delta \delta_e \\ \Delta \delta_r \end{Bmatrix} \end{aligned} \quad (10.39)$$

Many of these terms can be eliminated on the basis of symmetry.

The weight vector is given in Eq. (10.26). Retaining the linear terms of a Taylor series expansion for the weight vector with changes in orientation and evaluating these derivatives at the known particular solution gives

$$\begin{Bmatrix} \Delta W_{x_b} \\ \Delta W_{y_b} \\ \Delta W_{z_b} \end{Bmatrix} = \begin{bmatrix} \frac{\partial W_{x_b}}{\partial \phi} & \frac{\partial W_{x_b}}{\partial \theta} & \frac{\partial W_{x_b}}{\partial \psi} \\ \frac{\partial W_{y_b}}{\partial \phi} & \frac{\partial W_{y_b}}{\partial \theta} & \frac{\partial W_{y_b}}{\partial \psi} \\ \frac{\partial W_{z_b}}{\partial \phi} & \frac{\partial W_{z_b}}{\partial \theta} & \frac{\partial W_{z_b}}{\partial \psi} \end{bmatrix} \begin{Bmatrix} \Delta \phi \\ \Delta \theta \\ \Delta \psi \end{Bmatrix} = \begin{bmatrix} 0 & -W \cos \theta_o & 0 \\ W \cos \theta_o & 0 & 0 \\ 0 & -W \sin \theta_o & 0 \end{bmatrix} \begin{Bmatrix} \Delta \phi \\ \Delta \theta \\ \Delta \psi \end{Bmatrix} \quad (10.40)$$

Performing a similar analysis on the kinematic transformation equations and combining these with the results of Eq. (10.37) gives the linearized equations of motion. These can be divided into longitudinal and lateral equations, since within small-disturbance theory, they do not couple.

1. Linearized Longitudinal Equations

$$\begin{aligned} \begin{bmatrix} W/g - F_{x_b, \dot{u}} & -F_{x_b, \dot{w}} & 0 & 0 & 0 & 0 \\ -F_{z_b, \dot{u}} & W/g - F_{z_b, \dot{w}} & 0 & 0 & 0 & 0 \\ -M_{y_b, \dot{u}} & -M_{y_b, \dot{w}} & I_{yy_b} & 0 & 0 & 0 \\ 0 & 0 & 0 & 1 & 0 & 0 \\ 0 & 0 & 0 & 0 & 1 & 0 \\ 0 & 0 & 0 & 0 & 0 & 1 \end{bmatrix} \begin{Bmatrix} \Delta \dot{u} \\ \Delta \dot{w} \\ \Delta \dot{q} \\ \Delta \dot{x}_f \\ \Delta \dot{z}_f \\ \Delta \dot{\theta} \end{Bmatrix} &= \begin{Bmatrix} F_{x_b, \delta_e} \\ F_{z_b, \delta_e} \\ M_{y_b, \delta_e} \\ 0 \\ 0 \\ 0 \end{Bmatrix} \Delta \delta_e \\ &+ \begin{bmatrix} F_{x_b, u} & F_{x_b, w} & F_{x_b, q} & 0 & 0 & -W \cos \theta_o \\ F_{z_b, u} & F_{z_b, w} & F_{z_b, q} + V_o W/g & 0 & 0 & -W \sin \theta_o \\ M_{y_b, u} & M_{y_b, w} & M_{y_b, q} & 0 & 0 & 0 \\ \cos \theta_o & \sin \theta_o & 0 & 0 & 0 & -V_o \sin \theta_o \\ -\sin \theta_o & \cos \theta_o & 0 & 0 & 0 & -V_o \cos \theta_o \\ 0 & 0 & 1 & 0 & 0 & 0 \end{bmatrix} \begin{Bmatrix} \Delta u \\ \Delta w \\ \Delta q \\ \Delta x_f \\ \Delta z_f \\ \Delta \theta \end{Bmatrix} \end{aligned} \quad (10.41)$$

2. Linearized Lateral Equations

$$\begin{aligned}
& \begin{bmatrix} W/g & 0 & 0 & 0 & 0 & 0 \\ 0 & I_{xx_b} & -I_{xz_b} & 0 & 0 & 0 \\ 0 & -I_{xz_b} & I_{zz_b} & 0 & 0 & 0 \\ 0 & 0 & 0 & 1 & 0 & 0 \\ 0 & 0 & 0 & 0 & 1 & 0 \\ 0 & 0 & 0 & 0 & 0 & 1 \end{bmatrix} \begin{bmatrix} \Delta\dot{v} \\ \Delta\dot{p} \\ \Delta\dot{r} \\ \Delta\dot{y}_f \\ \Delta\dot{\phi} \\ \Delta\dot{\psi} \end{bmatrix} = \begin{Bmatrix} F_{y_b, \delta_a} & F_{y_b, \delta_r} \\ M_{x_b, \delta_a} & M_{x_b, \delta_r} \\ M_{z_b, \delta_a} & M_{z_b, \delta_r} \\ 0 & 0 \\ 0 & 0 \\ 0 & 0 \end{Bmatrix} \begin{Bmatrix} \Delta\delta_a \\ \Delta\delta_r \end{Bmatrix} \\
& + \begin{bmatrix} F_{y_b, v} & F_{y_b, p} & F_{y_b, r} - V_o W/g & 0 & W \cos \theta_o & 0 \\ M_{x_b, v} & M_{x_b, p} & M_{x_b, r} & 0 & 0 & 0 \\ M_{z_b, v} & M_{z_b, p} & M_{z_b, r} & 0 & 0 & 0 \\ 1 & 0 & 0 & 0 & 0 & V_o \cos \theta_o \\ 0 & 1 & \tan \theta_o & 0 & 0 & 0 \\ 0 & 0 & \sec \theta_o & 0 & 0 & 0 \end{bmatrix} \begin{Bmatrix} \Delta v \\ \Delta p \\ \Delta r \\ \Delta y_f \\ \Delta \phi \\ \Delta \psi \end{Bmatrix} \quad (10.42)
\end{aligned}$$

F. Force and Moment Derivatives

Wind tunnel experiments or computational fluid dynamics could be used to evaluate the pseudo aerodynamic force and moment derivatives required in Eqs. (10.41) and (10.42). However, these derivatives are not in a form that is particularly useful for aerodynamic analysis. These forces are traditionally written as

$$\begin{Bmatrix} F_{x_b} \\ F_{y_b} \\ F_{z_b} \end{Bmatrix} = \frac{1}{2} \rho V^2 S_w \begin{Bmatrix} C_X \\ C_Y \\ C_Z \end{Bmatrix} + T \begin{Bmatrix} \cos \alpha_{T0} \\ 0 \\ \sin \alpha_{T0} \end{Bmatrix} \quad (10.43)$$

$$\begin{Bmatrix} M_{x_b} \\ M_{y_b} \\ M_{z_b} \end{Bmatrix} = \frac{1}{2} \rho V^2 S_w \begin{Bmatrix} C_\ell b_w \\ C_m \bar{c}_w \\ C_n b_w \end{Bmatrix} + T \begin{Bmatrix} 0 \\ z_T \cos \alpha_{T0} + x_T \sin \alpha_{T0} \\ 0 \end{Bmatrix} \quad (10.44)$$

The force coefficients are traditionally written in terms of lift and drag coefficients as

$$\begin{Bmatrix} C_X \\ C_Y \\ C_Z \end{Bmatrix} = \begin{Bmatrix} C_L \sin \alpha - C_D \cos \alpha \\ C_Y \\ -C_L \cos \alpha - C_D \sin \alpha \end{Bmatrix} \quad (10.45)$$

At the equilibrium state we have chosen, the aerodynamic force and moment coefficients are

$$\begin{Bmatrix} C_X \\ C_Y \\ C_Z \\ C_\ell \\ C_m \\ C_n \end{Bmatrix} = \begin{Bmatrix} -C_{D0} \\ 0 \\ -C_{L0} \\ 0 \\ C_{m0} \\ 0 \end{Bmatrix} \quad (10.46)$$

where

$$C_{L0} = \frac{W \cos \theta_o}{\frac{1}{2} \rho V_o^2 S_w \cos \phi_o} \quad (10.47)$$

and

$$C_{D0} = C_{D0} + C_{D1} C_{L0} + C_{D2} C_{L0}^2 \quad (10.48)$$

1. Derivatives with respect to Velocity

Equations (10.41) and (10.42) require derivatives with respect to velocities in the body-fixed coordinate system. However, aerodynamic derivatives are traditionally known in terms of the total velocity, the angle of attack, and the sideslip velocity. From Eqs. (10.28) – (10.30), using the small-angle approximation and evaluating the derivatives at the equilibrium state ($u_o = V_o$, $v_o = w_o = 0$) gives

$$\frac{\partial V}{\partial u} = \frac{u}{\sqrt{u^2 + v^2 + w^2}} = 1, \quad \frac{\partial V}{\partial v} = \frac{v}{\sqrt{u^2 + v^2 + w^2}} = 0, \quad \frac{\partial V}{\partial w} = \frac{w}{\sqrt{u^2 + v^2 + w^2}} = 0 \quad (10.49)$$

$$\frac{\partial \alpha}{\partial u} \approx -\frac{w}{u^2} = 0, \quad \frac{\partial \alpha}{\partial v} = 0, \quad \frac{\partial \alpha}{\partial w} \approx \frac{1}{u} = \frac{1}{V_o} \quad (10.50)$$

$$\frac{\partial \beta}{\partial u} \approx -\frac{v}{u^2} = 0, \quad \frac{\partial \beta}{\partial v} \approx \frac{1}{u} = \frac{1}{V_o}, \quad \frac{\partial \beta}{\partial w} = 0 \quad (10.51)$$

Given an aerodynamic parameter that is a known function of $f(V, \alpha, \beta)$, we can compute the derivatives of that parameter with respect to u , v , and w at the equilibrium state by applying Eqs. (10.49)–(10.51)

$$\frac{\partial f}{\partial u} = \frac{\partial f}{\partial V} \frac{\partial V}{\partial u} + \frac{\partial f}{\partial \alpha} \frac{\partial \alpha}{\partial u} + \frac{\partial f}{\partial \beta} \frac{\partial \beta}{\partial u} = \frac{\partial f}{\partial V} \quad (10.52)$$

$$\frac{\partial f}{\partial v} = \frac{\partial f}{\partial V} \frac{\partial V}{\partial v} + \frac{\partial f}{\partial \alpha} \frac{\partial \alpha}{\partial v} + \frac{\partial f}{\partial \beta} \frac{\partial \beta}{\partial v} = \frac{1}{V_o} \frac{\partial f}{\partial \beta} \quad (10.53)$$

$$\frac{\partial f}{\partial w} = \frac{\partial f}{\partial V} \frac{\partial V}{\partial w} + \frac{\partial f}{\partial \alpha} \frac{\partial \alpha}{\partial w} + \frac{\partial f}{\partial \beta} \frac{\partial \beta}{\partial w} = \frac{1}{V_o} \frac{\partial f}{\partial \alpha} \quad (10.54)$$

Using Eqs. (10.43)–(10.46), and (10.52)–(10.54) and evaluating at the equilibrium condition gives the following derivatives.

Derivatives with respect to u

$$\begin{aligned} F_{x_b,u} &= -\frac{1}{2} \rho V_o^2 S_w \left(\frac{2C_{D0}}{V_o} \right) + T_{,V} \cos \alpha_{T0} \\ F_{y_b,u} &= 0 \\ F_{z_b,u} &= -\frac{1}{2} \rho V_o^2 S_w \left(\frac{2C_{L0}}{V_o} \right) - T_{,V} \sin \alpha_{T0} \\ M_{x_b,u} &= 0 \\ M_{y_b,u} &= \frac{1}{2} \rho V_o^2 S_w \left(\frac{2\bar{c}_w C_{mo}}{V_o} \right) + z_{T0} T_{,V} \\ M_{z_b,u} &= 0 \end{aligned} \quad (10.55)$$

where

$$z_{T0} = z_T \cos \alpha_{T0} + x_T \sin \alpha_{T0} \quad (10.56)$$

Derivatives with respect to v

$$\begin{aligned} F_{x_b,v} &= 0 \\ F_{y_b,v} &= \frac{1}{2} \rho V_o^2 S_w \left(\frac{C_{Y,\beta}}{V_o} \right) \\ F_{z_b,v} &= 0 \\ M_{x_b,v} &= \frac{1}{2} \rho V_o^2 S_w \left(\frac{b_w C_{\ell,\beta}}{V_o} \right) \\ M_{y_b,v} &= 0 \\ M_{z_b,v} &= \frac{1}{2} \rho V_o^2 S_w \left(\frac{b_w C_{n,\beta}}{V_o} \right) \end{aligned} \quad (10.57)$$

Derivatives with respect to w

$$\begin{aligned}
F_{x_b,w} &= \frac{1}{2}\rho V_o^2 S_w \left(\frac{C_{Lo} - C_{D,\alpha}}{V_o} \right) \\
F_{y_b,w} &= 0 \\
F_{z_b,w} &= \frac{1}{2}\rho V_o^2 S_w \left(\frac{-C_{Do} - C_{L,\alpha}}{V_o} \right) \\
M_{x_b,w} &= 0 \\
M_{y_b,w} &= \frac{1}{2}\rho V_o^2 S_w \left(\frac{\bar{c}_w C_{m,\alpha}}{V_o} \right) \\
M_{z_b,w} &= 0
\end{aligned} \tag{10.58}$$

where

$$C_{D,\alpha} = C_{D1}C_{L,\alpha} + 2C_{D2}C_{Lo}C_{L,\alpha} \tag{10.59}$$

2. Derivatives with respect to Rotation Rates

Derivatives with respect to p

$$\begin{aligned}
F_{x_b,p} &= 0 \\
F_{y_b,p} &= \frac{1}{2}\rho V_o^2 S_w C_{Y,p} \\
F_{z_b,p} &= 0 \\
M_{x_b,p} &= \frac{1}{2}\rho V_o^2 S_w b_w C_{\ell,p} \\
M_{y_b,p} &= 0 \\
M_{z_b,p} &= \frac{1}{2}\rho V_o^2 S_w b_w C_{n,p}
\end{aligned} \tag{10.60}$$

Derivatives with respect to q

$$\begin{aligned}
F_{x_b,q} &= -\frac{1}{2}\rho V_o^2 S_w C_{D,q} \\
F_{y_b,q} &= 0 \\
F_{z_b,q} &= -\frac{1}{2}\rho V_o^2 S_w C_{L,q} \\
M_{x_b,q} &= 0 \\
M_{y_b,q} &= \frac{1}{2}\rho V_o^2 S_w \bar{c}_w C_{m,q} \\
M_{z_b,q} &= 0
\end{aligned} \tag{10.61}$$

Derivatives with respect to r

$$\begin{aligned}
F_{x_b,r} &= 0 \\
F_{y_b,r} &= \frac{1}{2}\rho V_o^2 S_w C_{Y,r} \\
F_{z_b,r} &= 0 \\
M_{x_b,r} &= \frac{1}{2}\rho V_o^2 S_w b_w C_{\ell,r} \\
M_{y_b,r} &= 0 \\
M_{z_b,r} &= \frac{1}{2}\rho V_o^2 S_w b_w C_{n,r}
\end{aligned} \tag{10.62}$$

3. Derivatives with respect to Translational Acceleration

Derivatives with respect to translational acceleration can be difficult to obtain, but can be computed from unsteady CFD simulations. As a first approximation, we can assume that many of these are exactly zero for a symmetric aircraft, or negligible.

Derivatives with respect to \dot{u}

$$\begin{aligned}
F_{x_b, \dot{u}} &= -\frac{1}{2}\rho V_o^2 S_w C_{D, \dot{u}} \\
F_{y_b, \dot{u}} &= 0 \\
F_{z_b, \dot{u}} &= -\frac{1}{2}\rho V_o^2 S_w C_{L, \dot{u}} \\
M_{x_b, \dot{u}} &= 0 \\
M_{y_b, \dot{u}} &= \frac{1}{2}\rho V_o^2 S_w \bar{c}_w C_{m, \dot{u}} \\
M_{z_b, \dot{u}} &= 0
\end{aligned} \tag{10.63}$$

Derivatives with respect to \dot{v}

$$F_{x_b, \dot{v}} = F_{y_b, \dot{v}} = F_{z_b, \dot{v}} = M_{x_b, \dot{v}} = M_{y_b, \dot{v}} = M_{z_b, \dot{v}} = 0 \tag{10.64}$$

Derivatives with respect to \dot{w}

Derivatives with respect to \dot{w} can be pronounced on aircraft with a traditional horizontal tail due to the time it takes the shed vorticity from the main wing to propagate downstream to the tail. An estimate for derivatives for a conventional aircraft can be obtained from

$$\begin{aligned}
F_{x_b, \dot{w}} &= -\frac{1}{2}\rho V_o^2 S_w \frac{C_{D, \dot{\alpha}}}{V_o} \\
F_{y_b, \dot{w}} &= 0 \\
F_{z_b, \dot{w}} &= -\frac{1}{2}\rho V_o^2 S_w \frac{C_{L, \dot{\alpha}}}{V_o} \\
M_{x_b, \dot{w}} &= 0 \\
M_{y_b, \dot{w}} &= \frac{1}{2}\rho V_o^2 S_w \bar{c}_w \frac{C_{m, \dot{\alpha}}}{V_o} \\
M_{z_b, \dot{w}} &= 0
\end{aligned} \tag{10.65}$$

4. Derivatives with respect to Control Deflections

Derivatives with respect to aileron deflection

$$\begin{aligned}
F_{x_b, \delta_a} &= 0 \\
F_{y_b, \delta_a} &= \frac{1}{2}\rho V_o^2 S_w C_Y, \delta_a \\
F_{z_b, \delta_a} &= 0 \\
M_{x_b, \delta_a} &= \frac{1}{2}\rho V_o^2 S_w b_w C_{\ell, \delta_a} \\
M_{y_b, \delta_a} &= 0 \\
M_{z_b, \delta_a} &= \frac{1}{2}\rho V_o^2 S_w b_w C_{n, \delta_a}
\end{aligned} \tag{10.66}$$

Derivatives with respect to elevator deflection

$$\begin{aligned}
F_{x_b, \delta_e} &= -\frac{1}{2}\rho V_o^2 S_w C_{D, \delta_e} \\
F_{y_b, \delta_e} &= 0 \\
F_{z_b, \delta_e} &= -\frac{1}{2}\rho V_o^2 S_w C_{L, \delta_e} \\
M_{x_b, \delta_e} &= 0 \\
M_{y_b, \delta_e} &= \frac{1}{2}\rho V_o^2 S_w \bar{c}_w C_{m, \delta_e} \\
M_{z_b, \delta_e} &= 0
\end{aligned} \tag{10.67}$$

Derivatives with respect to rudder deflection

$$\begin{aligned}
F_{x_b, \delta_r} &= 0 \\
F_{y_b, \delta_r} &= \frac{1}{2} \rho V_o^2 S_w C_{Y, \delta_r} \\
F_{z_b, \delta_r} &= 0 \\
M_{x_b, \delta_r} &= \frac{1}{2} \rho V_o^2 S_w b_w C_{\ell, \delta_r} \\
M_{y_b, \delta_r} &= 0 \\
M_{z_b, \delta_r} &= \frac{1}{2} \rho V_o^2 S_w b_w C_{n, \delta_r}
\end{aligned} \tag{10.68}$$

G. Traditional Nondimensional Linearized Equations of Motion

The dimensional variables in the equations of motion can be written in nondimensional form with the following definitions

$$\Delta\mu \equiv \frac{\Delta u}{V_o}, \quad \Delta\beta \equiv \frac{\Delta v}{V_o}, \quad \Delta\alpha \equiv \frac{\Delta w}{V_o} \tag{10.69}$$

$$\Delta\hat{\alpha} \equiv \frac{\Delta\dot{\alpha} \bar{c}_w}{2V_o}, \quad \Delta\bar{p} \equiv \frac{\Delta p b_w}{2V_o}, \quad \Delta\bar{q} \equiv \frac{\Delta q \bar{c}_w}{2V_o}, \quad \Delta\bar{r} \equiv \frac{\Delta r b_w}{2V_o} \tag{10.70}$$

$$\Delta\xi_x \equiv \frac{2\Delta x_f}{\bar{c}_w}, \quad \Delta\xi_y \equiv \frac{2\Delta y_f}{b_w}, \quad \Delta\xi_z \equiv \frac{2\Delta z_f}{\bar{c}_w} \tag{10.71}$$

$$\tau_x \equiv \frac{2V_o t}{\bar{c}_w}, \quad \tau_y \equiv \frac{2V_o t}{b_w} \tag{10.72}$$

$$R_{gx} \equiv \frac{g \bar{c}_w}{2V_o^2}, \quad R_{gy} \equiv \frac{g b_w}{2V_o^2} \tag{10.73}$$

$$R_{\rho x} \equiv \frac{4W/g}{\rho S_w \bar{c}_w}, \quad R_{\rho y} \equiv \frac{4W/g}{\rho S_w b_w} \tag{10.74}$$

$$R_{xx} \equiv \frac{8I_{xx_b}}{\rho S_w b_w^3}, \quad R_{yy} \equiv \frac{8I_{yy_b}}{\rho S_w \bar{c}_w^3}, \quad R_{zz} \equiv \frac{8I_{zz_b}}{\rho S_w b_w^3}, \quad R_{xz} \equiv \frac{8I_{xz_b}}{\rho S_w b_w^3} \tag{10.75}$$

$$C_{T,V} = \frac{T,V}{\frac{1}{2} \rho V_o S_w} \tag{10.76}$$

1. Nondimensional Linearized Longitudinal Equations

$$\begin{aligned}
& \begin{bmatrix} (R_{\rho x} + C_{D,\hat{\mu}}) & C_{D,\hat{\alpha}} & 0 & 0 & 0 & 0 \\ C_{L,\hat{\mu}} & (R_{\rho x} + C_{L,\hat{\alpha}}) & 0 & 0 & 0 & 0 \\ -C_{m,\hat{\mu}} & -C_{m,\hat{\alpha}} & R_{yy} & 0 & 0 & 0 \\ 0 & 0 & 0 & 1 & 0 & 0 \\ 0 & 0 & 0 & 0 & 1 & 0 \\ 0 & 0 & 0 & 0 & 0 & 1 \end{bmatrix} \begin{Bmatrix} \Delta\hat{\mu} \\ \Delta\hat{\alpha} \\ \Delta\hat{q} \\ \Delta\hat{\xi}_x \\ \Delta\hat{\xi}_z \\ \Delta\hat{\theta} \end{Bmatrix} \\
= & \begin{bmatrix} (-2C_{Do} + C_{T,V} \cos \alpha_{T_0}) & (C_{Lo} - C_{D,\alpha}) & -C_{D,\bar{q}} & 0 & 0 & -R_{\rho x}R_{gx} \cos \theta_o \\ (-2C_{Lo} - C_{T,V} \sin \alpha_{T_0}) & (-C_{L,\alpha} - C_{Do}) & (-C_{L,\bar{q}} + R_{\rho x}) & 0 & 0 & -R_{\rho x}R_{gx} \sin \theta_o \\ (2C_{mo} + C_{T,V} z_{T_0}/\bar{c}_w) & C_{m,\alpha} & C_{m,\bar{q}} & 0 & 0 & 0 \\ \cos \theta_o & \sin \theta_o & 0 & 0 & 0 & -\sin \theta_o \\ -\sin \theta_o & \cos \theta_o & 0 & 0 & 0 & -\cos \theta_o \\ 0 & 0 & 1 & 0 & 0 & 0 \end{bmatrix} \begin{Bmatrix} \Delta\mu \\ \Delta\alpha \\ \Delta\bar{q} \\ \Delta\xi_x \\ \Delta\xi_z \\ \Delta\theta \end{Bmatrix} + \begin{Bmatrix} -C_{D,\delta_e} \\ -C_{L,\delta_e} \\ C_{m,\delta_e} \\ 0 \\ 0 \\ 0 \end{Bmatrix} \Delta\delta_e
\end{aligned} \tag{10.77}$$

2. Nondimensional Linearized Lateral Equations

$$\begin{aligned}
& \begin{bmatrix} R_{\rho y} & 0 & 0 & 0 & 0 & 0 \\ 0 & R_{xx} & -R_{xz} & 0 & 0 & 0 \\ 0 & -R_{xz} & R_{zz} & 0 & 0 & 0 \\ 0 & 0 & 0 & 1 & 0 & 0 \\ 0 & 0 & 0 & 0 & 1 & 0 \\ 0 & 0 & 0 & 0 & 0 & 1 \end{bmatrix} \begin{Bmatrix} \Delta\hat{\beta} \\ \Delta\hat{p} \\ \Delta\hat{r} \\ \Delta\hat{\xi}_y \\ \Delta\hat{\phi} \\ \Delta\hat{\psi} \end{Bmatrix} \\
= & \begin{bmatrix} C_{Y,\beta} & C_{Y,\bar{p}} & (C_{Y,\bar{r}} - R_{\rho y}) & 0 & R_{\rho y}R_{gy} \cos \theta_o & 0 \\ C_{\ell,\beta} & C_{\ell,\bar{p}} & C_{\ell,\bar{r}} & 0 & 0 & 0 \\ C_{n,\beta} & C_{n,\bar{p}} & C_{n,\bar{r}} & 0 & 0 & 0 \\ 1 & 0 & 0 & 0 & 0 & \cos \theta_o \\ 0 & 1 & \tan \theta_o & 0 & 0 & 0 \\ 0 & 0 & \sec \theta_o & 0 & 0 & 0 \end{bmatrix} \begin{Bmatrix} \Delta\beta \\ \Delta\bar{p} \\ \Delta\bar{r} \\ \Delta\xi_y \\ \Delta\phi \\ \Delta\psi \end{Bmatrix} + \begin{bmatrix} C_{Y,\delta_a} & C_{Y,\delta_r} \\ C_{\ell,\delta_a} & C_{\ell,\delta_r} \\ C_{n,\delta_a} & C_{n,\delta_r} \\ 0 & 0 \\ 0 & 0 \\ 0 & 0 \end{bmatrix} \begin{Bmatrix} \Delta\delta_a \\ \Delta\delta_r \end{Bmatrix}
\end{aligned} \tag{10.78}$$

Most of the required derivatives can be obtained quite simply from CFD or experimental results. The derivatives with respect to translational acceleration can be approximated as

$$\begin{aligned}
C_{D,\hat{\mu}} & \approx C_{L,\hat{\mu}} \approx C_{m,\hat{\mu}} \approx C_{D,\hat{\alpha}} \approx 0 \\
C_{L,\hat{\alpha}} & \approx 1.1 \frac{4S_h l_{wt}}{\pi b_w^2 \bar{c}_w} \eta_h C_{L_w,\alpha} C_{L_h,\alpha} \\
C_{m,\hat{\alpha}} & \approx \frac{x_{bh}}{\bar{c}_w} C_{L,\hat{\alpha}}
\end{aligned} \tag{10.79}$$

For a canard design or a flying-wing design, all derivatives with respect to $\hat{\alpha}$ can be approximated as zero.

H. Transformation of Stability Axes

The linearized equations of motion were developed by placing the x axis in the direction of the equilibrium velocity vector. This is called the stability coordinate system. This simplified the mathematics and allowed us to use small-angle approximations for deviations from that path. However, the aerodynamic and inertial information and derivatives may

not always be given in that coordinate system. Often the information is given in a coordinate system that was convenient for the aerodynamic and mass computations. If the information is given in another coordinate system, we must transform the data to the correct stability axes to use the linearized equations of motion.

Any vector given in the coordinate system b' that shares a plane of symmetry $x - z$ with the body-fixed coordinate system can be transformed to the body-fixed coordinate system from the rotation matrix

$$\begin{Bmatrix} v_{x_b} \\ v_{y_b} \\ v_{z_b} \end{Bmatrix} = \begin{bmatrix} \cos \varphi & 0 & \sin \varphi \\ 0 & 1 & 0 \\ -\sin \varphi & 0 & \cos \varphi \end{bmatrix} \begin{Bmatrix} v_{x_{b'}} \\ v_{y_{b'}} \\ v_{z_{b'}} \end{Bmatrix} \quad (10.80)$$

Applying this rotation to the inertia tensor gives

$$\begin{aligned} (I_{xx_b})' &= I_{xx_b} \cos^2 \varphi + 2I_{xz_b} \cos \varphi \sin \varphi + I_{zz_b} \sin^2 \varphi \\ (I_{yy_b})' &= I_{yy_b} \\ (I_{zz_b})' &= I_{zz_b} \cos^2 \varphi - 2I_{xz_b} \cos \varphi \sin \varphi + I_{xx_b} \sin^2 \varphi \\ (I_{xz_b})' &= I_{xz_b} (\cos^2 \varphi - \sin^2 \varphi) + (I_{zz_b} - I_{xx_b}) \cos \varphi \sin \varphi \end{aligned} \quad (10.81)$$

Rotations can also be applied to the aerodynamic derivatives to give

$$\begin{aligned} (C_{D,\hat{\mu}})' &= C_{D,\hat{\mu}} \cos^2 \varphi - (C_{D,\hat{\alpha}} + C_{L,\hat{\mu}}) \cos \varphi \sin \varphi + C_{L,\hat{\alpha}} \sin^2 \varphi \\ (C_{D,\hat{\alpha}})' &= C_{D,\hat{\alpha}} \cos^2 \varphi + (C_{D,\hat{\mu}} - C_{L,\hat{\alpha}}) \cos \varphi \sin \varphi - C_{L,\hat{\mu}} \sin^2 \varphi \\ (C_{D,\bar{q}})' &= C_{D,\bar{q}} \cos \varphi - C_{L,\bar{q}} \sin \varphi \\ (C_{D,\delta_e})' &= C_{D,\delta_e} \cos \varphi - C_{L,\delta_e} \sin \varphi \end{aligned} \quad (10.82)$$

$$\begin{aligned} (C_{L,\hat{\mu}})' &= C_{L,\hat{\mu}} \cos^2 \varphi + (C_{D,\hat{\mu}} - C_{L,\hat{\alpha}}) \cos \varphi \sin \varphi - C_{D,\hat{\alpha}} \sin^2 \varphi \\ (C_{L,\hat{\alpha}})' &= C_{L,\hat{\alpha}} \cos^2 \varphi + (C_{D,\hat{\alpha}} + C_{L,\hat{\mu}}) \cos \varphi \sin \varphi + C_{D,\hat{\mu}} \sin^2 \varphi \\ (C_{L,\bar{q}})' &= C_{L,\bar{q}} \cos \varphi + C_{D,\bar{q}} \sin \varphi \end{aligned} \quad (10.83)$$

$$\begin{aligned} (C_{L,\delta_e})' &= C_{L,\delta_e} \cos \varphi + C_{D,\delta_e} \sin \varphi \\ (C_{m,\hat{\mu}})' &= C_{m,\hat{\mu}} \cos \varphi - C_{m,\hat{\alpha}} \sin \varphi \\ (C_{m,\hat{\alpha}})' &= C_{m,\hat{\alpha}} \cos \varphi + C_{m,\hat{\mu}} \sin \varphi \\ (C_{m,\alpha})' &= C_{m,\alpha} \cos \varphi + C_{m,\mu} \sin \varphi \end{aligned} \quad (10.84)$$

$$\begin{aligned} (C_{m,\bar{q}})' &= C_{m,\bar{q}} \\ (C_{m,\delta_e})' &= C_{m,\delta_e} \\ (C_{Y,\beta})' &= C_{Y,\beta} \\ (C_{Y,\bar{p}})' &= C_{Y,\bar{p}} \cos \varphi - C_{Y,\bar{r}} \sin \varphi \\ (C_{Y,\bar{r}})' &= C_{Y,\bar{r}} \cos \varphi + C_{Y,\bar{p}} \sin \varphi \end{aligned} \quad (10.85)$$

$$\begin{aligned} (C_{Y,\delta_a})' &= C_{Y,\delta_a} \\ (C_{Y,\delta_r})' &= C_{Y,\delta_r} \end{aligned} \quad (10.86)$$

$$(C_{\ell,\beta})' = C_{\ell,\beta} \cos \varphi - C_{n,\beta} \sin \varphi$$

$$\begin{aligned} (C_{\ell,\bar{p}})' &= C_{\ell,\bar{p}} \cos^2 \varphi - (C_{\ell,\bar{r}} + C_{n,\bar{p}}) \cos \varphi \sin \varphi + C_{n,\bar{r}} \sin^2 \varphi \\ (C_{\ell,\bar{r}})' &= C_{\ell,\bar{r}} \cos^2 \varphi + (C_{\ell,\bar{p}} - C_{n,\bar{r}}) \cos \varphi \sin \varphi - C_{n,\bar{p}} \sin^2 \varphi \end{aligned} \quad (10.86)$$

$$(C_{\ell,\delta_a})' = C_{\ell,\delta_a} \cos \varphi - C_{n,\delta_a} \sin \varphi$$

$$(C_{\ell,\delta_r})' = C_{\ell,\delta_r} \cos \varphi - C_{n,\delta_r} \sin \varphi$$

$$(C_{n,\beta})' = C_{n,\beta} \cos \varphi + C_{\ell,\beta} \sin \varphi$$

$$\begin{aligned} (C_{n,\bar{p}})' &= C_{n,\bar{p}} \cos^2 \varphi + (C_{\ell,\bar{p}} - C_{n,\bar{r}}) \cos \varphi \sin \varphi - C_{\ell,\bar{r}} \sin^2 \varphi \\ (C_{n,\bar{r}})' &= C_{n,\bar{r}} \cos^2 \varphi + (C_{\ell,\bar{r}} + C_{n,\bar{p}}) \cos \varphi \sin \varphi + C_{\ell,\bar{p}} \sin^2 \varphi \end{aligned} \quad (10.87)$$

$$(C_{n,\delta_a})' = C_{n,\delta_a} \cos \varphi + C_{\ell,\delta_a} \sin \varphi$$

$$(C_{n,\delta_r})' = C_{n,\delta_r} \cos \varphi + C_{\ell,\delta_r} \sin \varphi$$

11. Linearized Dynamics

The generalized eigenproblem of a linear dynamic system can be written as

$$([\mathbf{A}] - \lambda[\mathbf{B}])\{\chi\} = 0 \quad (11.1)$$

The values of λ that satisfy this equation are the eigenvalues, and the corresponding vectors χ are the eigenvectors. The special eigenproblem of a linear dynamic system can be written as

$$([\mathbf{B}]^{-1}[\mathbf{A}] - \lambda[\mathbf{B}]^{-1}[\mathbf{B}])\{\chi\} = ([\mathbf{B}]^{-1}[\mathbf{A}] - \lambda[\mathbf{i}])\{\chi\} = 0 \quad (11.2)$$

A pair of eigenvalues exist for each degree of freedom within the dynamic system. In general, the eigenvalues and eigenvectors must be found numerically. Once these have been found, the frequency and damping properties of each set of eigenvalues can be obtained from

$$\text{damped natural frequency} \equiv \omega_d = |\text{imag}(\lambda)| \quad (11.3)$$

$$\text{damping rate} \equiv \sigma = -\text{real}(\lambda) \quad (11.4)$$

$$\lambda_{1,2} = -\sigma \pm \omega_d i \quad (11.5)$$

$$\text{undamped natural frequency} \equiv \omega_n = \sqrt{\lambda_1 \lambda_2} = \sqrt{\sigma^2 + \omega_d^2} \quad (11.6)$$

$$\text{damping ratio} \equiv \zeta = -\frac{\lambda_1 + \lambda_2}{2\sqrt{\lambda_1 \lambda_2}} = \frac{\sigma}{\omega_n} \quad (11.7)$$

The damping rate can be used to obtain the following

$$\text{time constant} = 1/\sigma \quad (11.8)$$

$$\text{time to half amplitude} = -\frac{\ln(0.5)}{\sigma} \quad (11.9)$$

$$99\% \text{ damping time} = -\frac{\ln(0.01)}{\sigma} \quad (11.10)$$

$$\text{doubling time} = -\frac{\ln(2)}{\sigma} \quad (11.11)$$

The damped natural frequency can be used to compute the period of the oscillation

$$\text{period} = \frac{2\pi}{\omega_d} \quad (11.12)$$

The eigenvectors contain information about the amplitude and phase of each independent variable within the system corresponding to each mode. The amplitude and phase of each eigenvector component χ_i can be found from

$$\text{amplitude} = \sqrt{[\text{real}(\chi_i)]^2 + [\text{imag}(\chi_i)]^2} \quad (11.13)$$

$$\text{phase} = \text{atan2}[\text{imag}(\chi_i), \text{real}(\chi_i)] \quad (11.14)$$

A. Linearized Longitudinal Dynamics

The generalized eigenproblem for longitudinal dynamics can be expressed as

$$\begin{aligned} & \begin{pmatrix} (-2C_{Do} + C_{T,V} \cos \alpha_{T_0}) & (C_{Lo} - C_{D,\alpha}) & -C_{D,\bar{q}} & 0 & 0 & -R_{\rho x} R_{gx} \cos \theta_o \\ (-2C_{Lo} - C_{T,V} \sin \alpha_{T_0}) & (-C_{L,\alpha} - C_{Do}) & (-C_{L,\bar{q}} + R_{\rho x}) & 0 & 0 & -R_{\rho x} R_{gx} \sin \theta_o \\ (2C_{mo} + C_{T,V} z_{T_0} / \bar{c}_w) & C_{m,\alpha} & C_{m,\bar{q}} & 0 & 0 & 0 \\ \cos \theta_o & \sin \theta_o & 0 & 0 & 0 & -\sin \theta_o \\ -\sin \theta_o & \cos \theta_o & 0 & 0 & 0 & -\cos \theta_o \\ 0 & 0 & 1 & 0 & 0 & 0 \end{pmatrix} \\ & -\lambda \begin{pmatrix} (R_{\rho x} + C_{D,\hat{\mu}}) & C_{D,\hat{\alpha}} & 0 & 0 & 0 & 0 \\ C_{L,\hat{\mu}} & (R_{\rho x} + C_{L,\hat{\alpha}}) & 0 & 0 & 0 & 0 \\ -C_{m,\hat{\mu}} & -C_{m,\hat{\alpha}} & R_{yy} & 0 & 0 & 0 \\ 0 & 0 & 0 & 1 & 0 & 0 \\ 0 & 0 & 0 & 0 & 1 & 0 \\ 0 & 0 & 0 & 0 & 0 & 1 \end{pmatrix} \begin{Bmatrix} \chi_\mu \\ \chi_\alpha \\ \chi_{\bar{q}} \\ \chi_{\xi_x} \\ \chi_{\xi_z} \\ \chi_\theta \end{Bmatrix} = \begin{Bmatrix} 0 \\ 0 \\ 0 \\ 0 \\ 0 \\ 0 \end{Bmatrix} \quad (11.15) \end{aligned}$$

Once the eigenvalues and eigenvectors have been found, the dimensional frequency and damping properties of each mode can be obtained from

$$\sigma = -\text{real}(\lambda) \frac{2V_o}{\bar{c}_w} \quad (11.16)$$

$$\omega_d = |\text{imag}(\lambda)| \frac{2V_o}{\bar{c}_w} \quad (11.17)$$

$$\zeta = -\frac{\lambda_1 + \lambda_2}{2\sqrt{\lambda_1 \lambda_2}} \quad (11.18)$$

$$\omega_n = \frac{2V_o}{\bar{c}_w} \sqrt{\lambda_1 \lambda_2} \quad (11.19)$$

1. Short-Period

The short-period mode is an interchange of rotational kinetic energy and potential energy. It is usually more damped than than the phugoid mode and typically lasts only a couple seconds before damping out. A closed-form approximation can be obtained by approximating $\Delta\mu = 0$ and setting the climb angle to $\theta = 0$. Using these approximations in the homogeneous form of Eq. (10.75) allows the second and third lines of that equation to decouple from the remaining terms in the linear system and gives

$$\begin{bmatrix} (R_{\rho x} + C_{L,\hat{\alpha}}) & 0 \\ -C_{m,\hat{\alpha}} & R_{yy} \end{bmatrix} \begin{Bmatrix} \Delta\hat{\alpha} \\ \Delta\hat{q} \end{Bmatrix} = \begin{bmatrix} (-C_{L,\alpha} - C_{Do}) & (-C_{L,\bar{q}} + R_{\rho x}) \\ C_{m,\alpha} & C_{m,\bar{q}} \end{bmatrix} \begin{Bmatrix} \Delta\alpha \\ \Delta\bar{q} \end{Bmatrix} \quad (11.20)$$

This formulation can be used to produce the eigenproblem

$$\begin{pmatrix} (-C_{L,\alpha} - C_{Do}) & (-C_{L,\bar{q}} + R_{\rho x}) \\ C_{m,\alpha} & C_{m,\bar{q}} \end{pmatrix} - \lambda \begin{pmatrix} (R_{\rho x} + C_{L,\hat{\alpha}}) & 0 \\ -C_{m,\hat{\alpha}} & R_{yy} \end{pmatrix} \begin{Bmatrix} \chi_\alpha \\ \chi_{\bar{q}} \end{Bmatrix} = \begin{Bmatrix} 0 \\ 0 \end{Bmatrix} \quad (11.21)$$

Taking the determinate gives the characteristic equation

$$A_{sp}\lambda_{sp}^2 + B_{sp}\lambda_{sp} + C_{sp} = 0 \quad (11.22)$$

where

$$A_{sp} = R_{yy}(R_{\rho x} + C_{L,\hat{\alpha}}) \quad (11.23)$$

$$B_{sp} = R_{yy}(C_{L,\alpha} + C_{Do}) - C_{m,\bar{q}}(R_{\rho x} + C_{L,\hat{\alpha}}) - C_{m,\hat{\alpha}}(R_{\rho x} - C_{L,\bar{q}}) \quad (11.24)$$

$$C_{sp} = -C_{m,\bar{q}}(C_{L,\alpha} + C_{Do}) - C_{m,\alpha}(R_{\rho x} - C_{L,\bar{q}}) \quad (11.25)$$

This gives the resulting approximation for the dimensionless eigenvalues

$$\lambda_{sp} \approx \frac{-B_{sp} \pm \sqrt{B_{sp}^2 - 4A_{sp}C_{sp}}}{2A_{sp}} = \frac{\bar{c}_w}{2V_o}(-\sigma_{sp} \pm \omega_{d_{sp}}i) \quad (11.26)$$

with dimensional damping and frequency of

$$\sigma_{sp} \approx -\frac{2V_o}{\bar{c}_w} \operatorname{real}(\lambda_{sp}) = \frac{V_o}{\bar{c}_w} \frac{B_{sp}}{A_{sp}} \quad (11.27)$$

$$\omega_{d_{sp}} \approx \frac{2V_o}{\bar{c}_w} |\operatorname{imag}(\lambda_{sp})| = \frac{V_o}{\bar{c}_w} \left| \frac{\sqrt{B_{sp}^2 - 4A_{sp}C_{sp}}}{A_{sp}} \right| \quad (11.28)$$

2. Phugoid

The phugoid mode is an interchange of translational kinetic energy and potential energy. It is typically lightly damped and can last several minutes. A closed-form approximation for the dimensionless phugoid eigenvalue of an aircraft in incompressible flow with constant thrust aligned with the direction of flight can be written as

$$\lambda_p \approx \frac{\bar{c}_w}{2V_o}(-\sigma_p \pm \omega_{d_p}i) \quad (11.29)$$

with dimensional damping and frequency of

$$\sigma_p \approx \sigma_D + \sigma_q + \sigma_\varphi \quad (11.30)$$

$$\omega_{d_p} \approx \sqrt{2 \left(\frac{g}{V_o} \right)^2 R_{ps} - (\sigma_D + \sigma_q)^2} \quad (11.31)$$

where

$$\sigma_D \equiv \text{phugoid drag damping} = \frac{g}{V_o} \frac{C_{Do}}{C_{Lo}} \quad (11.32)$$

$$\sigma_q \equiv \text{phugoid pitch damping} = \frac{g}{V_o} \left[\frac{(C_{Lo} - C_{D,\alpha})C_{m,\bar{q}}}{R_{\rho x}C_{m,\alpha} + (C_{Do} + C_{L,\alpha})C_{m,\bar{q}}} \right] \quad (11.33)$$

$$\sigma_\varphi \equiv \text{phugoid phase damping} = -\frac{g}{V_o} R_{gx} R_{ps} \left[\frac{R_{\rho x}C_{m,\bar{q}} - R_{yy}(C_{Do} + C_{L,\alpha})}{R_{\rho x}C_{m,\alpha} + (C_{Do} + C_{L,\alpha})C_{m,\bar{q}}} \right] \quad (11.34)$$

$$R_{ps} \equiv \text{phugoid stability ratio} = \frac{R_{\rho x}C_{m,\alpha}}{R_{\rho x}C_{m,\alpha} + (C_{Do} + C_{L,\alpha})C_{m,\bar{q}}} \quad (11.35)$$

B. Linearized Lateral Dynamics

The generalized eigenproblem for lateral dynamics can be expressed as

$$\begin{pmatrix} C_{Y,\beta} & C_{Y,\bar{p}} & (C_{Y,\bar{r}} - R_{\rho y}) & 0 & R_{\rho y}R_{gy} \cos \theta_o & 0 \\ C_{\ell,\beta} & C_{\ell,\bar{p}} & C_{\ell,\bar{r}} & 0 & 0 & 0 \\ C_{n,\beta} & C_{n,\bar{p}} & C_{n,\bar{r}} & 0 & 0 & 0 \\ 1 & 0 & 0 & 0 & 0 & \cos \theta_o \\ 0 & 1 & \tan \theta_o & 0 & 0 & 0 \\ 0 & 0 & \sec \theta_o & 0 & 0 & 0 \end{pmatrix} - \lambda \begin{bmatrix} R_{\rho y} & 0 & 0 & 0 & 0 & 0 \\ 0 & R_{xx} & -R_{xz} & 0 & 0 & 0 \\ 0 & -R_{xz} & R_{zz} & 0 & 0 & 0 \\ 0 & 0 & 0 & 1 & 0 & 0 \\ 0 & 0 & 0 & 0 & 1 & 0 \\ 0 & 0 & 0 & 0 & 0 & 1 \end{bmatrix} \begin{Bmatrix} \chi_\beta \\ \chi_{\bar{p}} \\ \chi_{\bar{r}} \\ \chi_{\xi_y} \\ \chi_\phi \\ \chi_\psi \end{Bmatrix} = \begin{Bmatrix} 0 \\ 0 \\ 0 \\ 0 \\ 0 \\ 0 \end{Bmatrix} \quad (11.36)$$

Once the eigenvalues and eigenvectors have been found, the dimensional frequency and damping properties of each mode can be obtained from

$$\sigma = -\text{real}(\lambda) \frac{2V_o}{b_w} \quad (11.37)$$

$$\omega_d = |\text{imag}(\lambda)| \frac{2V_o}{b_w} \quad (11.38)$$

$$\zeta = -\frac{\lambda_1 + \lambda_2}{2\sqrt{\lambda_1 \lambda_2}} \quad (11.39)$$

$$\omega_n = \sqrt{\lambda_1 \lambda_2} \frac{2V_o}{b_w} \quad (11.40)$$

1. Roll Mode

The roll mode is usually very heavily damped due to the roll damping from the wingspan of the main wing. An approximation can be obtained by recognizing that changes in sideslip angle and yawing rate are small compared to changes in rolling rate. Using $\beta = 0$ and $\bar{r} = 0$ in the linearized lateral equations gives

$$(C_{\ell,\bar{p}} - \lambda R_{xx}) \chi_{\bar{p}} = 0 \quad (11.41)$$

This can be solved to give the dimensionless eigenvalue

$$\lambda_r \cong C_{\ell,\bar{p}} / R_{xx} \quad (11.42)$$

which results in the dimensional damping rate

$$\sigma_r \cong -\frac{2V_o}{b_w} \left(\frac{\rho S_w b_w^3}{8I_{xx_b}} C_{\ell,\bar{p}} \right) = -\frac{\rho S_w b_w^2 V_o}{4I_{xx_b}} C_{\ell,\bar{p}} \quad (11.43)$$

2. Spiral Mode

The spiral mode is typically slowly convergent or slowly divergent. It is characterized mainly by changes in heading. It depends on the relative roll stability and yaw stability magnitudes of the aircraft. A closed-form approximation for the dimensionless eigenvalue can be written as

$$\lambda_s \cong -\frac{gb_w}{2V_o^2} \left(\frac{C_{\ell,\beta} C_{n,\bar{r}} - C_{\ell,\bar{r}} C_{n,\beta}}{C_{\ell,\beta} C_{n,\bar{p}} - C_{\ell,\bar{p}} C_{n,\beta}} \right) \quad (11.44)$$

which gives a dimensional damping rate of

$$\sigma_s \cong -\frac{2V_o}{b_w} \lambda_s = \frac{g}{V_o} \left(\frac{C_{\ell,\beta} C_{n,\bar{r}} - C_{\ell,\bar{r}} C_{n,\beta}}{C_{\ell,\beta} C_{n,\bar{p}} - C_{\ell,\bar{p}} C_{n,\beta}} \right) \quad (11.45)$$

3. Dutch Roll Approximation

Dutch roll is an oscillatory mode involving roll, yaw, and sideslip. An approximation for the dimensionless eigenvalues can be written as

$$\lambda_{DR} \approx \frac{b_w}{2V_o} (-\sigma_{DR} \pm \omega_{d_{DR}} i) \quad (11.46)$$

with dimensional damping and frequency of

$$\sigma_{DR} \cong -\frac{V_o}{b_w} \left(\frac{C_{Y,\beta}}{R_{\rho y}} + \frac{C_{n,\bar{r}}}{R_{zz}} - \frac{C_{\ell,\bar{r}} C_{n,\bar{p}}}{C_{\ell,\bar{p}} R_{zz}} + \frac{R_{gy}(C_{\ell,\bar{r}} C_{n,\beta} - C_{\ell,\beta} C_{n,\bar{r}})}{C_{\ell,\bar{p}} (C_{n,\beta} + C_{Y,\beta} C_{n,\bar{r}} / R_{\rho y})} - R_{xx} \frac{R_{Ds}}{C_{\ell,\bar{p}}} \right) \quad (11.47)$$

$$\omega_{d_{DR}} \cong \frac{2V_o}{b_w} \sqrt{\left(1 - \frac{C_{Y,\bar{r}}}{R_{\rho y}} \right) \frac{C_{n,\beta}}{R_{zz}} + \frac{C_{Y,\beta} C_{n,\bar{r}}}{R_{\rho y} R_{zz}} + R_{Ds} - \frac{1}{4} \left(\frac{C_{Y,\beta}}{R_{\rho y}} + \frac{C_{n,\bar{r}}}{R_{zz}} \right)^2} \quad (11.48)$$

where

$$R_{Ds} \equiv \text{Dutch roll stability ratio} = \frac{C_{\ell,\beta} [R_{gy} R_{\rho y} R_{zz} - (R_{\rho y} - C_{Y,\bar{r}}) C_{n,\bar{p}}] - C_{Y,\beta} C_{\ell,\bar{r}} C_{n,\bar{p}}}{R_{\rho y} R_{zz} C_{\ell,\bar{p}}} \quad (11.49)$$

The undamped natural frequency can be approximated as

$$\omega_{n_{DR}} = \frac{2V_o}{b_w} \sqrt{\omega_{\infty_{DR}}^2 + R_{Ds}} \quad (11.50)$$

where $\omega_{\infty_{DR}}$ is the dimensionless undamped natural frequency of the dutch roll in the case of infinite roll damping

$$\omega_{\infty_{DR}} = \sqrt{\frac{(1 - C_{Y,\bar{r}} / R_{\rho y}) C_{n,\beta} + C_{Y,\beta} C_{n,\bar{r}} / R_{\rho y}}{R_{zz}}} \quad (11.51)$$

12. Maneuverability

A. Longitudinal Trim with a Pitch Rate

Maneuverability is dominated by the ability to change the lift vector to point in the direction of desired acceleration. Hence, maneuverability depends on longitudinal trim with a pitching rate. A pitching rate creates a change in angle of attack on each lifting surface proportional to the pitch rate and distance the lifting surface is from the center of gravity. For our simplified analysis, the lift coefficients from the main wing and horizontal stabilizer are

$$C_{L_w} \equiv \frac{L_w}{\frac{1}{2}\rho V^2 S_w} = C_{L_w, \alpha} \left(\alpha + \alpha_{0w} - \alpha_{L0w} + \bar{q} \frac{2l_w}{\bar{c}_w} \right) \quad (12.1)$$

$$C_{L_h} \equiv \frac{L_h}{\frac{1}{2}\rho V^2 S_h} = C_{L_h, \alpha} \left(\alpha + \alpha_{0h} - \alpha_{L0h} - \varepsilon_d + \bar{q} \frac{2l_h}{\bar{c}_w} + \varepsilon_e \delta_e \right) \quad (12.2)$$

The lift and pitching moment equations required for trim are then

$$C_L = C_{L0} + C_{L, \alpha} \alpha + C_{L, \bar{q}} \bar{q} + C_{L, \delta_e} \delta_e = nC_W \quad (12.3)$$

$$C_m = C_{m0} + C_{m, \alpha} \alpha + C_{m, \bar{q}} \bar{q} + C_{m, \delta_e} \delta_e = 0 \quad (12.4)$$

where for our simplified wing and horizontal tail analysis,

$$C_{L0} = C_{L_w, \alpha} (\alpha_{0w} - \alpha_{L0w}) + \frac{S_h}{S_w} \eta_h C_{L_h, \alpha} (\alpha_{0h} - \alpha_{L0h} - \varepsilon_{d0}) \quad (12.5)$$

$$C_{L, \alpha} = C_{L_w, \alpha} + \frac{S_h}{S_w} \eta_h C_{L_h, \alpha} (1 - \varepsilon_{d, \alpha}) \quad (12.6)$$

$$C_{L, \bar{q}} = 2 \frac{l_w}{\bar{c}_w} C_{L_w, \alpha} + 2 \frac{l_h}{\bar{c}_w} \frac{S_h}{S_w} \eta_h C_{L_h, \alpha} \quad (12.7)$$

$$C_{L, \delta_e} = \frac{S_h}{S_w} \eta_h C_{L_h, \alpha} \varepsilon_e \quad (12.8)$$

$$C_{m0} = C_{m_w} + \frac{S_h \bar{c}_h}{S_w \bar{c}_w} \eta_h C_{m_h0} - \frac{l_w}{\bar{c}_w} C_{L_w, \alpha} (\alpha_{0w} - \alpha_{L0w}) - \frac{S_h l_h}{S_w \bar{c}_w} \eta_h C_{L_h, \alpha} (\alpha_{0h} - \alpha_{L0h} - \varepsilon_{d0}) \quad (12.9)$$

$$C_{m, \alpha} = -\frac{l_w}{\bar{c}_w} C_{L_w, \alpha} - \frac{S_h l_h}{S_w \bar{c}_w} \eta_h C_{L_h, \alpha} (1 - \varepsilon_{d, \alpha}) \quad (12.10)$$

$$C_{m, \bar{q}} = -2 \frac{l_w^2}{\bar{c}_w^2} C_{L_w, \alpha} - 2 \frac{l_h^2}{\bar{c}_w^2} \frac{S_h}{S_w} \eta_h C_{L_h, \alpha} \quad (12.11)$$

$$C_{m, \delta_e} = \frac{S_h \bar{c}_h}{S_w \bar{c}_w} \eta_h C_{m_h, \delta_e} - \frac{S_h l_h}{S_w \bar{c}_w} \eta_h C_{L_h, \alpha} \varepsilon_e \quad (12.12)$$

Equations (12.3) and (12.4) can be written as a system of equations as

$$\begin{bmatrix} C_{L, \alpha} & C_{L, \delta_e} \\ C_{m, \alpha} & C_{m, \delta_e} \end{bmatrix} \begin{Bmatrix} \alpha \\ \delta_e \end{Bmatrix} = \begin{Bmatrix} nC_W - C_{L0} - C_{L, \bar{q}} \bar{q} \\ -C_{m0} - C_{m, \bar{q}} \bar{q} \end{Bmatrix} \quad (12.13)$$

This can be solved directly to yield

$$\begin{Bmatrix} \alpha \\ \delta_e \end{Bmatrix} = \frac{1}{C_{L, \alpha} C_{m, \delta_e} - C_{L, \delta_e} C_{m, \alpha}} \begin{Bmatrix} (nC_W - C_{L0} - C_{L, \bar{q}} \bar{q}) C_{m, \delta_e} + C_{L, \delta_e} (C_{m0} + C_{m, \bar{q}} \bar{q}) \\ -(nC_W - C_{L0} - C_{L, \bar{q}} \bar{q}) C_{m, \alpha} - C_{L, \alpha} (C_{m0} + C_{m, \bar{q}} \bar{q}) \end{Bmatrix} \quad (12.14)$$

The nondimensional pitch rate can be expressed as a function of load factor as

$$\bar{q} = (n - 1) \frac{g \bar{c}_w}{2V^2} \quad (12.15)$$

Using this in Eq. (12.14) gives

$$\alpha = \frac{(nC_W - C_{L0}) C_{m, \delta_e} + C_{L, \delta_e} C_{m0} + (C_{L, \delta_e} C_{m, \bar{q}} - C_{L, \bar{q}} C_{m, \delta_e})(n - 1) g \bar{c}_w / (2V^2)}{C_{L, \alpha} C_{m, \delta_e} - C_{L, \delta_e} C_{m, \alpha}} \quad (12.16)$$

$$\delta_e = -\frac{(nC_W - C_{L0}) C_{m, \alpha} + C_{L, \alpha} C_{m0} + (C_{L, \alpha} C_{m, \bar{q}} - C_{L, \bar{q}} C_{m, \alpha})(n - 1) g \bar{c}_w / (2V^2)}{C_{L, \alpha} C_{m, \delta_e} - C_{L, \delta_e} C_{m, \alpha}} \quad (12.17)$$

B. Elevator Angle per g

Taking the derivative of Eq. (12.17) with respect to load factor gives the **elevator angle per g**

$$\frac{\partial \delta_e}{\partial n} = -\frac{C_{m,\alpha} C_W + (C_{L,\alpha} C_{m,\bar{q}} - C_{L,\bar{q}} C_{m,\alpha}) g \bar{c}_w / (2V^2)}{C_{L,\alpha} C_{m,\delta_e} - C_{L,\delta_e} C_{m,\alpha}} \quad (12.18)$$

From the definition of the neutral point, this can be rearranged to yield the center of gravity x -location that will give a zero elevator angle per g . This location is called the **maneuver point** and can be written as

$$\frac{x_{mp}}{\bar{c}_w} = \frac{x_{np}}{\bar{c}_w} - \frac{C_{m,\bar{q}} g \bar{c}_w / (2V^2)}{C_W - C_{L,\bar{q}} g \bar{c}_w / (2V^2)} \quad (12.19)$$

The **stick-fixed maneuver margin** is simply the distance between the maneuver point and the center of gravity normalized by the mean chord of the main wing

$$\frac{l_{mp}}{\bar{c}_w} \equiv \frac{x_{mp} - x_{cg}}{\bar{c}_w} = \frac{l_{np}}{\bar{c}_w} - \frac{C_{m,\bar{q}} g \bar{c}_w / (2V^2)}{C_W - C_{L,\bar{q}} g \bar{c}_w / (2V^2)} \quad (12.20)$$

Because the second term on the right-hand side of this equation combined with the minus sign is always positive, the maneuver point lies aft of the neutral point.

C. Dynamic Margin

The **dynamic pitch rate** is defined as the ratio of the centripetal acceleration to the gravitational acceleration

$$\tilde{q} \equiv \frac{Vq}{g} = \frac{2V^2}{g \bar{c}_w} \bar{q} \quad (12.21)$$

Because $C_W \gg C_{L,\bar{q}}$, the location of the maneuver point can be estimated as

$$l_{mp} = -\frac{\bar{c}_w C_{m,\alpha}}{C_{L,\alpha}} - \frac{\bar{c}_w C_{m,\bar{q}}}{C_W - C_{L,\bar{q}}} = -\frac{m,\alpha}{L,\alpha} - \frac{m,\bar{q}}{W} \quad (12.22)$$

The **Control Anticipation Parameter (CAP)** is

$$\text{Control Anticipation Parameter} \equiv \frac{\omega_{n_{sp}}^2}{C_{L,\alpha}/C_W} \quad (12.23)$$

From the closed-form approximation for the short-period mode, the undamped natural frequency can be estimated as

$$\omega_{n_{sp}} = \sqrt{-\frac{L,\alpha}{W} \frac{m,q}{I_{yyb}} \frac{g}{V} - \frac{m,\alpha}{I_{yyb}}} = \sqrt{\frac{gl_{mp} L,\alpha}{r_{yyb}^2 W}} \quad (12.24)$$

where the **pitch radius of gyration** is

$$r_{yyb} \equiv \sqrt{\frac{g I_{yyb}}{W}} \quad (12.25)$$

Using Eq. (12.24) in Eq. (12.23) gives

$$\text{CAP} = \frac{gl_{mp}}{r_{yyb}^2} \quad (12.26)$$

The **dynamic margin** is defined as

$$\frac{l_{mp}}{r_{yyb}} = -\frac{C_{m,\alpha}}{C_{L,\alpha}} - \frac{C_{m,\bar{q}}}{C_W} \quad (12.27)$$

where the **dynamic moment coefficient** is

$$C_{\tilde{m}} = \frac{m}{\frac{1}{2} \rho V^2 S_w r_{yyb}} = \frac{\bar{c}_w}{r_{yyb}} C_m \quad (12.28)$$

13. Flight Simulation

A. Flat-Earth Euler-Angle Formulation

The flat-earth development of the rigid-body Euler-angle equations of motion for an aircraft in constant wind can be summarized as

$$\begin{aligned} \begin{Bmatrix} \dot{u} \\ \dot{v} \\ \dot{w} \end{Bmatrix} &= \frac{g}{W} \begin{Bmatrix} F_{x_b} \\ F_{y_b} \\ F_{z_b} \end{Bmatrix} + g \begin{Bmatrix} -S_\theta \\ S_\phi C_\theta \\ C_\phi C_\theta \end{Bmatrix} + \begin{Bmatrix} rv - qw \\ pw - ru \\ qu - pv \end{Bmatrix} \\ \begin{Bmatrix} \dot{p} \\ \dot{q} \\ \dot{r} \end{Bmatrix} &= \begin{bmatrix} I_{xx_b} & -I_{xy_b} & -I_{xz_b} \\ -I_{xy_b} & I_{yy_b} & -I_{yz_b} \\ -I_{xz_b} & -I_{yz_b} & I_{zz_b} \end{bmatrix}^{-1} \begin{bmatrix} 0 & -h_{zb} & h_{yb} \\ h_{zb} & 0 & -h_{xb} \\ -h_{yb} & h_{xb} & 0 \end{bmatrix} \begin{Bmatrix} p \\ q \\ r \end{Bmatrix} \\ &+ \begin{Bmatrix} M_{x_b} + (I_{yy_b} - I_{zz_b})qr + I_{yz_b}(q^2 - r^2) + I_{xz_b}pq - I_{xy_b}pr \\ M_{y_b} + (I_{zz_b} - I_{xx_b})pr + I_{xz_b}(r^2 - p^2) + I_{xy_b}qr - I_{yz_b}pq \\ M_{z_b} + (I_{xx_b} - I_{yy_b})pq + I_{xy_b}(p^2 - q^2) + I_{yz_b}pr - I_{xz_b}qr \end{Bmatrix} \\ \begin{Bmatrix} \dot{x}_f \\ \dot{y}_f \\ \dot{z}_f \end{Bmatrix} &= \begin{bmatrix} C_\theta C_\psi & S_\phi S_\theta C_\psi - C_\phi S_\psi & C_\phi S_\theta C_\psi + S_\phi S_\psi \\ C_\theta S_\psi & S_\phi S_\theta S_\psi + C_\phi C_\psi & C_\phi S_\theta S_\psi - S_\phi C_\psi \\ -S_\theta & S_\phi C_\theta & C_\phi C_\theta \end{bmatrix} \begin{Bmatrix} u \\ v \\ w \end{Bmatrix} + \begin{Bmatrix} V_{wx_f} \\ V_{wy_f} \\ V_{wz_f} \end{Bmatrix} \\ \begin{Bmatrix} \dot{\phi} \\ \dot{\theta} \\ \dot{\psi} \end{Bmatrix} &= \begin{bmatrix} 1 & S_\phi S_\theta / C_\theta & C_\phi S_\theta / C_\theta \\ 0 & C_\phi & -S_\phi \\ 0 & S_\phi / C_\theta & C_\phi / C_\theta \end{bmatrix} \begin{Bmatrix} p \\ q \\ r \end{Bmatrix} \end{aligned}$$

B. Euler Axis

$$\begin{Bmatrix} E_{x_f} \\ E_{y_f} \\ E_{z_f} \end{Bmatrix} = \begin{Bmatrix} E_{x_b} \\ E_{y_b} \\ E_{z_b} \end{Bmatrix} \equiv \begin{Bmatrix} E_x \\ E_y \\ E_z \end{Bmatrix} \quad (13.1)$$

$$E_x^2 + E_y^2 + E_z^2 \equiv 1 \quad (13.2)$$

$$\begin{Bmatrix} v_{x_b} \\ v_{y_b} \\ v_{z_b} \end{Bmatrix} = \begin{bmatrix} E_{xx} + C_\Theta & E_{xy} + E_z S_\Theta & E_{xz} - E_y S_\Theta \\ E_{xy} - E_z S_\Theta & E_{yy} + C_\Theta & E_{yz} + E_x S_\Theta \\ E_{xz} + E_y S_\Theta & E_{yz} - E_x S_\Theta & E_{zz} + C_\Theta \end{bmatrix} \begin{Bmatrix} v_{x_f} \\ v_{y_f} \\ v_{z_f} \end{Bmatrix} \quad (13.3)$$

where $E_{ij} = E_i E_j (1 - C_\Theta)$.

$$\begin{Bmatrix} \dot{\Theta} \\ \dot{E}_x \\ \dot{E}_y \\ \dot{E}_z \end{Bmatrix} = \frac{1}{2} \begin{bmatrix} 2E_x & 2E_y & 2E_z \\ E'_{xx} + (C_{\Theta/2})/(S_{\Theta/2}) & E'_{xy} - E_z & E'_{xz} + E_y \\ E'_{xy} + E_z & E'_{yy} + (C_{\Theta/2})/(S_{\Theta/2}) & E'_{yz} - E_x \\ E'_{xz} - E_y & E'_{yz} + E_x & E'_{zz} + (C_{\Theta/2})/(S_{\Theta/2}) \end{bmatrix} \begin{Bmatrix} p \\ q \\ r \end{Bmatrix} \quad (13.4)$$

where $E'_{ij} = -E_i E_j (C_{\Theta/2})/(S_{\Theta/2})$.

C. Euler-Rodriguez Quaternion

$$\begin{Bmatrix} e_0 \\ e_x \\ e_y \\ e_z \end{Bmatrix} \equiv \begin{Bmatrix} \cos(\Theta/2) \\ E_x \sin(\Theta/2) \\ E_y \sin(\Theta/2) \\ E_z \sin(\Theta/2) \end{Bmatrix} \quad (13.5)$$

$$e_0^2 + e_x^2 + e_y^2 + e_z^2 = 1 \quad (13.6)$$

$$\begin{Bmatrix} v_{x_b} \\ v_{y_b} \\ v_{z_b} \end{Bmatrix} = \begin{bmatrix} e_x^2 + e_0^2 - e_y^2 - e_z^2 & 2(e_x e_y + e_z e_0) & 2(e_x e_z - e_y e_0) \\ 2(e_x e_y - e_z e_0) & e_y^2 + e_0^2 - e_x^2 - e_z^2 & 2(e_y e_z + e_x e_0) \\ 2(e_x e_z + e_y e_0) & 2(e_y e_z - e_x e_0) & e_z^2 + e_0^2 - e_x^2 - e_y^2 \end{bmatrix} \begin{Bmatrix} v_{x_f} \\ v_{y_f} \\ v_{z_f} \end{Bmatrix} \quad (13.7)$$

$$\begin{Bmatrix} v_{x_f} \\ v_{y_f} \\ v_{z_f} \end{Bmatrix} = \begin{bmatrix} e_x^2 + e_0^2 - e_y^2 - e_z^2 & 2(e_x e_y - e_z e_0) & 2(e_x e_z + e_y e_0) \\ 2(e_x e_y + e_z e_0) & e_y^2 + e_0^2 - e_x^2 - e_z^2 & 2(e_y e_z - e_x e_0) \\ 2(e_x e_z - e_y e_0) & 2(e_y e_z + e_x e_0) & e_z^2 + e_0^2 - e_x^2 - e_y^2 \end{bmatrix} \begin{Bmatrix} v_{x_b} \\ v_{y_b} \\ v_{z_b} \end{Bmatrix} \quad (13.8)$$

$$\begin{Bmatrix} W_{x_b} \\ W_{y_b} \\ W_{z_b} \end{Bmatrix} = W \begin{Bmatrix} 2(e_x e_z - e_y e_0) \\ 2(e_y e_z + e_x e_0) \\ e_z^2 + e_0^2 - e_x^2 - e_y^2 \end{Bmatrix} \quad (13.9)$$

$$\begin{Bmatrix} \dot{x}_f \\ \dot{y}_f \\ \dot{z}_f \end{Bmatrix} = \begin{Bmatrix} V_{w x_f} \\ V_{w y_f} \\ V_{w z_f} \end{Bmatrix} + \begin{bmatrix} e_x^2 + e_0^2 - e_y^2 - e_z^2 & 2(e_x e_y - e_z e_0) & 2(e_x e_z + e_y e_0) \\ 2(e_x e_y - e_z e_0) & e_y^2 + e_0^2 - e_x^2 - e_z^2 & 2(e_y e_z - e_x e_0) \\ 2(e_x e_z - e_y e_0) & 2(e_y e_z + e_x e_0) & e_z^2 + e_0^2 - e_x^2 - e_y^2 \end{bmatrix} \begin{Bmatrix} u \\ v \\ w \end{Bmatrix} \quad (13.10)$$

$$\begin{Bmatrix} \dot{e}_0 \\ \dot{e}_x \\ \dot{e}_y \\ \dot{e}_z \end{Bmatrix} = \frac{1}{2} \begin{bmatrix} -e_x & -e_y & -e_z \\ e_0 & -e_z & e_y \\ e_z & e_0 & -e_x \\ -e_y & e_x & e_0 \end{bmatrix} \begin{Bmatrix} p \\ q \\ r \end{Bmatrix} \quad (13.11)$$

D. Quaternion Algebra

$$\{\mathbf{Q}\} \equiv Q_0 + Q_x \mathbf{i}_x + Q_y \mathbf{i}_y + Q_z \mathbf{i}_z \quad (13.12)$$

$$\begin{aligned} \mathbf{i}_x \otimes \mathbf{i}_x &\equiv -1, & \mathbf{i}_x \otimes \mathbf{i}_y &\equiv \mathbf{i}_z, & \mathbf{i}_x \otimes \mathbf{i}_z &\equiv -\mathbf{i}_y, \\ \mathbf{i}_y \otimes \mathbf{i}_x &\equiv -\mathbf{i}_z, & \mathbf{i}_y \otimes \mathbf{i}_y &\equiv -1, & \mathbf{i}_y \otimes \mathbf{i}_z &\equiv \mathbf{i}_x, \\ \mathbf{i}_z \otimes \mathbf{i}_x &\equiv \mathbf{i}_y, & \mathbf{i}_z \otimes \mathbf{i}_y &\equiv -\mathbf{i}_x, & \mathbf{i}_z \otimes \mathbf{i}_z &\equiv -1 \end{aligned} \quad (13.13)$$

$$\begin{aligned} \{\mathbf{A}\} \otimes \{\mathbf{B}\} &= (A_0 + A_x \mathbf{i}_x + A_y \mathbf{i}_y + A_z \mathbf{i}_z) \otimes (B_0 + B_x \mathbf{i}_x + B_y \mathbf{i}_y + B_z \mathbf{i}_z) \\ &= (A_0 B_0 - A_x B_x - A_y B_y - A_z B_z) \\ &\quad + (A_0 B_x + A_x B_0 + A_y B_z - A_z B_y) \mathbf{i}_x \\ &\quad + (A_0 B_y - A_x B_z + A_y B_0 + A_z B_x) \mathbf{i}_y \\ &\quad + (A_0 B_z + A_x B_y - A_y B_x + A_z B_0) \mathbf{i}_z \end{aligned} \quad (13.14)$$

$$\begin{aligned} \mathbf{A} \otimes \mathbf{B} &= -(A_x B_x + A_y B_y + A_z B_z) \\ &\quad + (A_y B_z - A_z B_y) \mathbf{i}_x \\ &\quad + (A_z B_x - A_x B_z) \mathbf{i}_y \\ &\quad + (A_x B_y - A_y B_x) \mathbf{i}_z = -\mathbf{A} \cdot \mathbf{B} + \mathbf{A} \times \mathbf{B} \end{aligned} \quad (13.15)$$

$$|\{\mathbf{Q}\}| \equiv \sqrt{Q_0^2 + Q_x^2 + Q_y^2 + Q_z^2} \quad (13.16)$$

$$\{\mathbf{Q}\}^* \equiv Q_0 - Q_x \mathbf{i}_x - Q_y \mathbf{i}_y - Q_z \mathbf{i}_z \quad (13.17)$$

$$\{\mathbf{Q}\} \otimes \{\mathbf{Q}\}^* = Q_0^2 + Q_x^2 + Q_y^2 + Q_z^2 = |\{\mathbf{Q}\}|^2 \quad (13.18)$$

$$\begin{pmatrix} v_{xb} \\ v_{yb} \\ v_{zb} \end{pmatrix} = \begin{pmatrix} e_0 \\ -e_x \\ -e_y \\ -e_z \end{pmatrix} \otimes \left(\begin{pmatrix} 0 \\ v_{xf} \\ v_{yf} \\ v_{zf} \end{pmatrix} \otimes \begin{pmatrix} e_0 \\ e_x \\ e_y \\ e_z \end{pmatrix} \right) \quad (13.19)$$

$$\begin{pmatrix} v_{xf} \\ v_{yf} \\ v_{zf} \end{pmatrix} = \begin{pmatrix} e_0 \\ e_x \\ e_y \\ e_z \end{pmatrix} \otimes \left(\begin{pmatrix} 0 \\ v_{xb} \\ v_{yb} \\ v_{zb} \end{pmatrix} \otimes \begin{pmatrix} e_0 \\ -e_x \\ -e_y \\ -e_z \end{pmatrix} \right) \quad (13.20)$$

E. Relations to Other Attitude Descriptors

The transformation matrices for the Euler-angle and quaternion representations must be equal.

$$\begin{bmatrix} e_x^2 + e_0^2 - e_y^2 - e_z^2 & 2(e_x e_y + e_z e_0) & 2(e_x e_z - e_y e_0) \\ 2(e_x e_y - e_z e_0) & e_y^2 + e_0^2 - e_x^2 - e_z^2 & 2(e_y e_z + e_x e_0) \\ 2(e_x e_z + e_y e_0) & 2(e_y e_z - e_x e_0) & e_z^2 + e_0^2 - e_x^2 - e_y^2 \end{bmatrix} = \begin{bmatrix} C_\theta C_\psi & C_\theta S_\psi & -S_\theta \\ S_\phi S_\theta C_\psi - C_\phi S_\psi & S_\phi S_\theta S_\psi + C_\phi C_\psi & S_\phi C_\theta \\ C_\phi S_\theta C_\psi + S_\phi S_\psi & C_\phi S_\theta S_\psi - S_\phi C_\psi & C_\phi C_\theta \end{bmatrix} \quad (13.21)$$

1. Euler Angles to Quaternion

$$\begin{pmatrix} e_0 \\ e_x \\ e_y \\ e_z \end{pmatrix} = \pm \begin{cases} C_{\phi/2} C_{\theta/2} C_{\psi/2} + S_{\phi/2} S_{\theta/2} S_{\psi/2} \\ S_{\phi/2} C_{\theta/2} C_{\psi/2} - C_{\phi/2} S_{\theta/2} S_{\psi/2} \\ C_{\phi/2} S_{\theta/2} C_{\psi/2} + S_{\phi/2} C_{\theta/2} S_{\psi/2} \\ C_{\phi/2} C_{\theta/2} S_{\psi/2} - S_{\phi/2} S_{\theta/2} C_{\psi/2} \end{cases} \quad (13.22)$$

2. Quaternion to Euler Angles

$$\begin{aligned} & \text{if}(e_0 e_y - e_x e_z = 0.5) \\ & \quad \begin{cases} \phi \\ \theta \\ \psi \end{cases} = \begin{cases} 2 \sin^{-1}[e_x / \cos(\pi/4)] + \psi \\ \pi/2 \\ \text{arbitrary} \end{cases} \\ & \text{if}(e_0 e_y - e_x e_z = -0.5) \\ & \quad \begin{cases} \phi \\ \theta \\ \psi \end{cases} = \begin{cases} 2 \sin^{-1}[e_x / \cos(\pi/4)] - \psi \\ -\pi/2 \\ \text{arbitrary} \end{cases} \\ & \text{else} \\ & \quad \begin{cases} \phi \\ \theta \\ \psi \end{cases} = \begin{cases} \text{atan2}[2(e_0 e_x + e_y e_z), (e_0^2 + e_z^2 - e_x^2 - e_y^2)] \\ \sin^{-1}[2(e_0 e_y - e_x e_z)] \\ \text{atan2}[2(e_0 e_z + e_x e_y), (e_0^2 + e_x^2 - e_y^2 - e_z^2)] \end{cases} \end{aligned} \quad (13.23)$$

F. Quaternion Renormalization

1. Exact Solution

$$\{\mathbf{e}\}_r = \frac{\{\mathbf{e}\}}{|\{\mathbf{e}\}|} = \frac{\{\mathbf{e}\}}{\sqrt{e_0^2 + e_x^2 + e_y^2 + e_z^2}} \quad (13.24)$$

2. Approximate Solution

$$\{\mathbf{e}\}_r \equiv \{\mathbf{e}\}[1.5 - 0.5(e_0^2 + e_x^2 + e_y^2 + e_z^2)] \quad (13.25)$$

G. Flat-Earth Quaternion Formulation

$$\begin{Bmatrix} \dot{u} \\ \dot{v} \\ \dot{w} \end{Bmatrix} = \frac{g}{W} \begin{Bmatrix} F_{xb} \\ F_{yb} \\ F_{zb} \end{Bmatrix} + g \begin{Bmatrix} 2(e_x e_z - e_y e_0) \\ 2(e_y e_z + e_x e_0) \\ e_z^2 + e_0^2 - e_x^2 - e_y^2 \end{Bmatrix} + \begin{Bmatrix} rv - qw \\ pw - ru \\ qu - pv \end{Bmatrix} \quad (13.26)$$

$$\begin{Bmatrix} \dot{p} \\ \dot{q} \\ \dot{r} \end{Bmatrix} = \begin{Bmatrix} I_{xx_b} & -I_{xy_b} & -I_{xz_b} \\ -I_{xy_b} & I_{yy_b} & -I_{yz_b} \\ -I_{xz_b} & -I_{yz_b} & I_{zz_b} \end{Bmatrix}^{-1} \begin{Bmatrix} 0 & -h_{zb} & h_{yb} \\ h_{zb} & 0 & -h_{xb} \\ -h_{yb} & h_{xb} & 0 \end{Bmatrix} \begin{Bmatrix} p \\ q \\ r \end{Bmatrix} + \begin{Bmatrix} M_{xb} + (I_{yy_b} - I_{zz_b})qr + I_{yz_b}(q^2 - r^2) + I_{xz_b}pq - I_{xy_b}pr \\ M_{yb} + (I_{zz_b} - I_{xx_b})pr + I_{xz_b}(r^2 - p^2) + I_{xy_b}qr - I_{yz_b}pq \\ M_{zb} + (I_{xx_b} - I_{yy_b})pq + I_{xy_b}(p^2 - q^2) + I_{yz_b}pr - I_{xz_b}qr \end{Bmatrix} \quad (13.27)$$

$$\begin{Bmatrix} \dot{x}_f \\ \dot{y}_f \\ \dot{z}_f \end{Bmatrix} = \begin{Bmatrix} e_0 \\ e_x \\ e_y \\ e_z \end{Bmatrix} \otimes \left(\begin{Bmatrix} 0 \\ u \\ v \\ w \end{Bmatrix} \otimes \begin{Bmatrix} e_0 \\ -e_x \\ -e_y \\ -e_z \end{Bmatrix} \right) + \begin{Bmatrix} V_{wx_f} \\ V_{wy_f} \\ V_{wz_f} \end{Bmatrix} \quad (13.28)$$

$$\begin{Bmatrix} \dot{e}_0 \\ \dot{e}_x \\ \dot{e}_y \\ \dot{e}_z \end{Bmatrix} = \frac{1}{2} \begin{Bmatrix} -e_x & -e_y & -e_z \\ e_0 & -e_z & e_y \\ e_z & e_0 & -e_x \\ -e_y & e_x & e_0 \end{Bmatrix} \begin{Bmatrix} p \\ q \\ r \end{Bmatrix} \quad (13.29)$$

H. Geographic Coordinates

Latitude is defined in the range

$$-\pi/2 \leq \Phi \leq \pi/2 \quad (13.30)$$

Longitude is defined in the range

$$-\pi \leq \Psi \leq \pi \quad (13.31)$$

1. Mean-Sea-Level Ellipsoid Approximation

The currently accepted polar radius is the minor radius of the ellipse and defined as

$$R_p = 6,356.7516 \text{ km} \quad (13.32)$$

The currently accepted equatorial radius is the major radius of the ellipse and defined as

$$R_e \equiv 6,378.1363 \text{ km} \quad (13.33)$$

The eccentricity ε of the ellipse is defined by

$$\varepsilon^2 \equiv 1 - \left(\frac{R_p}{R_e} \right)^2 = 0.0066943850 \quad (13.34)$$

At mean-sea level, the change in latitude, longitude, and altitude can be computed from

$$\begin{Bmatrix} \dot{\Phi} \\ \dot{\Psi} \\ \dot{H} \end{Bmatrix} = \begin{Bmatrix} \dot{x}_f (1 - \varepsilon^2 \sin^2 \Phi)^{3/2} / [R_e (1 - \varepsilon^2)] \\ \dot{y}_f (1 - \varepsilon^2 \sin^2 \Phi)^{1/2} / (R_e \cos \Phi) \\ -\dot{z}_f \end{Bmatrix} \quad (13.35)$$

At an altitude above mean-sea level of H , the change in latitude, longitude, and altitude can be computed from

$$\begin{Bmatrix} \dot{\Phi} \\ \dot{\Psi} \\ \dot{H} \end{Bmatrix} = \begin{Bmatrix} \dot{x}_f / (R_x + H) \\ \dot{y}_f / [(R_y + H) \cos \Phi] \\ -\dot{z}_f \end{Bmatrix} \quad (13.36)$$

where R_x and R_y are the primary radii of curvature

$$R_x \equiv \frac{R_e (1 - \varepsilon^2)}{(1 - \varepsilon^2 \sin^2 \Phi)^{3/2}} \quad (13.37)$$

$$R_y \equiv \frac{R_e}{(1 - \varepsilon^2 \sin^2 \Phi)^{1/2}} \quad (13.38)$$

For small changes in latitude, longitude, and altitude, this can be approximated using the following first-order approximation algorithm. Given an initial latitude Φ_1 , longitude Ψ_1 , and altitude H_1 , as well as displacements in flat-earth coordinates $(\Delta x_f, \Delta y_f, \Delta z_f)$, the latitude, longitude, and altitude at the next time step can be computed from

$$\begin{aligned} \begin{Bmatrix} \Theta_x \\ \Theta_y \end{Bmatrix} &\equiv \begin{Bmatrix} \Delta x_f / (R_x + H_1 - \Delta z_f / 2) \\ \Delta y_f / (R_y + H_1 - \Delta z_f / 2) \end{Bmatrix} \\ \begin{Bmatrix} \hat{x} \\ \hat{y} \\ \hat{z} \end{Bmatrix} &\equiv \begin{Bmatrix} (1 - \varepsilon^2)[\cos(\Phi_1 + \Theta_x) - \cos \Phi_1] + (1 - \varepsilon^2 \sin^2 \Phi_1) \cos \Theta_y \cos \Phi_1 \\ (1 - \varepsilon^2 \sin^2 \Phi_1) \sin \Theta_y \\ (1 - \varepsilon^2)[\sin(\Phi_1 + \Theta_x) - \sin \Phi_1] + (1 - \varepsilon^2 \sin^2 \Phi_1)(\cos \Theta_y - \varepsilon^2) \sin \Phi_1 \end{Bmatrix} \\ \begin{Bmatrix} \Phi_2 \\ \Psi_2 \\ H_2 \end{Bmatrix} &\approx \begin{Bmatrix} \text{atan2}[\hat{z}, (\hat{x}^2 + \hat{y}^2)^{1/2}] \\ \Psi_1 + \text{atan2}(\hat{y}, \hat{x}) \\ H_1 - \Delta z_f \end{Bmatrix} \\ \Delta \psi_g &\approx (\Psi_2 - \Psi_1) \sin[(\Phi_2 + \Phi_1)/2] (1 - \varepsilon^2) / (1 - \varepsilon^2 \sin^2 \Phi_1) \end{aligned} \quad (13.39)$$

This algorithm is most correctly applied at every step within a high-order integration scheme, such as a fourth-order Runge-Kutta integration method. However, if the distance traveled in a single complete time step is small compared to the local radii of curvature, this algorithm can be applied at the end of each complete time step with very good results.

2. Spherical Earth Approximation

From the definition of the historical nautical mile, the radius of the earth can be approximated as

$$R_E \equiv 6,366.707 \text{ km} \quad (13.40)$$

The change in longitude, latitude, and altitude at any altitude based on a spherical earth can be computed from

$$\begin{Bmatrix} \dot{\Phi} \\ \dot{\Psi} \\ \dot{H} \end{Bmatrix} = \begin{Bmatrix} \dot{x}_f / (R_E + H) \\ \dot{y}_f / [(R_E + H) \cos \Phi] \\ -\dot{z}_f \end{Bmatrix} \quad (13.41)$$

For small changes in latitude, longitude, and altitude, this can be approximated using the following first-order approximation algorithm. Given an initial latitude Φ_1 , longitude Ψ_1 , and altitude H_1 , as well as displacements in flat-earth coordinates $(\Delta x_f, \Delta y_f, \Delta z_f)$ and an initial bearing ψ_{g1} , the latitude, longitude, and altitude at the next time step can be computed from

$$\begin{aligned}
d &= \sqrt{\Delta x_f^2 + \Delta y_f^2} \\
\text{if } (d < \varepsilon_t) \text{ then} \\
&\quad \Phi_2 = \Phi_1 \\
&\quad \Psi_2 = \Psi_1 \\
&\quad \Delta \psi_g = 0 \\
\text{else} \\
&\quad \Theta = d / (R_E + H_1 - \Delta z_f / 2) \\
&\quad \hat{x} = \cos \Phi_1 \cos \Theta - \sin \Phi_1 \sin \Theta \cos \psi_{g1} \\
&\quad \hat{y} = \sin \Theta \sin \psi_{g1} \\
&\quad \hat{z} = \sin \Phi_1 \cos \Theta + \cos \Phi_1 \sin \Theta \cos \psi_{g1} \\
&\quad \hat{x}' = -\cos \Phi_1 \sin \Theta - \sin \Phi_1 \cos \Theta \cos \psi_{g1} \\
&\quad \hat{y}' = \cos \Theta \sin \psi_{g1} \\
&\quad \hat{z}' = -\sin \Phi_1 \sin \Theta + \cos \Phi_1 \cos \Theta \cos \psi_{g1} \\
&\quad \hat{r} = \sqrt{\hat{x}^2 + \hat{y}^2} \\
&\quad \Phi_2 = \text{atan2}(\hat{z}, \hat{r}) \\
&\quad \Psi_2 = \Psi_1 + \text{atan2}(\hat{y}, \hat{x}) \\
&\quad C = \hat{x}^2 \hat{y}' \\
&\quad S = (\hat{x} \hat{y}' - \hat{y} \hat{x}') \cos^2 \Phi_2 \cos^2 (\Psi_2 - \Psi_1) \\
&\quad \Delta \psi_g = \text{atan2}(S, C) - \psi_{g1} \\
\text{end if} \\
H_2 &= H_1 - \Delta z_f
\end{aligned} \tag{13.42}$$

where ε_t is a number on the order of the square root of machine precision, and is used as a tolerance to avoid an indeterminate calculation for vertical flight.

14. Aerodynamic Coordinate Transformations

A. Traditional Aerodynamic Angles

The forces and moments on the aircraft depend on two aerodynamic angles called the angle of attack and sideslip angle. Traditionally, the aerodynamic angles are defined as

$$\alpha \equiv \tan^{-1} \left(\frac{w}{u} \right) \quad (14.1)$$

$$\beta \equiv \sin^{-1} \left(\frac{v}{V} \right) \quad (14.2)$$

These angles can be used to define the direction of the freestream relative to the body-fixed coordinate system of the aircraft. Because the dynamics of an aircraft depend on the forces and moments, and because the forces and moments are related to the aerodynamic angles, it is often convenient to consider the forces and moments in two coordinate systems related to the aerodynamic angles. These coordinate systems are the stability coordinate system and the wind coordinate system.

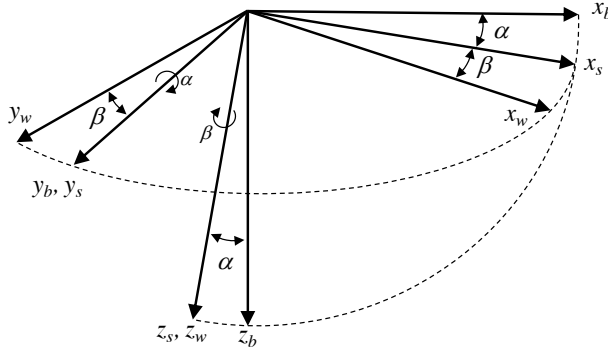


Fig. 14.1 Body-Fixed, Stability, and Wind Coordinate Systems.

B. Stability Coordinate System

The stability coordinate system is obtained by rotating the body-fixed coordinate system about the y_b -axis by the angle of attack α . The transformation of an arbitrary vector in the body-fixed coordinate system to the stability coordinate system is

$$\begin{Bmatrix} v_{x_s} \\ v_{y_s} \\ v_{z_s} \end{Bmatrix} = \begin{bmatrix} c_\alpha & 0 & s_\alpha \\ 0 & 1 & 0 \\ -s_\alpha & 0 & c_\alpha \end{bmatrix} \begin{Bmatrix} v_{x_b} \\ v_{y_b} \\ v_{z_b} \end{Bmatrix} \quad (14.3)$$

and the inverse transformation is

$$\begin{Bmatrix} v_{x_b} \\ v_{y_b} \\ v_{z_b} \end{Bmatrix} = \begin{bmatrix} c_\alpha & 0 & -s_\alpha \\ 0 & 1 & 0 \\ s_\alpha & 0 & c_\alpha \end{bmatrix} \begin{Bmatrix} v_{x_s} \\ v_{y_s} \\ v_{z_s} \end{Bmatrix} \quad (14.4)$$

C. Wind Coordinate System

The wind coordinate system is obtained by rotating the stability coordinate system about the z_s -axis by the sideslip angle β . The transformation of an arbitrary vector in the stability coordinate system to the wind coordinate system is

$$\begin{Bmatrix} v_{x_w} \\ v_{y_w} \\ v_{z_w} \end{Bmatrix} = \begin{bmatrix} c_\beta & s_\beta & 0 \\ -s_\beta & c_\beta & 0 \\ 0 & 0 & 1 \end{bmatrix} \begin{Bmatrix} v_{x_s} \\ v_{y_s} \\ v_{z_s} \end{Bmatrix} \quad (14.5)$$

and the inverse transformation is

$$\begin{Bmatrix} v_{x_s} \\ v_{y_s} \\ v_{z_s} \end{Bmatrix} = \begin{bmatrix} c_\beta & -s_\beta & 0 \\ s_\beta & c_\beta & 0 \\ 0 & 0 & 1 \end{bmatrix} \begin{Bmatrix} v_{x_w} \\ v_{y_w} \\ v_{z_w} \end{Bmatrix} \quad (14.6)$$

Combining Eqs. (14.3) and (14.5), the transformation of a vector from the body-fixed coordinate system to the wind coordinate system is

$$\begin{Bmatrix} v_{x_w} \\ v_{y_w} \\ v_{z_w} \end{Bmatrix} = \begin{bmatrix} c_\beta & s_\beta & 0 \\ -s_\beta & c_\beta & 0 \\ 0 & 0 & 1 \end{bmatrix} \begin{bmatrix} c_\alpha & 0 & s_\alpha \\ 0 & 1 & 0 \\ -s_\alpha & 0 & c_\alpha \end{bmatrix} \begin{Bmatrix} v_{x_b} \\ v_{y_b} \\ v_{z_b} \end{Bmatrix} = \begin{bmatrix} c_\alpha c_\beta & s_\beta & s_\alpha c_\beta \\ -c_\alpha s_\beta & c_\beta & -s_\alpha s_\beta \\ -s_\alpha & 0 & c_\alpha \end{bmatrix} \begin{Bmatrix} v_{x_b} \\ v_{y_b} \\ v_{z_b} \end{Bmatrix} \quad (14.7)$$

Combining Eqs. (14.4) and (14.6), the transformation of a vector from the wind coordinate system to the body-fixed coordinate system is

$$\begin{Bmatrix} v_{x_b} \\ v_{y_b} \\ v_{z_b} \end{Bmatrix} = \begin{bmatrix} c_\alpha & 0 & -s_\alpha \\ 0 & 1 & 0 \\ s_\alpha & 0 & c_\alpha \end{bmatrix} \begin{bmatrix} c_\beta & -s_\beta & 0 \\ s_\beta & c_\beta & 0 \\ 0 & 0 & 1 \end{bmatrix} \begin{Bmatrix} v_{x_w} \\ v_{y_w} \\ v_{z_w} \end{Bmatrix} = \begin{bmatrix} c_\alpha c_\beta & -c_\alpha s_\beta & -s_\alpha \\ s_\beta & c_\beta & 0 \\ s_\alpha c_\beta & -s_\alpha s_\beta & c_\alpha \end{bmatrix} \begin{Bmatrix} v_{x_w} \\ v_{y_w} \\ v_{z_w} \end{Bmatrix} \quad (14.8)$$

1. Velocity Components

Equation (14.8) can be used to compute the velocity vector in the body-fixed coordinate system from a velocity magnitude in the wind coordinate system and the two aerodynamic angles. This gives

$$\begin{Bmatrix} u \\ v \\ w \end{Bmatrix} = \begin{Bmatrix} V_{x_b} \\ V_{y_b} \\ V_{z_b} \end{Bmatrix} = \begin{bmatrix} c_\alpha c_\beta & -c_\alpha s_\beta & -s_\alpha \\ s_\beta & c_\beta & 0 \\ s_\alpha c_\beta & -s_\alpha s_\beta & c_\alpha \end{bmatrix} \begin{Bmatrix} V \\ 0 \\ 0 \end{Bmatrix} = V \begin{Bmatrix} c_\alpha c_\beta \\ s_\beta \\ s_\alpha c_\beta \end{Bmatrix} \quad (14.9)$$

D. Flank Angle

The sideslip angle defined in Eq. (14.2) is not the only method for defining sideslip. The traditional definition given in Eq. (14.2) is useful for defining the wind coordinate system relative to the stability coordinate system. It is often used in wind-tunnel testing. Because this traditional definition is the angle between the stability coordinate system and the wind coordinate system, it is not a direct analog to angle of attack, which is relative to the body-fixed coordinate system. The sideslip angle of the freestream velocity vector relative to the body-fixed coordinate system is sometimes known as the flank angle [5], and is defined as

$$\beta_f \equiv \tan^{-1} \left(\frac{v}{u} \right) \quad (14.10)$$

Notice that Eq. (14.10) is a direct analog to the definition of angle of attack given in Eq. (14.1). This is because both the angle of attack and flank angle are measured relative to the body-fixed coordinate system. The flank angle is sometimes the sideslip angle of choice in analytic work or numerical simulations. It is also the angle usually measured by a wind vane in a flight test.

The freestream velocity vector given in Eq. (14.9) is shown as a function of the angle of attack and traditional sideslip angle. This vector can also be expressed in terms of the angle of attack and flank angle. The velocity magnitude is related to the velocity components in the body-fixed coordinate system according to

$$V^2 = u^2 + v^2 + w^2 \quad (14.11)$$

From the definitions of angle of attack and flank angle given in Eqs. (14.1) and (14.10), we can write

$$v = u \tan \beta_f \quad (14.12)$$

$$w = u \tan \alpha \quad (14.13)$$

Using Eqs. (14.12) and (14.13) in Eq. (14.11), applying trigonometric identities, and applying the result to Eqs. (14.12) and (14.13) gives

$$\begin{Bmatrix} u \\ v \\ w \end{Bmatrix} = \frac{V}{\sqrt{1 - s_\alpha^2 s_{\beta_f}^2}} \begin{Bmatrix} c_\alpha c_{\beta_f} \\ c_\alpha s_{\beta_f} \\ s_\alpha c_{\beta_f} \end{Bmatrix} \quad (14.14)$$

The relationship between the traditional sideslip angle and the flank angle can be found by applying the velocity components given in Eq. (14.9) to Eq. (14.10). This gives

$$\tan \beta_f = \frac{\tan \beta}{\cos \alpha} \quad (14.15)$$

At small angles of attack, the traditional sideslip angle and the flank angle are very nearly equal, and at an angle of attack of zero, the sideslip and flank angles are identical. However, at large angles of attack, these two angles are significantly different. Both angles are useful in different situations. The key is to be aware of how the angle is defined for any analysis, and to be consistent in application. In any case, if the angle of attack and one definition of sideslip angle is known, the other definition of sideslip angle can be found from Eq. (14.15).

E. Aerodynamic Force Components

The aerodynamic force on an aircraft can be expressed as a single vector with the origin at the center of gravity. This vector is often expressed in components in the body-fixed coordinate system, the stability coordinate system, or the wind coordinate system. In the body-fixed coordinate system, these force components are commonly referred to as axial, side, and normal forces. In the stability and wind coordinate systems, the force components are commonly referred to as drag, side force, and lift. Because the stability coordinate system is a rotation of the body-fixed coordinate system about the y_b -axis, the side force is the same in the body-fixed and stability coordinate systems. Because the wind coordinate system is a rotation of the stability coordinate system about the z_s -axis, the lift is the same in the stability and wind coordinate systems. The side force and drag in the stability coordinate system are not equivalent to the side force and drag in the wind coordinate system. Therefore, we denote the side force and drag components in the wind coordinate system as S and D respectively. These force components are labeled in Fig. 1 and defined in Tables 14.1–14.3.

Using Eqs. (14.4) and (14.8), the force components in the body-fixed coordinate system can be expressed as a function of the force components in the stability and wind coordinate systems. This is shown in Table 14.1. In a similar manner, the force components in the stability coordinate system can be expressed as a function of the force components in the body-fixed and wind coordinate systems as shown in Table 14.2. Likewise, the force components in the wind coordinate system can be expressed as a function of the force components in the body-fixed and stability coordinate systems as shown in Table 14.3.

Table 14.1 Force components in the body-fixed coordinate system.

| Force Component | Symbol | Definition | From Stability | From Wind |
|-----------------|--------|-------------------|-------------------------------|--|
| Axial | A | $\equiv -F_{x_b}$ | $= D_s c_\alpha - L s_\alpha$ | $= D c_\alpha c_\beta + S c_\alpha s_\beta - L s_\alpha$ |
| Side | Y | $\equiv F_{y_b}$ | $= Y$ | $= S c_\beta - D s_\beta$ |
| Normal | N | $\equiv -F_{z_b}$ | $= L c_\alpha + D_s s_\alpha$ | $= D s_\alpha c_\beta + S s_\alpha s_\beta + L c_\alpha$ |

F. Aerodynamic Moment Components

The aerodynamic moment on an aircraft can also be expressed as a single vector with the origin at the center of gravity. This vector is most often expressed in components in the body-fixed coordinate system or the stability coordinate system. However, in some cases it may be useful to consider these components in the wind coordinate system

Table 14.2 Force components in the stability coordinate system.

| Force Component | Symbol | Definition | From Body-Fixed | From Wind |
|-----------------|--------|-------------------|---------------------------|-------------------------|
| Drag | D_s | $\equiv -F_{x_s}$ | $= Ac_\alpha + Ns_\alpha$ | $= Dc_\beta + Ss_\beta$ |
| Side | Y | $\equiv F_{y_s}$ | $= Y$ | $= Ds_\beta + Sc_\beta$ |
| Lift | L | $\equiv -F_{z_s}$ | $= Nc_\alpha - As_\alpha$ | $= L$ |

Table 14.3 Force components in the wind coordinate system.

| Force Component | Symbol | Definition | From Body-Fixed | From Stability |
|-----------------|--------|-------------------|--|--------------------------|
| Drag | D | $\equiv -F_{x_w}$ | $= Ac_\alpha c_\beta - Ys_\beta + Ns_\alpha c_\beta$ | $= Dsc_\beta - Ys_\beta$ |
| Side | S | $\equiv F_{y_w}$ | $= Ac_\alpha s_\beta + Yc_\beta + Ns_\alpha s_\beta$ | $= Dss_\beta + Yc_\beta$ |
| Lift | L | $\equiv -F_{z_w}$ | $= Nc_\alpha - As_\alpha$ | $= L$ |

as well. In the body-fixed coordinate system, these components are referred to as rolling, pitching, and yawing moments. Here we will use this terminology for all three coordinate systems, and use subscripts to denote which coordinate system the moment components pertain to. These moment components are defined in Tables 14.4–14.6. Using Eqs. (14.2)–(14.8), the moments in any of the three coordinate systems can be computed from known moment components in one of the other coordinate systems.

Table 14.4 Moment components in the body-fixed coordinate system.

| Moment Component | Symbol | Definition | From Stability | From Wind |
|------------------|--------|------------------|------------------------------------|---|
| Roll | ℓ | $\equiv M_{x_b}$ | $= \ell_s c_\alpha - n_s s_\alpha$ | $= \ell_w c_\alpha c_\beta - m_w c_\alpha s_\beta - n_w s_\alpha$ |
| Pitch | m | $\equiv M_{y_b}$ | $= m_s$ | $= \ell_w s_\beta + m_w c_\beta$ |
| Yaw | n | $\equiv M_{z_b}$ | $= \ell_s s_\alpha + n_s c_\alpha$ | $= \ell_w s_\alpha c_\beta - m_w s_\alpha s_\beta + n_w c_\alpha$ |

Table 14.5 Moment components in the stability coordinate system.

| Moment Component | Symbol | Definition | From Body-Fixed | From Wind |
|------------------|----------|------------------|-------------------------------|----------------------------------|
| Roll | ℓ_s | $\equiv M_{x_s}$ | $= \ell c_\alpha + ns_\alpha$ | $= \ell_w c_\beta - m_w s_\beta$ |
| Pitch | m_s | $\equiv M_{y_s}$ | $= m$ | $= \ell_w s_\beta + m_w c_\beta$ |
| Yaw | n_s | $\equiv M_{z_s}$ | $= nc_\alpha - \ell s_\alpha$ | $= n_w$ |

Table 14.6 Moment components in the wind coordinate system.

| Moment Component | Symbol | Definition | From Body-Fixed | From Stability |
|------------------|----------|------------------|--|----------------------------------|
| Roll | ℓ_w | $\equiv M_{x_w}$ | $= \ell c_\alpha c_\beta + ms_\beta + ns_\alpha c_\beta$ | $= \ell_s c_\beta + m_s s_\beta$ |
| Pitch | m_w | $\equiv M_{y_w}$ | $= mc_\beta - \ell c_\alpha s_\beta - ns_\alpha s_\beta$ | $= m_s c_\beta - \ell_s s_\beta$ |
| Yaw | n_w | $\equiv M_{z_w}$ | $= nc_\alpha - \ell s_\alpha$ | $= n_s$ |

G. Pseudo Aerodynamic Forces and Moments

Aerodynamic forces are commonly evaluated in either the stability or wind coordinate system. However, the equations that govern the dynamics of the aircraft are usually written in the body-fixed coordinate system. Using the

traditional aerodynamic angles given in Eqs. (14.1) and (14.2), from the results shown in Table 14.1, the aerodynamic forces including thrust can be expressed in the body-fixed coordinate system as

$$\begin{aligned} \begin{Bmatrix} F_{x_b} \\ F_{y_b} \\ F_{z_b} \end{Bmatrix} &= \begin{Bmatrix} F_{P_x} \\ F_{P_y} \\ F_{P_z} \end{Bmatrix} + \frac{1}{2} \rho V^2 S_w \begin{Bmatrix} -C_A \\ C_Y \\ -C_N \end{Bmatrix} \\ &= \begin{Bmatrix} F_{P_x} \\ F_{P_y} \\ F_{P_z} \end{Bmatrix} + \frac{1}{2} \rho V^2 S_w \begin{Bmatrix} C_L s_\alpha - C_{D_s} c_\alpha \\ C_Y \\ -C_L c_\alpha - C_{D_s} s_\alpha \end{Bmatrix} \\ &= \begin{Bmatrix} F_{P_x} \\ F_{P_y} \\ F_{P_z} \end{Bmatrix} + \frac{1}{2} \rho V^2 S_w \begin{Bmatrix} C_L s_\alpha - C_S c_\alpha s_\beta - C_D c_\alpha c_\beta \\ C_S c_\beta - C_D s_\beta \\ -C_L c_\alpha - C_S s_\alpha s_\beta - C_D s_\alpha c_\beta \end{Bmatrix} \end{aligned} \quad (14.16)$$

where F_{P_x} , F_{P_y} , and F_{P_z} are the propulsion force components in the body-fixed coordinate system, and all aerodynamic force coefficients are nondimensionalized by the dynamic pressure and wing area.

The aerodynamic moment vector can be evaluated in any of the three coordinate systems considered, but are usually applied to the equations of motion in the body-fixed coordinate system. Using the results shown in Table 14.4, the aerodynamic moment components including thrust can be expressed in the body-fixed coordinate system as

$$\begin{aligned} \begin{Bmatrix} M_{x_b} \\ M_{y_b} \\ M_{z_b} \end{Bmatrix} &= \begin{Bmatrix} M_{P_x} \\ M_{P_y} \\ M_{P_z} \end{Bmatrix} + \frac{1}{2} \rho V^2 S_w \begin{Bmatrix} b_w C_\ell \\ \bar{c}_w C_m \\ b_w C_n \end{Bmatrix} \\ &= \begin{Bmatrix} M_{P_x} \\ M_{P_y} \\ M_{P_z} \end{Bmatrix} + \frac{1}{2} \rho V^2 S_w \begin{Bmatrix} b_w (C_{\ell_s} c_\alpha - C_{n_s} s_\alpha) \\ \bar{c}_w C_{m_s} \\ b_w (C_{\ell_s} s_\alpha + C_{n_s} c_\alpha) \end{Bmatrix} \\ &= \begin{Bmatrix} M_{P_x} \\ M_{P_y} \\ M_{P_z} \end{Bmatrix} + \frac{1}{2} \rho V^2 S_w \begin{Bmatrix} b_w (C_{\ell_w} c_\alpha c_\beta - C_{n_w} s_\alpha) - \bar{c}_w C_{m_w} c_\alpha s_\beta \\ b_w C_{\ell_w} s_\beta + \bar{c}_w C_{m_w} c_\beta \\ b_w (C_{\ell_w} s_\alpha c_\beta + C_{n_w} c_\alpha) - \bar{c}_w C_{m_w} s_\alpha s_\beta \end{Bmatrix} \end{aligned} \quad (14.17)$$

where M_{P_x} , M_{P_y} , and M_{P_z} are the propulsion moment components in the body-fixed coordinate system, and all aerodynamic moment coefficients are nondimensionalized by the dynamic pressure, wing area, and longitudinal or lateral reference length.

H. Center of Gravity Movement

The body-fixed, stability, and wind coordinate systems shown in Fig. 14.1 share an origin at the center of gravity of the aircraft. Due to fuel consumption and other passenger, cargo, or armament movement or changes during a flight, it is not uncommon for the center of gravity to shift during flight. Additionally, because each flight of an aircraft can contain different cargo, the center of gravity of the aircraft may be different for each flight.

When an aerodynamic model for an aircraft is constructed, the roll, pitch, and yaw moments must be reported about some chosen location. However, this location may be different from the location of the center of gravity of the aircraft at any instance in time. Hence, in order to accurately model the forces and moments on an aircraft in flight, we must be able to transfer the moments from one body-fixed coordinate location to another body-fixed coordinate location.

If the pseudo aerodynamic forces and moments such as those given in Eqs. (14.16) and (14.17) are known at the origin in body-fixed coordinates, the pseudo aerodynamic moments about another location $P_1 = (x_1, y_1, z_1)$ can be found using the relation

$$\begin{Bmatrix} M_{x_1} \\ M_{y_1} \\ M_{z_1} \end{Bmatrix} = \begin{Bmatrix} M_{x_b} \\ M_{y_b} \\ M_{z_b} \end{Bmatrix} - \begin{Bmatrix} x_1 \\ y_1 \\ z_1 \end{Bmatrix} \times \begin{Bmatrix} F_{x_b} \\ F_{y_b} \\ F_{z_b} \end{Bmatrix} \quad (14.18)$$

15. Aerodynamic Models

The aerodynamic forces and moments acting on an aircraft depend on many parameters including the velocity vector, velocity magnitude, angular rates, translational accelerations, and control-surface deflections. The velocity vector is defined relative to the body-fixed coordinate system using aerodynamic angles α , β and/or β_f . The velocity magnitude is defined in terms of two nondimensional numbers known as the Reynolds number

$$R_e \equiv \frac{\rho V \bar{c}}{\mu} \quad (15.1)$$

and Mach number

$$M \equiv \frac{V}{a} \quad (15.2)$$

where a is the speed of sound. Because the aerodynamic forces and moments are proportional to the dynamic pressure, these forces and moments are traditionally written in dimensionless form in terms of coefficients that are normalized by the dynamic pressure. At high Reynolds numbers and Mach numbers below 0.3, the aerodynamic force and moment coefficients are nearly independent of velocity magnitude. The angular rates are traditionally written in nondimensional form as

$$\bar{p} \equiv \frac{pb}{2V} \quad (15.3)$$

$$\bar{q} \equiv \frac{q\bar{c}_w}{2V} \quad (15.4)$$

$$\bar{r} \equiv \frac{rb}{2V} \quad (15.5)$$

and the translational accelerations are usually written in nondimensional form as

$$\hat{\alpha} \equiv \frac{\dot{\alpha}\bar{c}_w}{2V} \quad (15.6)$$

$$\hat{\beta} \equiv \frac{\dot{\beta}b}{2V} \quad (15.7)$$

Finally, the control-surface deflections vary widely depending on aircraft. However, the traditional controls included on most aircraft are an aileron, elevator, and rudder.

A. Aerodynamic Model Below Stall

At small angles of attack, small sideslip angles, and small control-surface deflections, the lift, drag, and side force can be estimated by assuming linear relations with the aerodynamic angles, angular rates, control-surface deflections, and translational accelerations. Applying these approximations to the aerodynamic forces in the **wind coordinate system** gives

$$C_L = C_{L_0} + C_{L,\alpha}\alpha + C_{L,\beta}\beta + C_{L,\bar{p}}\bar{p} + C_{L,\bar{q}}\bar{q} + C_{L,\bar{r}}\bar{r} + C_{L,\hat{\alpha}}\hat{\alpha} + C_{L,\hat{\beta}}\hat{\beta} + \sum_{i=1}^{N_c} C_{L,\delta_i}\delta_i \quad (15.8)$$

$$C_S = C_{S_0} + C_{S,\alpha}\alpha + C_{S,\beta}\beta + C_{S,\bar{p}}\bar{p} + C_{S,\bar{q}}\bar{q} + C_{S,\bar{r}}\bar{r} + C_{S,\hat{\alpha}}\hat{\alpha} + C_{S,\hat{\beta}}\hat{\beta} + \sum_{i=1}^{N_c} C_{S,\delta_i}\delta_i \quad (15.9)$$

$$C_D = C_{D_0} + C_{D,\alpha}\alpha + C_{D,\beta}\beta + C_{D,\bar{p}}\bar{p} + C_{D,\bar{q}}\bar{q} + C_{D,\bar{r}}\bar{r} + C_{D,\hat{\alpha}}\hat{\alpha} + C_{D,\hat{\beta}}\hat{\beta} + \sum_{i=1}^{N_c} C_{D,\delta_i}\delta_i \quad (15.10)$$

where C_{L_0} , C_{S_0} , and C_{D_0} are the lift, side, and drag coefficients at zero angle of attack, zero sideslip angle, zero rotational rates, zero translation acceleration, and zero control surface deflection. Within this small-angle region, the rolling, pitching, and yawing moments can also be estimated to be nearly linear functions of the aerodynamic angles, angular rates, and control-surface deflections. These aerodynamic moments can be written in any of the three coordinate systems discussed above. However, they are most conveniently expressed in terms of the **body-fixed coordinate system** as

$$C_\ell = C_{\ell_0} + C_{\ell,\alpha}\alpha + C_{\ell,\beta}\beta + C_{\ell,\bar{p}}\bar{p} + C_{\ell,\bar{q}}\bar{q} + C_{\ell,\bar{r}}\bar{r} + C_{\ell,\hat{\alpha}}\hat{\alpha} + C_{\ell,\hat{\beta}}\hat{\beta} + \sum_{i=1}^{N_c} C_{\ell,\delta_i}\delta_i \quad (15.11)$$

$$C_m = C_{m_0} + C_{m,\alpha}\alpha + C_{m,\beta}\beta + C_{m,\bar{p}}\bar{p} + C_{m,\bar{q}}\bar{q} + C_{m,\bar{r}}\bar{r} + C_{m,\hat{\alpha}}\hat{\alpha} + C_{m,\hat{\beta}}\hat{\beta} + \sum_{i=1}^{N_c} C_{m,\delta_i}\delta_i \quad (15.12)$$

$$C_n = C_{n_0} + C_{n,\alpha}\alpha + C_{n,\beta}\beta + C_{n,\bar{p}}\bar{p} + C_{n,\bar{q}}\bar{q} + C_{n,\bar{r}}\bar{r} + C_{n,\hat{\alpha}}\hat{\alpha} + C_{n,\hat{\beta}}\hat{\beta} + \sum_{i=1}^{N_c} C_{n,\delta_i}\delta_i \quad (15.13)$$

where C_{ℓ_0} , C_{m_0} , and C_{n_0} are the rolling, pitching, and yawing moment coefficients at zero angle of attack, zero sidelip angle, zero rotational rates, zero translation acceleration, and zero control surface deflection.

These equations can be further simplified and refined for many common aircraft designs. For example, many aircraft have only three control surfaces including an elevator δ_e , aileron δ_a , and rudder δ_r . Furthermore, most aircraft are very nearly symmetrical. For the case of a **symmetric aircraft at small sideslip angles**, the change in longitudinal aerodynamic forces and moments with respect to the sideslip angle and lateral accelerations, rotation rates, and control surfaces are very nearly zero

$$\begin{aligned} C_{L,\beta} &\approx C_{L,\bar{p}} \approx C_{L,\bar{r}} \approx C_{L,\hat{\beta}} \approx C_{L,\delta_a} \approx C_{L,\delta_r} \approx 0 \\ C_{D,\beta} &\approx C_{D,\bar{p}} \approx C_{D,\bar{r}} \approx C_{D,\hat{\beta}} \approx C_{D,\delta_a} \approx C_{D,\delta_r} \approx 0 \\ C_{m,\beta} &\approx C_{m,\bar{p}} \approx C_{m,\bar{r}} \approx C_{m,\hat{\beta}} \approx C_{m,\delta_a} \approx C_{m,\delta_r} \approx 0 \end{aligned} \quad (15.14)$$

These terms are exactly zero or very nearly zero due to the fact that changes in the lateral terms will have an identical effect on the longitudinal forces and moments whether they are positive or negative. For example, the change in drag with respect to sideslip angle may be nonzero. However, since we are using a linear model relative to the case of no sideslip, for a symmetric aircraft a positive sideslip angle will produce the same change in drag as a negative sideslip angle. Therefore, the first derivative of the drag with respect to sideslip angle is zero.

Additionally, due to symmetry, the change in lateral aerodynamic forces and moments with respect to the angle of attack and lateral accelerations, rotation rates, and elevator deflection are nearly zero

$$\begin{aligned} C_{S,\alpha} &\approx C_{S,\bar{q}} \approx C_{S,\hat{\alpha}} \approx C_{S,\delta_e} \approx 0 \\ C_{\ell,\alpha} &\approx C_{\ell,\bar{q}} \approx C_{\ell,\hat{\alpha}} \approx C_{\ell,\delta_e} \approx 0 \\ C_{n,\alpha} &\approx C_{n,\bar{q}} \approx C_{n,\hat{\alpha}} \approx C_{n,\delta_e} \approx 0 \end{aligned} \quad (15.15)$$

Finally, the following terms are also zero for **perfectly symmetric aircraft**

$$C_{S_0} = C_{\ell_0} = C_{n_0} = 0 \quad (15.16)$$

Applying Eqs. (15.14)–(15.16) to Eqs. (15.8)–(15.13) gives

$$C_L = C_{L_0} + C_{L,\alpha}\alpha + C_{L,\bar{q}}\bar{q} + C_{L,\hat{\alpha}}\hat{\alpha} + C_{L,\delta_e}\delta_e \quad (15.17)$$

$$C_S = C_{S,\beta}\beta + C_{S,\bar{p}}\bar{p} + C_{S,\bar{r}}\bar{r} + C_{S,\hat{\beta}}\hat{\beta} + C_{S,\delta_a}\delta_a + C_{S,\delta_r}\delta_r \quad (15.18)$$

$$C_D = C_{D_0} + C_{D,\alpha}\alpha + C_{D,\bar{q}}\bar{q} + C_{D,\hat{\alpha}}\hat{\alpha} + C_{D,\delta_e}\delta_e \quad (15.19)$$

$$C_\ell = C_{\ell,\beta}\beta + C_{\ell,\bar{p}}\bar{p} + C_{\ell,\bar{r}}\bar{r} + C_{\ell,\hat{\beta}}\hat{\beta} + C_{\ell,\delta_a}\delta_a + C_{\ell,\delta_r}\delta_r \quad (15.20)$$

$$C_m = C_{m_0} + C_{m,\alpha}\alpha + C_{m,\bar{q}}\bar{q} + C_{m,\hat{\alpha}}\hat{\alpha} + C_{m,\delta_e}\delta_e \quad (15.21)$$

$$C_n = C_{n,\beta}\beta + C_{n,\bar{p}}\bar{p} + C_{n,\bar{r}}\bar{r} + C_{n,\hat{\beta}}\hat{\beta} + C_{n,\delta_a}\delta_a + C_{n,\delta_r}\delta_r \quad (15.22)$$

The aerodynamic model given in Eqs. (15.17)–(15.22) is accurate only for very small angles of attack, sidelip angles, and control-surface deflections. To improve this model to capture the relevant aerodynamics over a larger range of angles of attack below stall, some nonlinear relationships should be included. Many of these nonlinear terms come from our understanding of the relationship between lift and drag. From lifting-line theory and a host of computational and experimental results, it is well understood that drag below stall can be approximated as a quadratic function of the lift coefficient. Likewise, because the side force on a traditional aircraft is dominated by the lateral force on the vertical stabilizer, the effects of side force on drag can be approximated using a quadratic. Using these quadratic approximations gives

$$C_D \approx C_{D,L_0} + C_{D,L}C_L + C_{D,L^2}C_L^2 + C_{D,S^2}C_S^2 \quad (15.23)$$

where $C_{D_{L0}}$ is the drag at zero lift and zero side force. Notice that we have not included the linear term $C_{D,S}C_S$ due to the assumption that the aircraft is symmetric about the $x - z$ plane. Equation (15.23) can be used to develop a drag model superior to that given in Eq. (15.19) and account for the changes in drag that can be expected due to angle of attack, pitch rate, normal acceleration, and elevator deflection. Applying Eq. (15.17) to Eq. (15.23) gives

$$C_D \approx C_{D_{L0}} + C_{D,S^2}C_S^2 + C_{D,L}(C_{L_0} + C_{L,\alpha}\alpha + C_{L,\bar{q}}\bar{q} + C_{L,\hat{\alpha}}\hat{\alpha} + C_{L,\delta_e}\delta_e) + C_{D,L^2}(C_{L_0} + C_{L,\alpha}\alpha + C_{L,\bar{q}}\bar{q} + C_{L,\hat{\alpha}}\hat{\alpha} + C_{L,\delta_e}\delta_e)^2 \quad (15.24)$$

To assist in this analysis, we define a pseudo lift coefficient that neglects changes in lift due to pitch rate, normal acceleration, or elevator deflection

$$C_{L_1} = C_{L_0} + C_{L,\alpha}\alpha \quad (15.25)$$

Using this definition in Eq. (15.24) and rearranging gives

$$\begin{aligned} C_D \approx & C_{D_{L0}} + C_{D,S^2}C_S^2 + C_{D,L}(C_{L_1} + C_{L,\bar{q}}\bar{q} + C_{L,\hat{\alpha}}\hat{\alpha} + C_{L,\delta_e}\delta_e) \\ & + C_{D,L^2}[C_{L_1}^2 + (C_{L,\bar{q}}\bar{q})^2 + (C_{L,\hat{\alpha}}\hat{\alpha})^2 + (C_{L,\delta_e}\delta_e)^2] \\ & + 2C_{D,L^2}(C_{L_1}C_{L,\bar{q}}\bar{q} + C_{L_1}C_{L,\hat{\alpha}}\hat{\alpha} + C_{L_1}C_{L,\delta_e}\delta_e) \\ & + 2C_{D,L^2}(C_{L,\bar{q}}C_{L,\hat{\alpha}}\hat{\alpha} + C_{L,\bar{q}}C_{L,\delta_e}\delta_e + C_{L,\hat{\alpha}}C_{L,\delta_e}\delta_e) \end{aligned} \quad (15.26)$$

Since $C_{L,\bar{q}}$, $C_{L,\hat{\alpha}}$, C_{L,δ_e} , $C_{D,L}$, and C_{D,L^2} are constants, combinations of these constants can be renamed. Additionally, we will drop the interaction terms $\bar{q}\hat{\alpha}$, $\bar{q}\delta_e$, and $\hat{\alpha}\delta_e$ and assume the nonlinear terms \bar{q}^2 and $\hat{\alpha}^2$ are small and can be neglected in comparison to other terms. Dropping these terms and combining constants gives

$$\begin{aligned} C_D \approx & C_{D_{L0}} + C_{D,L}C_{L_1} + C_{D,L^2}C_{L_1}^2 + C_{D,S^2}C_S^2 + (C_{D,L}\bar{q}C_{L_1} + C_{D,\bar{q}})C_{L_1} \\ & + (C_{D,L}\hat{\alpha}C_{L_1} + C_{D,\hat{\alpha}})\hat{\alpha} + (C_{D,L}\delta_eC_{L_1} + C_{D,\delta_e})\delta_e + C_{D,\delta_e^2}\delta_e^2 \end{aligned} \quad (15.27)$$

This drag model can be significantly more accurate than that given in Eq. (15.19).

From lifting-line theory it can be shown that the effects of rolling rate and aileron deflection on the yawing moment can each be approximated as a linear function of lift. Hence, the influence of rolling rate on yawing moment can be approximated as $(C_{n,L}\bar{p}C_{L_1} + C_{n,\bar{p}})\bar{p}$, and the influence of aileron deflection on yawing moment can be approximated as $(C_{n,L}\delta_aC_{L_1} + C_{n,\delta_a})\delta_a$. Additionally, an analytic approximation by Phillips [] shows that the change in rolling moment with respect to yawing rate depends in a linear fashion on the lift coefficient of the main wing. This can be approximated as $(C_{\ell,L}\bar{r}C_{L_1} + C_{\ell,\bar{r}})\bar{r}$. Finally, the change in side force with respect to rolling rate can also be a function of lift coefficient and can be modeled in the form $(C_{S,L}\bar{p}C_{L_1} + C_{S,\bar{p}})\bar{p}$. Applying these approximations along with the result given in Eq. (15.27) to Eqs. (15.17)–(15.22) gives the simplified aerodynamic model below stall

$$C_L = C_{L_1} + C_{L,\bar{q}}\bar{q} + C_{L,\hat{\alpha}}\hat{\alpha} + C_{L,\delta_e}\delta_e \quad (15.28)$$

$$C_S = C_{S,\beta}\beta + (C_{S,L}\bar{p}C_{L_1} + C_{S,\bar{p}})\bar{p} + C_{S,\bar{r}}\bar{r} + C_{S,\hat{\beta}}\hat{\beta} + C_{S,\delta_a}\delta_a + C_{S,\delta_r}\delta_r \quad (15.29)$$

$$\begin{aligned} C_D = & C_{D_{L0}} + C_{D,L}C_{L_1} + C_{D,L^2}C_{L_1}^2 + C_{D,S^2}C_S^2 + (C_{D,L}\bar{q}C_{L_1} + C_{D,\bar{q}})C_{L_1} \\ & + (C_{D,L}\hat{\alpha}C_{L_1} + C_{D,\hat{\alpha}})\hat{\alpha} + (C_{D,L}\delta_eC_{L_1} + C_{D,\delta_e})\delta_e + C_{D,\delta_e^2}\delta_e^2 \end{aligned} \quad (15.30)$$

$$C_\ell = C_{\ell,\beta}\beta + C_{\ell,\bar{p}}\bar{p} + (C_{\ell,L}\bar{r}C_{L_1} + C_{\ell,\bar{r}})\bar{r} + C_{\ell,\hat{\beta}}\hat{\beta} + C_{\ell,\delta_a}\delta_a + C_{\ell,\delta_r}\delta_r \quad (15.31)$$

$$C_m = C_{m_0} + C_{m,\alpha}\alpha + C_{m,\bar{q}}\bar{q} + C_{m,\hat{\alpha}}\hat{\alpha} + C_{m,\delta_e}\delta_e \quad (15.32)$$

$$C_n = C_{n,\beta}\beta + (C_{n,L}\bar{p}C_{L_1} + C_{n,\bar{p}})\bar{p} + C_{n,\bar{r}}\bar{r} + C_{n,\hat{\beta}}\hat{\beta} + (C_{n,L}\delta_aC_{L_1} + C_{n,\delta_a})\delta_a + C_{n,\delta_r}\delta_r \quad (15.33)$$

where C_{L_1} is given in Eq. (15.25). Equations (15.28)–(15.33) comprise a reasonable aerodynamic model below stall for traditional aircraft.

B. Aerodynamic Coefficient Estimation

Most aerodynamic coefficients needed for Eqs. (15.22)–(15.27) can be obtained through relatively straight-forward processes from wind-tunnel testing or computational fluid dynamics. Note that the coefficients needed in Eqs. (15.22)–(15.24) are defined in the wind coordinate system, and those needed in Eqs. (15.25)–(15.27) are defined in the body-fixed coordinate system. These coefficients can be obtained from measurements in any coordinate system by use of the transformation equations given in Tables 14.1–14.6.

The derivatives with respect to translational accelerations needed in Eqs. (15.22)–(15.27) can be a bit more difficult to evaluate. In general, these coefficients must be obtained through an unsteady flow analysis. As a first approximation, Phillips [6] provides an estimate for the change in lift and pitching moment with respect to the vertical acceleration $\dot{\alpha}$. In nondimensional form, this can be written as

$$\begin{aligned} C_{L,\hat{\alpha}} &\approx \eta_h \frac{4S_h l_{wt}}{\pi b^2 \bar{c}_w} \frac{\partial C_{Lw}}{\partial \alpha} \frac{\partial C_{Lh}}{\partial \alpha} \\ C_{m,\hat{\alpha}} &\approx -\frac{x_{bh}}{\bar{c}_w} C_{L,\hat{\alpha}} \end{aligned} \quad (15.34)$$

where

$$l_{wt} = \begin{cases} 1.1(x_{bwingtip} - x_{bh}), & x_{bwingtip} > x_{bh} \\ 0.0, & x_{bh} > x_{bwingtip} \end{cases} \quad (15.35)$$

Phillips [6] suggests that, as a first approximation, all other changes in forces and moments with respect to changes in translational acceleration are zero or negligible. This gives

$$C_{D,\hat{\alpha}} \approx C_{S,\hat{\beta}} \approx C_{\ell,\hat{\beta}} \approx C_{n,\hat{\beta}} \approx 0 \quad (15.36)$$

C. Ground Effect

When a wing comes in the presence of the ground, the downwash is reduced across the wing. This produces an increase in lift and a decrease in induced drag. One estimate that can be used for the influence of ground effect on lift is the ratio of the lift in ground effect to that of the lift out of ground effect, both computed at the same angle of attack

$$\text{lift influence ratio} = \frac{[C_L(\alpha)]_h}{[C_L(\alpha)]_\infty} \quad (15.37)$$

where h is the height of the wing above ground. Since the induced-drag coefficient for a wing without twist is proportional to the lift coefficient squared, a common measure of the influence of the ground on induced drag is computed by the ratio of the induced drag divided by the square of the lift coefficient evaluated in ground effect to that of the same ratio out of ground effect

$$\text{induced-drag influence ratio} = \frac{(C_{Di}/C_L^2)_h}{(C_{Di}/C_L^2)_\infty} \quad (15.38)$$

1. Phillips and Hunsaker Model

Many approximations have been developed for the induced-drag influence ratio, including approximations by Hoerner and Borst [], McCormick [multiple], and Torenbeek []. Most of models are strong functions of the ratio of the wing height above ground h to the wing span b . More recently, Phillips and Hunsaker [] used a numerical lifting-line algorithm to conducted a large computational study on ground effect for wings without twist over a range of planforms, aspect ratios, and taper ratios. Closed-form relations were fit to the computational results, and can be used as an approximation for computing both lift and induced-drag influence ratios in the presence of the ground. The resulting lift and induced-drag influence ratios can be computed from

$$R_L \equiv \frac{[C_L(\alpha)]_h}{[C_L(\alpha)]_\infty} = \frac{1 + 288\delta_L(h/b)^{0.787} \exp[-9.14(h/b)^{0.327}]/R_A^{0.882}}{\beta_L} \quad (15.39)$$

$$R_D \equiv \frac{(C_{Di}/C_L^2)_h}{(C_{Di}/C_L^2)_\infty} = \{1 - \delta_D \exp[-4.74(h/b)^{0.814}] - (h/b)^2 \exp[-3.88(h/b)^{0.758}]\}\beta_D \quad (15.40)$$

where

$$\beta_L = 1 + \frac{0.269 C_{L_h}^{1.45}}{R_A^{3.18} (h/b)^{1.12}} \quad (15.41)$$

$$\beta_D = 1 + \frac{0.0361 C_{L_h}^{1.21}}{R_A^{1.19} (h/b)^{1.51}} \quad (15.42)$$

and C_{L_h} is the lift coefficient in ground effect. For an elliptic wing, $\delta_L = \delta_D = 1.0$. For linearly tapered wings,

$$\delta_L = 1 - 2.25(R_T^{0.00273} - 0.997)(R_A^{0.717} + 13.6) \quad (15.43)$$

$$\delta_D = 1 - 0.157(R_T^{0.775} - 0.373)(R_A^{0.417} - 1.27) \quad (15.44)$$

Note that if CL is negative, you can get complex numbers by raising it to a power of 1.45.

Because C_{L_h} in these equations is the lift coefficient in ground effect, these relations are rather straight forward to apply for the case when the lift of the aircraft is supporting the weight of the aircraft in a trim condition near the ground. In this case, the lift coefficient is equal to the weight coefficient, and can be easily found from the weight, velocity, and altitude of the aircraft. However, these equations are not as straight forward to implement in a simulation environment, where the lift coefficient in ground effect is an unknown. In fact, the purpose of applying these relations to a simulation environment is to solve for the lift in ground effect as a function of the state of the aircraft and control inputs.

For the case of flight simulation, the aerodynamic model of the aircraft can be used to obtain the lift coefficient at a given angle of attack in the absence of ground effect. This is then used in Eqs. (15.39) to obtain the lift coefficient in ground effect. However, since the lift coefficient in ground effect is needed in Eq. (15.41) to solve for β_L , solving for the lift coefficient in ground effect requires an iterative process. Using the lift in the absence of ground effect as the initial guess for C_{L_h} , Eqs. (15.41) and (15.39) can be solved. This gives a new estimate for the lift in ground effect, and the process can be repeated using this updated value for C_{L_h} . This iterative process converges very rapidly and typically requires about 10 iterations to converge to machine precision running double-precision computation.

It is often helpful to minimize computational time required to predict the aerodynamics of the aircraft in a flight simulator. In this case, one may choose not to perform any iterations to solve for the lift in ground effect, and rather use the lift out of ground effect as an approximation for C_{L_h} . This method typically produces errors in Eq. (15.39) of less than 0.5%. Since most aerodynamic models are not accurate to within 1%, this method can be used to speed up computation time with little loss in total simulation accuracy. Once Eq. (15.39) has been solved for the lift in ground effect, the results can be applied to Eqs. (15.42) and (15.40) to obtain the change in induced-drag due to ground effect.

2. Application to a Typical Aerodynamic Model

Approximations for ground effect can be added to the aerodynamic model given in Eqs. (15.28) – (15.33) by making a few assumptions. First we assume that the lift on the aircraft is dominated by the lift on the main wing, and that in ground effect, that lift is dominated by the angle of attack. Therefore, we will use Eq. (15.39) to alter C_{L_1} as

$$(C_{L_1})_h = R_L(C_{L_1})_\infty \quad (15.45)$$

The quantity $(C_{L_1})_h$ is then used in Eqs. (15.28), (15.30), (15.31), and (15.33) for every occurrence of the term C_{L_1} . Additionally, we will assume that the induced drag is the dominant effect in the term C_{D,L^2} which appears in Eq. (15.30). Hence, we can simply use Eq. (15.40) directly in Eq. (15.30) to yield an estimate for the total drag in ground effect

$$C_D = C_{D,L_0} + C_{D,L} C_{L_1} + R_D C_{D,L^2} C_{L_1}^2 + C_{D,S^2} C_S^2 + (C_{D,L\bar{q}} C_{L_1} + C_{D,\bar{q}}) \bar{q} \\ + (C_{D,L\hat{\alpha}} C_{L_1} + C_{D,\hat{\alpha}}) \hat{\alpha} + (C_{D,L\delta_e} C_{L_1} + C_{D,\delta_e}) \delta_e + C_{D,\delta_e^2} \delta_e^2 \quad (15.46)$$

To include an approximation for ground effect on drag, Eq. (15.46) can be used instead of Eq. (15.30).

D. Stall

Fixed-wing aircraft stall at high angles of attack. The stall characteristics of each aircraft are different, and depend on the aircraft design. For an excellent overview of the aerodynamics of aircraft at high angles of attack, see Phillips [MoF 6.6].

Any realistic simulator must have some method for approximating the aerodynamics of aircraft at high angles of attack. Because aircraft do not normally fly for extended periods of time in a stalled condition, the aerodynamics of stall must not be particularly accurate for most flight simulators. However, some representation for the forces and moments in a stalled condition must be in the simulator to produce a somewhat realistic simulator. If aerodynamic information at high angles of attack is available, it can be used in a table lookup or interpolation method. However, in the absence of this information, an approximate stall model can be developed by modifying the longitudinal aerodynamic forces and moments.

At high angles of attack, the lift and drag forces on the aircraft can be approximated from our understanding of flow over a flat plate at high incidence angles. The pitching moment of aircraft at high angles of attack can vary widely, and depends on the design of the aircraft. However, most aircraft are designed to produce a strong negative pitching moment when the aircraft stalls. This helps with stall recovery. As a first approximation, the lift [? ?], drag, and pitching moment can be modeled as

$$(C_L)_{\text{plate}} = 2 \text{sign}(\alpha) \sin^2 \alpha \cos \alpha \quad (15.47)$$

$$(C_D)_{\text{plate}} = 2 \sin^{(3/2)}(|\alpha|) \quad (15.48)$$

$$(C_m)_{\text{plate}} = -0.8 \sin \alpha \quad (15.49)$$

These can be blended with the aerodynamic model below stall using a sigmoid function. Beard and McLain [?] suggest the blending function

$$\sigma = \frac{1 + e^{-M(\alpha - \alpha_b)} + e^{M(\alpha + \alpha_b)}}{[1 + e^{-M(\alpha - \alpha_b)}][1 + e^{M(\alpha + \alpha_b)}]} \quad (15.50)$$

where α_b is a transition location and M is a blending rate parameter. This function produces a value near 1.0 outside of the range $-\alpha_b < \alpha < \alpha_b$ and a value near 0 inside this range. At $\alpha = \alpha_b$, the function has a value of $\sigma = 0.5$. Typical aircraft stall in the range of 15 to 25 degrees, and would have a α_b of 20 to 30 degrees. A blending rate of 20 to 100 usually produces reasonable results, with $M = 20$ for a soft stall and $M = 100$ for an abrupt stall.

Equations (15.47)–(15.49) can be blended with the aerodynamic model given in Eqs. (15.28)–(15.33) using the blending function given in Eq. (15.50). This gives

$$C_L = (1 - \sigma)(C_L)_{\text{model}} + \sigma(C_L)_{\text{plate}} \quad (15.51)$$

$$C_D = (1 - \sigma)(C_D)_{\text{model}} + \sigma(C_D)_{\text{plate}} \quad (15.52)$$

$$C_m = (1 - \sigma)(C_m)_{\text{model}} + \sigma(C_m)_{\text{plate}} \quad (15.53)$$

where the subscript *model* refers to the original coefficients from Eqs. (15.28), (15.30), and (15.32). Some aircraft are designed to maintain control effectiveness at high angles of attack to assist with stall recovery and control. For these cases, modifications to this very simple model can be made.

If more information about the aerodynamics of the aircraft beyond stall are known, modifications to the lateral forces and moments (rolling and yawing moments and side force) can also be made. These are particularly useful for modeling the effectiveness of control surfaces on the moments at high angles of attack. However, accurate models for lateral forces and moments above stall are usually not as important as models for the longitudinal forces and moments above stall.

E. Propulsion

The total propulsive force on an aircraft is a summation of those from the individual propulsive elements including jet engines, propellers, and exhaust nozzles, and can be expressed as

$$\begin{Bmatrix} F_{P_x} \\ F_{P_y} \\ F_{P_z} \end{Bmatrix} = \sum_{i=1}^{N_P} \mathbf{F}_{P_i} \quad (15.54)$$

where N_P is the number of propulsive elements. The propulsive force from a single propulsive element \mathbf{F}_P depends on both thrust produced by the element and the drag on the element, and can be written as

$$\mathbf{F}_P = (T \mathbf{u}_P + D_P \mathbf{u}_\infty) \quad (15.55)$$

where T and D_P are the thrust and drag of propulsive element, and \mathbf{u}_P is the unit vector in the direction of the thrust of propulsive element. The thrust from various propulsion methods can often be closely modeled as a quadratic function of velocity and is proportional to the density. This can be written as

$$T = \tau(\rho/\rho_0)^a (T_0 + T_1 V + T_2 V^2) \quad (15.56)$$

where T_0 , T_1 , and T_2 are the constants of the parabolic function, a is a constant related to the density ratio, and τ is the throttle setting, and ρ_0 is the standard sea-level density. The constants required in Eq. (15.33) can be found by fitting the equation to predicted or measured thrust data from a propulsive element. The drag on a propulsive element can be modeled as

$$D_P = \frac{1}{2} \rho V^2 S_P C_{DP} \quad (15.57)$$

where S_P is the characteristic area and C_{DP} is the drag coefficient of the propulsive element. The drag coefficient for the propulsive element can also be obtained from predicted or measured data. Once the propulsion model has been constructed, these results can be used in Eqs. (15.31) and (15.32) to predict the total propulsive force vector on the system.

The total propulsive moment vector can be obtained from

$$\begin{Bmatrix} M_{Px} \\ M_{Py} \\ M_{Pz} \end{Bmatrix} = \sum_{i=1}^{N_P} (\mathbf{r}_{Pi} \times \mathbf{F}_{Pi}) \quad (15.58)$$

where \mathbf{r}_{Pi} is the vector from the aircraft center of gravity to propulsive element i .

F. Gust Modeling

Disturbances in the air including unsteady wind, gusts, and thermals are common encounters for aircraft. Including these types of disturbances in flight simulation can be valuable for assessing the response of the aircraft to disturbances of varying magnitude and duration.

The equations of motion developed previously for rigid-body motion were developed under the assumption that the atmospheric coordinate system is not accelerating relative to the earth-fixed coordinate system. This assumption allowed the atmospheric coordinate system to be used as an inertial coordinate system. Such a development naturally accounts for the effects of constant wind velocity relative to the earth-fixed coordinate system, and the appropriate terms were included in that formulation.

Although atmospheric disturbances can result from a number of sources such as thermals, local turbulence, gusts, etc., each of these disturbances can be modeled in a similar manner. Here we will refer to any disturbance or deviation from the average wind as a gust. Accurately capturing the physics of gusts is challenging. However, the effects of gusts can be approximated quite simply by including the disturbances only in the aerodynamic model of the aircraft. Such a formulation assumes that the integral of the gusts relative to the average wind over a long period of time is zero. This allows the average wind atmospheric coordinate system to be used for the inertial coordinate system. The effects of the gust are incorporated into the equations of motion through their effects on the aerodynamics of the vehicle. This approach is suggested as the solution of choice by several authors (Beal JoGCD 16.1 1993, MIL 8785, MIL 1797). For example, MIL 1797 "4.9.3 Application of disturbance models in analyses" states, "The gust and turbulence velocities shall be applied to the aircraft equations of motion through the aerodynamic terms only, and the direct effect on the aerodynamic sensors shall be included when such sensors are part of the aircraft augmentation system."

In the aerodynamic models presented above, the pseudo aerodynamic force and moment vectors are functions of the body-fixed velocities u, v, w as well as the body-fixed rotation rates p, q, r

$$\begin{Bmatrix} F_{xb} \\ F_{yb} \\ F_{zb} \end{Bmatrix} = f(u, v, w, p, q, r) \quad (15.59)$$

$$\begin{Bmatrix} M_{xb} \\ M_{yb} \\ M_{zb} \end{Bmatrix} = f(u, v, w, p, q, r) \quad (15.60)$$

The suggested approach is simply to replace the velocity and rate components u, v, w, p, q, r within these functions with the components plus a fluctuating component due to the gust $u_g, v_g, w_g, p_g, q_g, r_g$ to yield

$$\begin{Bmatrix} F_{x_b} \\ F_{y_b} \\ F_{z_b} \end{Bmatrix} = f(u + u_g, v + v_g, w + w_g, p + p_g, q + q_g, r + r_g) \quad (15.61)$$

$$\begin{Bmatrix} M_{x_b} \\ M_{y_b} \\ M_{z_b} \end{Bmatrix} = f(u + u_g, v + v_g, w + w_g, p + p_g, q + q_g, r + r_g) \quad (15.62)$$

In this way, the gusts are modeled as a disturbance to the aerodynamics, but not a disturbance to the atmosphere. This method is very similar to modeling the gust disturbance as a disturbance in control-surface deflection.

Several gust models have been suggested. Here we consider three such models that can be used for various applications. Some gust models are prescribed in the earth-fixed coordinate system, where others are prescribed in the body-fixed coordinate system. If a gust model is prescribed in the earth-fixed coordinate system, the gust components $u_g, v_g, w_g, p_g, q_g, r_g$ can be obtained from the general vector rotation from earth-fixed coordinates to body-fixed coordinates. This gives

$$\begin{Bmatrix} V_{x_b} \\ V_{y_b} \\ V_{z_b} \end{Bmatrix} = \begin{bmatrix} C_\theta C_\psi & C_\theta S_\psi & -S_\theta \\ S_\phi S_\theta C_\psi - C_\phi S_\psi & S_\phi S_\theta S_\psi + C_\phi C_\psi & S_\phi C_\theta \\ C_\phi S_\theta C_\psi + S_\phi S_\psi & C_\phi S_\theta S_\psi - S_\phi C_\psi & C_\phi C_\theta \end{bmatrix} \begin{Bmatrix} V_{x_f} \\ V_{y_f} \\ V_{z_f} \end{Bmatrix} \quad (15.63)$$

if the aircraft orientation is known in terms of Euler angles, and

$$\begin{Bmatrix} V_{x_b} \\ V_{y_b} \\ V_{z_b} \end{Bmatrix} = \begin{bmatrix} e_x^2 + e_0^2 - e_y^2 - e_z^2 & 2(e_x e_y + e_z e_0) & 2(e_x e_z - e_y e_0) \\ 2(e_x e_y - e_z e_0) & e_y^2 + e_0^2 - e_x^2 - e_z^2 & 2(e_y e_z + e_x e_0) \\ 2(e_x e_z + e_y e_0) & 2(e_y e_z - e_x e_0) & e_z^2 + e_0^2 - e_x^2 - e_y^2 \end{bmatrix} \begin{Bmatrix} V_{x_f} \\ V_{y_f} \\ V_{z_f} \end{Bmatrix} = \begin{Bmatrix} e_0 \\ -e_x \\ -e_y \\ -e_z \end{Bmatrix} \otimes \left(\begin{Bmatrix} 0 \\ V_{x_f} \\ V_{y_f} \\ V_{z_f} \end{Bmatrix} \otimes \begin{Bmatrix} e_0 \\ e_x \\ e_y \\ e_z \end{Bmatrix} \right) \quad (15.64)$$

if the aircraft orientation is known in terms of the quaternion formulation.

1. Damped Sinusoidal Gust Model

A simple gust model can be constructed by using a sinusoidal variation in velocity with amplitude that varies with time. We will assume the velocity vector of the gust can be expressed in earth-fixed coordinates as

$$\mathbf{V}_g = A_g e^{-\lambda_g t} \sin(\omega_g t) \hat{\mathbf{i}}_g \quad (15.65)$$

where A_g is the gust amplitude, λ_g is the gust decay constant, ω_g is the gust frequency, t is the time since the gust began, and $\hat{\mathbf{i}}_g$ is the unit vector in the direction of the gust velocity in either earth-fixed coordinates or body-fixed coordinates. The time to half-amplitude is $\ln(2)/\lambda_g$, and the gust period is $2\pi/\omega_g$. To simulate gusts of random strength and duration, the amplitude, decay constant, frequency, and gust direction can be randomized. Additionally, several sine waves of this form having varying amplitude, frequency, decay constants, and even starting times can be superimposed to produce more realistic turbulent fluctuations.

2. von Kármán Atmospheric Turbulence Model

Atmospheric measurements have been made to estimate the probability of gust encounters, and models based on these measurements have been developed. One such model suggested for use by the FAA and military for aircraft design and simulation is the von Kármán Atmospheric Turbulence Model. This model falls under a category of atmospheric models often called *frozen field* models, in which the turbulent fluctuations are assumed to vary with aircraft location, but not time. This model is a one-dimensional location model, meaning that the turbulence depends only on the x -location of the aircraft. The u_g, v_g , and w_g fluctuation terms are modeled independently, but each only depends on the x -location

of the aircraft. The model can be incorporated into a flight simulator [?] by using a summation of sine waves of the form

$$u_g(x) = \sum_{i=1}^N A_{u_i} \sin(\omega_{u_i}x + \phi_{u_i}) \quad (15.66)$$

$$v_g(x) = \sum_{i=1}^N A_{v_i} \sin(\omega_{v_i}x + \phi_{v_i}) \quad (15.67)$$

$$w_g(x) = \sum_{i=1}^N A_{w_i} \sin(\omega_{w_i}x + \phi_{w_i}) \quad (15.68)$$

where A_{u_i} , A_{v_i} , and A_{w_i} are the amplitudes of individual sine waves, ω_{u_i} , ω_{v_i} , and ω_{w_i} are the frequencies of individual sine waves, and ϕ_{u_i} , ϕ_{v_i} , and ϕ_{w_i} are the phases of individual sine waves. The phase of each sine wave is randomly generated using an even distribution between $-\pi$ and π . The amplitudes and frequencies are determined from spectral density information from atmospheric measurements.

The spectral-density functions for this model can be written as

$$\Phi_u(\omega) = \sigma_u^2 \frac{2L_u}{\pi} \frac{1}{[1 + (1.339L_u\omega)^2]^{5/6}} \quad (15.69)$$

$$\Phi_v(\omega) = \sigma_v^2 \frac{L_v}{\pi} \frac{1 + (8/3)(1.339L_v\omega)^2}{[1 + (1.339L_v\omega)^2]^{11/6}} \quad (15.70)$$

$$\Phi_w(\omega) = \sigma_w^2 \frac{L_w}{\pi} \frac{1 + (8/3)(1.339L_w\omega)^2}{[1 + (1.339L_w\omega)^2]^{11/6}} \quad (15.71)$$

where σ_u , σ_v , and σ_w are standard deviations and L_u , L_v , and L_w are length scales. Note that the spectral densities Φ_v and Φ_w are identical. The values for standard deviation depend on the turbulence level. The length scales for this model are defined as

$$L_u = L_v = L_w = 2500 \text{ ft} \quad (15.72)$$

Note that the gust disturbances predicted by this model are in the body-fixed coordinate system. Such an approach is most suited for fixed-wing aircraft, in which the velocity of the aircraft is predominantly in the body-fixed x direction. Additionally, note that because this model is a frozen-field model, it is not suitable for aircraft with the ability to hover, such as rotorcraft. In the case of hover, the turbulence properties are fixed and do not change with time. This is clearly unrealistic.

3. Atmospheric Database

In some instances, an atmospheric database is available that gives the

How to compute roll, pitch, and yaw rate disturbances from those. Two ways: query the velocity at each location along the wing and apply it to the aerodynamics. Or estimate p_g , q_g , and r_g by taking derivative of u_g etc. like what is done in von Karman model.

16. Six-Degree-of-Freedom Static Trim

In general, for a flight condition specified by the altitude, velocity, climb angle, and type of trim, we wish to find the states of the aircraft that will produce a trim condition. This includes solving for the angle of attack, sideslip angle, elevation angle, bank angle, roll rate, pitch rate, yaw rate, control-surface deflections, and thrust required to maintain trim. We begin by considering the governing equations of motion for a rigid-body aircraft.

A. Governing Rigid-Body Equations of Motion

The governing equations of motion for a rigid-body aircraft can be obtained from Newton's Second Law and written in the body-fixed coordinate system in the form

$$\frac{W}{g} \begin{Bmatrix} \dot{u} \\ \dot{v} \\ \dot{w} \end{Bmatrix} = \begin{Bmatrix} F_{x_b} \\ F_{y_b} \\ F_{z_b} \end{Bmatrix} + W \begin{Bmatrix} -s_\theta \\ s_\phi c_\theta \\ c_\phi c_\theta \end{Bmatrix} + \frac{W}{g} \begin{Bmatrix} rv - qw \\ pw - ru \\ qu - pv \end{Bmatrix} \quad (16.1)$$

$$\begin{Bmatrix} I_{xx} & -I_{xy} & -I_{xz} \\ -I_{xy} & I_{yy} & -I_{yz} \\ -I_{xz} & -I_{yz} & I_{zz} \end{Bmatrix} \begin{Bmatrix} \dot{p} \\ \dot{q} \\ \dot{r} \end{Bmatrix} = \begin{Bmatrix} M_{x_b} \\ M_{y_b} \\ M_{z_b} \end{Bmatrix} + \begin{Bmatrix} 0 & -h_z & h_y \\ h_z & 0 & -h_x \\ -h_y & h_x & 0 \end{Bmatrix} \begin{Bmatrix} p \\ q \\ r \end{Bmatrix} + \begin{Bmatrix} (I_{yy} - I_{zz})qr + I_{yz}(q^2 - r^2) + I_{xz}pq - I_{xy}pr \\ (I_{zz} - I_{xx})pr + I_{xz}(r^2 - p^2) + I_{xy}qr - I_{yz}pq \\ (I_{xx} - I_{yy})pq + I_{xy}(p^2 - q^2) + I_{yz}pr - I_{xz}qr \end{Bmatrix} \quad (16.2)$$

For the purposes of considering a trim condition, we have chosen to apply the Euler-angle formulation. Applying a local flat-earth approximation, the change in earth-fixed coordinates can be written as

$$\begin{Bmatrix} \dot{x}_f \\ \dot{y}_f \\ \dot{z}_f \end{Bmatrix} = \begin{Bmatrix} c_\theta c_\psi & s_\phi s_\theta c_\psi - c_\phi s_\psi & c_\phi s_\theta c_\psi + s_\phi s_\psi \\ c_\theta s_\psi & s_\phi s_\theta s_\psi + c_\phi c_\psi & c_\phi s_\theta s_\psi - s_\phi c_\psi \\ -s_\theta & s_\phi c_\theta & c_\phi c_\theta \end{Bmatrix} \begin{Bmatrix} u \\ v \\ w \end{Bmatrix} + \begin{Bmatrix} V_{wx_f} \\ V_{wy_f} \\ V_{wz_f} \end{Bmatrix} \quad (16.3)$$

Using the Euler-angle formulation, the change in aircraft orientation can be written as

$$\begin{Bmatrix} \dot{\phi} \\ \dot{\theta} \\ \dot{\psi} \end{Bmatrix} = \begin{Bmatrix} 1 & s_\phi t_\theta & c_\phi t_\theta \\ 0 & c_\phi & -s_\phi \\ 0 & s_\phi/c_\theta & c_\phi/c_\theta \end{Bmatrix} \begin{Bmatrix} p \\ q \\ r \end{Bmatrix} \quad (16.4)$$

In a trim state, the equations of motion must be satisfied such that the aerodynamic velocities and rotation rates do not change with time. This requires that the left-hand side of Eqs. (16.1) and (16.2) are zero. Additionally, there must be no changes in the bank and elevation angles with time. Therefore, the first two equations within the system of equations given in Eq. (16.4) are zero. Applying these constraints, Eqs. (16.1), (16.2), and (16.4) can be rearranged to yield

$$\begin{Bmatrix} F_{x_b} \\ F_{y_b} \\ F_{z_b} \end{Bmatrix} = -W \begin{Bmatrix} -s_\theta \\ s_\phi c_\theta \\ c_\phi c_\theta \end{Bmatrix} - \frac{W}{g} \begin{Bmatrix} rv - qw \\ pw - ru \\ qu - pv \end{Bmatrix} \quad (16.5)$$

$$\begin{Bmatrix} M_{x_b} \\ M_{y_b} \\ M_{z_b} \end{Bmatrix} = - \begin{Bmatrix} 0 & -h_z & h_y \\ h_z & 0 & -h_x \\ -h_y & h_x & 0 \end{Bmatrix} \begin{Bmatrix} p \\ q \\ r \end{Bmatrix} - \begin{Bmatrix} (I_{yy} - I_{zz})qr + I_{yz}(q^2 - r^2) + I_{xz}pq - I_{xy}pr \\ (I_{zz} - I_{xx})pr + I_{xz}(r^2 - p^2) + I_{xy}qr - I_{yz}pq \\ (I_{xx} - I_{yy})pq + I_{xy}(p^2 - q^2) + I_{yz}pr - I_{xz}qr \end{Bmatrix} \quad (16.6)$$

$$p = -(qs_\phi + rc_\phi)t_\theta \quad (16.7)$$

$$q = rt_\phi \quad (16.8)$$

Equations (16.5)–(16.8) represent our core system of equations for trim. Each of these relations must be true for an aircraft to be in a trim state. Because we have eight equations, these can be used to solve for eight unknowns. Given

mass, propulsion, gyroscopic, and aerodynamic information for a traditional aircraft, the unknowns in these equations include the angle of attack, sideslip angle, elevation angle, bank angle, roll rate, pitch rate, yaw rate, aileron deflection, elevator deflection, rudder deflection, and throttle setting. Since we have eleven unknowns and only eight equations, additional information is required to close this system of equations. Two of these additional relations usually come in the form of a specified state of the aircraft, and the final constraint comes from the type of trim.

For example, the elevation angle and bank angle could be specified by the user. This leaves one final constraint that depends on the type of trim. The elevation angle and bank angles can be specified directly. However, these are directly related to the climb rate and the normal load factor, which are perhaps more useful input parameters.

B. Climb Rate

It is often convenient to specify the state of an aircraft in terms of the climb rate V_c or climb angle γ rather than an elevation angle θ . The climb rate is defined as the change in vertical location with respect to time, i.e. $V_c \equiv -\dot{z}_f$. The climb angle is related to the climb rate according to

$$V_c = V s_\gamma = -\dot{z}_f \quad (16.9)$$

The climb rate can be related to the aircraft orientation and velocity components using the third equation within Eq. (16.3),

$$\dot{z}_f = -s_\theta u + s_\phi c_\theta v + c_\phi c_\theta w + V_{wz_f} \quad (16.10)$$

Neglecting any vertical component of wind (i.e. $V_{wz_f} = 0$) and using Eq. (16.9) in Eq. (16.10) gives a relationship between the climb angle, bank angle, elevation angle, and body-fixed velocity components

$$V s_\gamma = u s_\theta - (v s_\phi + w c_\phi) c_\theta \quad (16.11)$$

Rearranging and squaring gives

$$V^2 s_\gamma^2 - 2u V s_\theta s_\gamma + u^2 s_\theta^2 = (v s_\phi + w c_\phi)^2 c_\theta^2 \quad (16.12)$$

Using the trigonometric identity $c_\theta^2 = 1 - s_\theta^2$ and rearranging gives a quadratic in s_θ

$$[u^2 + (v s_\phi + w c_\phi)^2] s_\theta^2 - 2u V s_\gamma s_\theta + V^2 s_\gamma^2 - (v s_\phi + w c_\phi)^2 = 0 \quad (16.13)$$

This equation can be solved using the quadratic formula to yield

$$s_\theta = \frac{u V s_\gamma \pm (v s_\phi + w c_\phi) \sqrt{u^2 + (v s_\phi + w c_\phi)^2 - V^2 s_\gamma^2}}{u^2 + (v s_\phi + w c_\phi)^2} \quad (16.14)$$

Equation (16.14) yields two solutions. The correct solution is the root that satisfies Eq. (16.11). Given the aerodynamic velocity components of the aircraft, Eqs. (16.14) and (16.11) can be used to solve for the elevation angle for a specified climb angle.

C. Ground Track

It is often convenient to specify the state of an aircraft in terms of the ground-track angle Ψ_g , which is defined as

$$\tan \Psi_g = \frac{\dot{y}_f}{\dot{x}_f} \quad (16.15)$$

The ground-track angle Ψ_g is related to the bank angle, elevation angle, heading or azimuthal angle, velocity components, and constant wind components through the first two equations given in Eq. (16.3). Using these two equations in Eq. (16.15) gives

$$\tan \Psi_g = \frac{c_\theta s_\psi u + (s_\phi s_\theta s_\psi + c_\phi c_\psi) v + (c_\phi s_\theta s_\psi - s_\phi c_\psi) w + V_{wy_f}}{c_\theta c_\psi u + (s_\phi s_\theta c_\psi - c_\phi s_\psi) v + (c_\phi s_\theta c_\psi + s_\phi s_\psi) w + V_{wx_f}} \quad (16.16)$$

This equation can be used to solve for either the required bank angle or the required heading angle given a specified ground track angle.

1. Given Bank Angle

For a given ground-track angle and bank angle, Eq. (16.16) can be used to solve for the required heading angle. Equation (16.16) can be rearranged to yield

$$K_1 c_\psi = K_2 s_\psi + K_3 \quad (16.17)$$

where

$$K_1 = b + a \tan \Psi_g \quad (16.18)$$

$$K_2 = a - b \tan \Psi_g \quad (16.19)$$

$$K_3 = V_{wyf} - V_{wx_f} \tan \Psi_g \quad (16.20)$$

$$a = c_\theta u + s_\phi s_\theta v + c_\phi s_\theta w \quad (16.21)$$

$$b = s_\phi w - c_\phi v \quad (16.22)$$

Squaring both sides of Eq. (16.17), applying the trigonometric identity $c_\psi^2 = 1 - s_\psi^2$ and rearranging gives a quadratic in s_ψ

$$(K_1^2 + K_2^2)s_\psi^2 + 2K_2 K_3 s_\psi + K_3^2 - K_1^2 = 0 \quad (16.23)$$

This equation can now be solved using the quadratic equation to yield

$$s_\psi = \frac{-K_2 K_3 \pm K_1 \sqrt{K_1^2 + K_2^2 - K_3^2}}{K_1^2 + K_2^2} \quad (16.24)$$

This equation yields two solutions. The correct solution is that which satisfies Eq. (16.17).

A common special case of this solution is the case for zero bank angle. This solution is often used during cross-wind landings to minimize the chance of a wing-tip strike. In this case, the ground-track angle must match that of the runway, and the heading angle is used to "crab" the aircraft into the wind. When the main landing gear of the aircraft touch down, the rudder is used to rotate the nose of the aircraft in line with the runway before setting the nose landing gear down.

2. Given Heading Angle

For a given ground-track angle and heading angle, Eq. (16.16) can be used to solve for the required bank angle. Equation (16.16) can be rearranged to yield

$$K_1 c_\phi = K_2 s_\phi + K_3 \quad (16.25)$$

where

$$K_1 = \tan \Psi_g (s_\theta c_\psi w - s_\psi v) - (s_\theta s_\psi w + c_\psi v) \quad (16.26)$$

$$K_2 = -\tan \Psi_g (s_\theta c_\psi v + s_\psi w) + s_\theta s_\psi v - c_\psi w \quad (16.27)$$

$$K_3 = c_\theta u (s_\psi - \tan \Psi_g c_\psi) + V_{wyf} - V_{wx_f} \tan \Psi_g \quad (16.28)$$

Squaring both sides of Eq. (16.25), applying the trigonometric identity $c_\phi^2 = 1 - s_\phi^2$ and rearranging gives a quadratic in s_ϕ

$$(K_1^2 + K_2^2)s_\phi^2 + 2K_2 K_3 s_\phi + K_3^2 - K_1^2 = 0 \quad (16.29)$$

This equation can now be solved using the quadratic equation to yield

$$s_\phi = \frac{-K_2 K_3 \pm K_1 \sqrt{K_1^2 + K_2^2 - K_3^2}}{K_1^2 + K_2^2} \quad (16.30)$$

This equation yields two solutions. The correct solution is that which satisfies Eq. (16.25).

For the special case when the heading angle is aligned with the ground-track angle, i.e. $\psi = \Psi_g$, Eq. (16.30) simplifies to

$$s_\phi = \frac{w c_\psi (V_{wyf} - V_{wx_f}) \pm v \sqrt{v^2 + w^2 - c_\psi^2 (V_{wyf} - V_{wx_f})^2}}{v^2 + w^2} \quad (16.31)$$

D. Load Factor

The load factor is a ratio of the negative pseudo aerodynamic force relative to the weight of the aircraft. It is 3-component vector that can be defined in body-fixed coordinates as $\mathbf{n}_b \equiv -\mathbf{F}_b/W = (-F_{x_b}/W, -F_{y_b}/W, -F_{z_b}/W)$.

1. General Relation to Bank Angle

It is sometimes convenient to specify a normal load factor for the trim condition rather than a bank angle. The term *load factor* is nearly universally defined as the ratio of lift to weight, i.e. L/W . Note that this is the ratio of the aerodynamic force perpendicular to the direction of flight in the plane of symmetry of the aircraft to the aircraft weight. However, in application and discussion, it is treated nearly universally as the ratio of pseudo aerodynamic force in the lift direction to the weight. This is an important difference, since the pseudo aerodynamic force includes thrust, whereas the lift is the aerodynamic force without thrust. Therefore, the load factor can be more accurately defined as

$$n_a \equiv \frac{-F_{z_s}}{W} = \frac{-F_{z_w}}{W} = \frac{-F_{z_b} c_\alpha + F_{x_b} s_\alpha}{W} \quad (16.32)$$

Solving for F_{z_b} in terms of the load factor gives

$$F_{z_b} = (F_{x_b} s_\alpha - W n_a) / c_\alpha \quad (16.33)$$

The load factor can be related to the bank angle through the third equation in Eq. (16.5). Using Eq. (16.33) in the third equation in Eq. (16.5) and solving for the bank angle gives

$$\phi = \cos^{-1} \left[\frac{n_a - F_{x_b} s_\alpha / W - (qu - pv) c_\alpha / g}{c_\theta c_\alpha} \right] \quad (16.34)$$

This is the general solution for the bank angle as a function of load factor.

2. Traditional Approximation

The general relationship between bank angle and load factor shown in Eq. (16.34) is slightly different from the commonly used relationship that is discussed in many text books. The most commonly used relationship between bank angle and load factor can be obtained from Eq. (16.34) by applying the assumptions that the body-fixed coordinate system and thrust are aligned with the direction of flight, and that the aircraft is in a steady-coordinated turn. For the special case when the body-fixed coordinate system is aligned with the direction of flight, $\alpha = \beta = v = w = 0$ and $u = V$. If the thrust is aligned with the direction of flight and the body-fixed x_b axis, $F_{P_z} = 0$. Hence, for this special case, Eq. (16.32) simplifies to the traditional approximation

$$n_a = \frac{L}{W} \quad (16.35)$$

Furthermore, for this special case, Eq. (16.11) simplifies to

$$\gamma = \theta \quad (16.36)$$

Additionally, as will be shown in a following section, for the case of a steady coordinated turn, the pitch rate is

$$q = \frac{g s_\phi^2 c_\theta}{V c_\phi} \quad (16.37)$$

Hence, for this special case, Eq. (16.34) reduces to

$$\phi = \cos^{-1} \left(\frac{c_\gamma}{n_a} \right) \quad (16.38)$$

Although Eq. (16.38) is widely used as the correct relationship between load factor, bank angle, and climb angle, it is technically only true for the special case when the body-fixed coordinate system and thrust are aligned with the direction of flight, and the aircraft is in a steady-coordinated turn. For most cases, the general solution given in Eqs. (16.34) should be used.

E. Steady-Coordinated Turn

In order to close the formulation for trim in a steady-coordinated turn, we need one additional constraint to our equations of motion. In a steady coordinated turn, the side force due to gravity and the bank angle perfectly balance the side force produced by rotational velocities. Therefore, the aerodynamic side force on the vehicle is zero, i.e. $F_{y_b} = 0$. From Eq. (16.5), this requires

$$gs_\phi c_\theta = ru - pw \quad (16.39)$$

This is our final constraint. Combining Eqs. (16.7), (16.8), and (16.39) gives three equations that can be solved for the rotation rates in the steady-coordinated turn as a function of the freestream velocities and orientation. This gives

$$\begin{Bmatrix} p \\ q \\ r \end{Bmatrix} = \frac{gs_\phi c_\theta}{uc_\theta c_\phi + ws_\theta} \begin{Bmatrix} -s_\theta \\ s_\phi c_\theta \\ c_\phi c_\theta \end{Bmatrix} \quad (16.40)$$

Equations (16.5), (16.6), and (16.40) comprise our full set of nine equations for a steady-coordinated turn. Given an elevation angle and bank angle, these can be solved for the nine unknowns, which are angle of attack, sideslip angle, rolling rate, pitching rate, yawing rate, aileron deflection, elevator deflection, rudder deflection, and thrust or throttle setting. If a climb angle is given instead of an elevation angle, Eq. (16.14) can be used to compute the appropriate elevation angle.

F. Steady-Heading Sideslip

Steady-heading sideslip is a trim condition in which the aircraft is sustaining some sideslip and maintaining heading. This case can be specified by either a sideslip angle β or a bank angle ϕ . However, once one of these angles is specified, the other becomes a dependent variable and is fixed. For the case of steady-heading sideslip, the aircraft has no rotational velocity. Therefore,

$$\begin{Bmatrix} p \\ q \\ r \end{Bmatrix} = 0 \quad (16.41)$$

Equations (16.5), (16.6), and (16.41) comprise our full set of nine equations for steady-heading sideslip. Given an elevation angle and either bank angle or sideslip angle, these can be solved for the nine remaining unknowns, which are angle of attack, sideslip angle or bank angle, rolling rate, pitching rate, yawing rate, aileron deflection, elevator deflection, rudder deflection, and thrust or throttle setting. If a climb angle is given instead of an elevation angle, Eq. (16.14) can be used to compute the appropriate elevation angle.

G. Vertical Barrel Roll

A vertical barrel roll is also a case that can be considered a trim condition. Technically, the control deflections and throttle setting would only be constant over time if density did not change with altitude. Since this is not the case, the vertical barrel roll can only be trimmed for a specific altitude, and will deviate from trim immediately. This is a challenge of trimming an aircraft in any climbing or descending trim state, including a steady-coordinated turn or steady-heading sideslip with a non-zero climb angle.

The vertical barrel roll is a trim case in which the aircraft is climbing or descending vertically and rotating about the wind axis. The rotation rate is defined in wind coordinates by a roll rate of p_w , with the pitch and yaw rates in the wind axis exactly zero,

$$q_w = r_w = 0 \quad (16.42)$$

Using Eq. (14.8), the rotation rates in the body-fixed coordinates can be related to the rotation rates in the wind coordinate system as

$$\begin{Bmatrix} p \\ q \\ r \end{Bmatrix} = \begin{Bmatrix} p_w c_\alpha c_\beta - q_w c_\alpha s_\beta - r_w s_\alpha \\ p_w s_\beta + q_w c_\beta \\ p_w s_\alpha c_\beta - q_w s_\alpha s_\beta + r_w c_\alpha \end{Bmatrix} \quad (16.43)$$

Applying Eq. (16.42) to Eq. (16.43) gives

$$\begin{Bmatrix} p \\ q \\ r \end{Bmatrix} = p_w \begin{Bmatrix} c_\alpha c_\beta \\ s_\beta \\ s_\alpha c_\beta \end{Bmatrix} \quad (16.44)$$

H. Solution Process

A trim algorithm can be used to solve for the trim state of an aircraft in a steady-coordinated turn or with steady-heading sideslip. The flight condition is specified by a freestream velocity, altitude, heading, and either a climb angle or elevation angle for both cases. Additionally, for the steady-coordinated turn, the load factor or bank angle must be specified, whereas for the case of steady-heading sideslip, the bank angle or sideslip angle must be specified. With this information, the following algorithm can be used to compute the trim state of a traditional aircraft:

- 1) Begin with the initial guess of all aerodynamic angles and controls set to zero ($\alpha = \beta = \delta_a = \delta_e = \delta_r = \tau = 0$).
- 2) Initialize the rotation rates to zero ($p = q = r = 0$).
- 3) For the case of steady-heading sideslip, set the bank angle or sideslip angle according to the user input.
- 4) Calculate the body-fixed velocities from Eq. (14.9) for the traditional definition of sideslip, or (14.14) if sideslip is defined as the flank angle.
- 5) If the climb angle is specified instead of the elevation angle, calculate the elevation angle from Eq. (16.14).
- 6) For the case of a steady-coordinated turn, if the load factor is specified instead of the bank angle, calculate the bank angle from Eq. (16.34).
- 7) For the case of a steady-coordinated turn, use Eq. (16.40) to compute the rotation rates.
- 8) For the case of a vertical barrel roll, use Eq. (16.43) to compute the rotation rates.
- 9) For the case of a steady-coordinated turn, vertical barrel roll, or for the case of a steady-heading sideslip with bank angle specified, use the aerodynamic model or database to find the aerodynamic angles, thrust, and control-surface deflections that satisfy Eqs. (16.5) and (16.6).
- 10) For the case of a steady-heading sideslip with sideslip angle specified, use the aerodynamic model or database to find the angle of attack, bank angle, thrust, and control-surface deflections that satisfy Eqs. (16.5) and (16.6).
- 11) Using the updated values for the orientation, aerodynamic angles, thrust, and control-surface deflections, repeat steps 4–10 until the solution converges.

Note that either Step 9 or Step 10 will be executed for a given trim condition. For an aircraft with only three control surfaces (aileron, elevator, and rudder), Steps 9 and 10 provide six equations and six unknowns. The six equations in Steps 8 and 9 are given in Eqs. (16.5) and (16.6). The six unknowns for Step 9 are the angle of attack, sideslip or flank angle, thrust, aileron deflection, elevator deflection, and rudder deflection. The six unknowns for Step 10 are the bank angle, angle of attack, thrust, aileron deflection, elevator deflection, and rudder deflection. Within the nearly linear aerodynamics usually encountered for trim conditions below stall, Step 9 or 10 results in only a single solution. This can be solved a number of ways including various linear algebra methods and optimization techniques. Perhaps the simplest method is by fixed-point iteration.

1. Fixed-Point Iteration

Fixed-point iteration can be used to solve the system of six equations given in Eqs. (16.5) and (16.6) along with a traditional aerodynamic model below stall. This is accomplished by using each equation in succession to solve for the unknown that is dominant in that particular equation. Table 16.1 shows the dominant terms for each of the pseudo aerodynamic forces and moments of traditional aircraft.

For example, the thrust or throttle setting is typically dominant in the first equation within Eq. (16.5). Hence, we will use the first equation in Eq. (16.5)

$$F_{x_b} = Ws_\theta - (rv - qw)W/g \quad (16.45)$$

to solve for the thrust. Using Eq. (14.16) in Eq. (16.45) and rearranging gives

$$F_{P_x} = Ws_\theta - (rv - qw)W/g + Dc_\alpha c_\beta + Sc_\alpha s_\beta - Ls_\alpha \quad (16.46)$$

Any root finding method could be used to solve Eq. (16.46) for the thrust or throttle setting. Eqs. (15.37) – (15.39) can

Table 16.1 Dominant terms in the pseudo aerodynamic forces and moments.

| Pseudo Aerodynamic Force/Moment | Dominant Term |
|---------------------------------|---------------|
| F_{x_b} | τ |
| F_{y_b} | β |
| F_{z_b} | α |
| M_{x_b} | δ_a |
| M_{y_b} | δ_e |
| M_{z_b} | δ_r |

be used in Eq. (16.46) and rearranged to yield

$$\tau = \frac{Ws_\theta - (rv - qw)W/g + Dc_\alpha c_\beta + Sc_\alpha s_\beta - Ls_\alpha - \sum_{i=1}^{N_p} D_{P_i} u_{\infty_x}}{\sum_{i=1}^{N_p} (\rho/\rho_0)^{a_i} (T_{0_i} + T_{1_i} V + T_{2_i} V^2) u_{P_{xi}}} \quad (16.47)$$

Closed-form solutions for this fixed-point iteration scheme can also be obtained for the remaining unknowns by applying the aerodynamic model given in Eqs. (15.28) – (15.33). For example, the dominant term in the pseudo aerodynamic side force is typically the sideslip angle. Recall that for a steady-coordinated turn, $F_{y_b} = 0$. Again, any root finding method could be used to solve this expression for the sideslip angle. Using Eq. (14.16) and rearranging gives

$$C_S c_\beta = C_D s_\beta - \frac{F_{P_y}}{\frac{1}{2} \rho V^2 S_w} \quad (16.48)$$

Applying the aerodynamic model given in Eq. (15.29) and solving for β gives

$$\beta = \left[\frac{C_D s_\beta}{c_\beta} - \frac{F_{P_y}}{c_\beta \frac{1}{2} \rho V^2 S_w} - (C_{S,L} \bar{p} C_{L_1} + C_{S,\bar{p}}) \bar{p} - C_{S,\bar{r}} \bar{r} - C_{S,\hat{\beta}} \hat{\beta} - C_{S,\delta_a} \delta_a - C_{S,\delta_r} \delta_r \right] / C_{S,\beta} \quad (16.49)$$

A similar process can be used to obtain solutions for the remaining unknowns given in Table 16.1. However, a perhaps more general and simple iterative process can be developed by using information from the previous iteration. At any point in the iterative scheme we have an estimate for each of the unknowns given in Table 6. Therefore, we can also obtain an estimate for each of the pseudo aerodynamic forces and moments and use this in the iterative scheme. For example, rearranging Eq. (16.47) gives

$$\tau_{i+1} = \tau_i - \frac{F_{x_b} - Ws_\theta + (rv - qw)W/g}{\sum_{i=1}^{N_p} (\rho/\rho_0)^{a_i} (T_{0_i} + T_{1_i} V + T_{2_i} V^2) u_{P_{xi}}} \quad (16.50)$$

where the right-hand side has been computed using the current estimate for the throttle setting τ_i . A similar process can be followed to obtain improved estimates for the other unknowns

$$\beta_{i+1} = \beta_i - \frac{F_{y_b} + Ws_\phi c_\theta + (pw - ru)W/g}{\frac{1}{2} \rho V^2 S_w C_{S,\beta} c_\beta} \quad (16.51)$$

$$\alpha_{i+1} = \alpha_i + \frac{F_{z_b} + Wc_\phi c_\theta + (qu - pv)W/g}{\frac{1}{2} \rho V^2 S_w C_{L,\alpha} c_\alpha} \quad (16.52)$$

$$\delta_{a_{i+1}} = \delta_{a_i} - \frac{M_{x_b} - h_z q + h_y r + (I_{yy} - I_{zz}) qr + I_{yz} (q^2 - r^2) + I_{xz} pq - I_{xy} pr}{\frac{1}{2} \rho V^2 S_w b_w C_{\ell,\delta_a}} \quad (16.53)$$

$$\delta_{e_{i+1}} = \delta_{e_i} - \frac{M_{y_b} + h_z p - h_x r + (I_{zz} - I_{xx}) pr + I_{xz} (r^2 - p^2) + I_{xy} qr - I_{yz} pq}{\frac{1}{2} \rho V^2 S_w \bar{c}_w C_{m,\delta_e}} \quad (16.54)$$

$$\delta_{r_{i+1}} = \delta_{r_i} - \frac{M_{z_b} - h_y p + h_x q + (I_{xx} - I_{yy}) pq + I_{xy} (p^2 - q^2) + I_{yz} pr - I_{xz} qr}{\frac{1}{2} \rho V^2 S_w b_w C_{n,\delta_r}} \quad (16.55)$$

Equations (16.50) – (16.55) can be used in the iterative solution process discussed above to solve for the aerodynamic angles, throttle setting, and control-surface deflections needed in Step 6. Although we have developed them by considering the aerodynamic model given in Eqs. (15.28) – (15.33), they could be used within any aerodynamic model or database as long as a local proportionality constant can be obtained for the variable of interest. For example, Eq. (16.51) can be used to evaluate a new guess for the sideslip angle as long as the local change in side force with respect to sideslip $C_{S,\beta}$ can be computed.

2. Newton's Method

Newton's method can also be used to solve the system of equations given in Eqs. (16.5) and (16.6). Newton's method can require less iterations but in general uses more computational power per iteration. Equation (16.5) and (16.6) can be written in the form

$$\mathbf{f}(\mathbf{G}) = \begin{bmatrix} F_{x_b} - W s_\theta + (rv - qw)W/g \\ F_{y_b} + W s_\phi c_\theta + (pw - ru)W/g \\ F_{z_b} + W c_\phi c_\theta + (qu - pv)W/g \\ M_{x_b} - h_z q + h_y r + (I_{yy} - I_{zz})qr + I_{yz}(q^2 - r^2) + I_{xz}pq - I_{xy}pr \\ M_{y_b} + h_z p - h_x r + (I_{zz} - I_{xx})pr + I_{xz}(r^2 - p^2) + I_{xy}qr - I_{yz}pq \\ M_{z_b} - h_y p + h_x q + (I_{xx} - I_{yy})pq + I_{xy}(p^2 - q^2) + I_{yz}pr - I_{xz}qr \end{bmatrix} = \mathbf{R} \quad (16.56)$$

where \mathbf{G} represents a vector containing the unknowns and \mathbf{R} is a vector of the resulting residual for each equation. We seek the solution to \mathbf{G} such that each component in \mathbf{R} goes to zero. Therefore, we wish the change in the residual to be $-\mathbf{R}$. Beginning with an estimate for the unknowns \mathbf{G} , we can estimate the change in the residual using the Jacobian

$$J_{ij} = \frac{\partial f_i}{\partial G_j} \quad (16.57)$$

For example, if the vector of unknowns is $\mathbf{G} = \{\alpha, \beta, \delta_a, \delta_e, \delta_r, \tau\}$, the Jacobian matrix is constructed from the following partial derivatives

$$[\mathbf{J}] = \begin{bmatrix} \frac{\partial f_1}{\partial \alpha} & \frac{\partial f_1}{\partial \beta} & \frac{\partial f_1}{\partial \delta_a} & \frac{\partial f_1}{\partial \delta_e} & \frac{\partial f_1}{\partial \delta_r} & \frac{\partial f_1}{\partial \tau} \\ \frac{\partial f_2}{\partial \alpha} & \frac{\partial f_2}{\partial \beta} & \frac{\partial f_2}{\partial \delta_a} & \frac{\partial f_2}{\partial \delta_e} & \frac{\partial f_2}{\partial \delta_r} & \frac{\partial f_2}{\partial \tau} \\ \frac{\partial f_3}{\partial \alpha} & \frac{\partial f_3}{\partial \beta} & \frac{\partial f_3}{\partial \delta_a} & \frac{\partial f_3}{\partial \delta_e} & \frac{\partial f_3}{\partial \delta_r} & \frac{\partial f_3}{\partial \tau} \\ \frac{\partial f_4}{\partial \alpha} & \frac{\partial f_4}{\partial \beta} & \frac{\partial f_4}{\partial \delta_a} & \frac{\partial f_4}{\partial \delta_e} & \frac{\partial f_4}{\partial \delta_r} & \frac{\partial f_4}{\partial \tau} \\ \frac{\partial f_5}{\partial \alpha} & \frac{\partial f_5}{\partial \beta} & \frac{\partial f_5}{\partial \delta_a} & \frac{\partial f_5}{\partial \delta_e} & \frac{\partial f_5}{\partial \delta_r} & \frac{\partial f_5}{\partial \tau} \\ \frac{\partial f_6}{\partial \alpha} & \frac{\partial f_6}{\partial \beta} & \frac{\partial f_6}{\partial \delta_a} & \frac{\partial f_6}{\partial \delta_e} & \frac{\partial f_6}{\partial \delta_r} & \frac{\partial f_6}{\partial \tau} \end{bmatrix} \quad (16.58)$$

The partial derivatives can be estimated through finite differencing. The Jacobian can then be used in Newton's method to obtain the change in \mathbf{G} from the equation

$$\Delta \mathbf{G} = -[\mathbf{J}]^{-1} \mathbf{R} \quad (16.59)$$

The estimate for \mathbf{G} is updated with each iteration using a relaxation factor Γ through the equation

$$\mathbf{G}_{i+1} = \mathbf{G}_i + \Gamma \Delta \mathbf{G} \quad (16.60)$$

This process is repeated until the solution converges. Convergence can be measured by computing the length of the residual vector \mathbf{R} after each iteration. Alternately, it can also be computed by simply using the largest component of \mathbf{R} . Once the length or the largest component of \mathbf{R} is below some tolerance, the solution is considered to be converged.